

ASSESSING THE USE OF MULTISPECTRAL REMOTE SENSING IN MAPPING THE
SPATIO-TEMPORAL VARIATIONS OF SOIL EROSION IN SEKHUKHUNE DISTRICT,
SOUTH AFRICA

TERRENCE KOENA SEPURU

A DISSERTATION SUBMITTED IN THE FULFILMENT FOR THE DEGREE OF MASTER
OF SCIENCE IN GEOGRAPHY IN THE DEPARTMENT OF GEOGRAPHY AND
ENVIRONMENTAL STUDIES, SCHOOL OF AGRICULTURAL AND ENVIRONMENTAL
SCIENCES, FACULTY OF SCIENCE AND AGRICULTURE, UNIVERSITY OF LIMPOPO,
SOUTH AFRICA

SUPERVISOR: Dr. TIMOTHY DUBE

JUNE, 2018

Abstract

Soil erosion, which is a critical component of land degradation, is one of the serious global environmental problems often threatening food security, water resources, and biodiversity. A comprehensive assessment and analysis of remote sensing applications in the spatial soil erosion mapping and monitoring over time and space is therefore, important for providing effective management and rehabilitation approaches at local, national and regional scales. The overall aim of the study was to assess the use of multispectral remote sensing sensors in mapping and monitoring the spatio-temporal variations in levels of soil erosion in the former homelands of Sekhukhune district, South Africa. Firstly, the effectiveness of the new and freely available moderate-resolution multispectral remote sensing data (Landsat 8 Operation Land Imager: OLI and Sentinel-2 Multi-Spectral Instrument: MSI) derived spectral bands, vegetation indices, and a combination of spectral bands and vegetation indices in mapping the spatio-temporal variation of soil erosion in the former homelands of Sekhukhune District, South Africa is compared. The study further determines the most optimal individual sensor variables that can accurately map soil erosion. The results showed that the integration of spectral bands and spectral vegetation indices yielded high soil erosion overall classification accuracies for both sensors. Sentinel-2 data produced an OA of 83, 81% whereas Landsat 8 has an OA of 82.86%. The study further established that Sentinel-2 MSI bands located in the NIR (0.785-0.900 μm), red edge (0.698-0.785 μm) and SWIR (1.565-2.280 μm) regions were the most optimal for discriminating degraded soils from other land cover types. For Landsat 8 OLI, only the SWIR (1.560-2.300 μm), NIR (0.845-0.885 μm) region were selected as the best regions. Of the eighteen spectral vegetation indices computed, Normalized Difference Vegetation Index (NDVI) and Soil Adjusted Vegetation Index (SAVI) and Global Environmental Monitoring Index (GEMI) were selected as the most suitable for detecting and mapping soil erosion.

Secondly, the study assessed soil erosion in the former homelands of Sekhukhune, South Africa by applying a time-series analysis (2002 and 2017), to track changes of areas affected by varying degrees of erosion. Specifically, the study assessed and mapped changes of eroded areas (wet and dry season), using multi-date Landsat products 8 OLI and 7 Enhanced Thematic Mapper (ETM+)). Additionally, the study used extracted eroded areas and overlay analysis was performed together with geology, slope and the Topographic Wetness Index (TWI) of the area under study to assess whether and to what extent the observed erosional trends can be explained.

Time series analysis indicated that the dry season of 2002, experienced 16.61 % (224733 ha) of erosion whereas in 2017 19.71% was observed. A similar trend was also observed in the wet season. This work also indicates that the dominant geology type Lebowa granite: and Rustenburg layered its lithology strata experienced more erosional disturbances than other geological types. Slopes between 2-5% (Nearly level) experienced more erosion and vice-versa. On the hand, the relationship between TWI and eroded areas showed that much erosion occurred between 3 and 6 TWI values in all the seasons for the two different years, however, the dry season of 2002 had a slightly higher relationship and vice-versa. We, therefore, recommend use and integration of freely and readily available new and free generation broadband sensors, such as Landsat data and environmental variables if soil erosion has to be well documented for purposes of effective soil rehabilitation and conservation.

Keywords: Food security Global changes, Land degradation, Land-based ecosystems, Land management practices, Satellite data, Soil conservation, Sustainable Development; Topographic Wetness Index; Time series analysis.

Preface

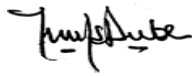
This study was conducted in the Department of Geography and Environment Studies, School of Agriculture and Environmental Science, University of Limpopo, Limpopo Province, South Africa, from February 2017 to June 2018, under the supervision of Dr. Timothy Dube.

I declare that the work presented in this thesis has never been submitted in any form to any other institution. This work represents my original work except where due acknowledgments are made.

Terrence Koena Sepuru Signed Date.....

As the candidate's supervisor, I certify the aforementioned statement and have approved this dissertation for submission.

Dr. Timothy Dube Signed



Date.....

Declaration

I Terrence Koena Sepuru, declare that:

1. The research reported in this dissertation, except where otherwise indicated is my original research.
2. This dissertation has not been submitted for any degree or examination at any other institution.
3. This thesis does not contain other person's data, pictures, graphs or other information unless specifically acknowledged as being sourced from other persons.
4. This dissertation does not contain other persons writing unless specifically acknowledged as being sourced from other researchers. Where other written sources have been quoted:
 - I. Their words have been re-written and the general information attributed to them has been referenced.
 - II. Where their exact words have been used, their writing has been placed inside quotation marks and referenced
5. This thesis does not contain text, graphics or tables copied and pasted from the internet, unless specifically acknowledged, and the source being detailed in the thesis and in the references section.

Signed..... Date.....

Declaration 2: Publications and Manuscripts

1. Sepuru, T.K., and Dube, T., 2017. An appraisal on the progress of remote sensing applications in soil erosion mapping and monitoring. *Remote Sensing Applications: Society and Environment* 9 (2018) 1–9.
2. Sepuru, T.K., and Dube, T., 2018. Understanding the spatial distribution of eroded areas in the former rural homelands of South Africa: Comparative evidence from two new non-commercial multispectral sensors. *International Journal of Applied Earth Observation and Geoinformation*, 69, pp.119-132.
3. Sepuru, T.K., and Dube, T., “A time-series analysis of soil erosion spatial extent in the former homelands of Sekhukhune, Limpopo using multi-date Landsat series data” at *International Journal of Remote Sensing*. Manuscript ID TRES-PAP-2018-0529

Dedication

I dedicate this dissertation to my family, for trusting me in the potential that I have to achieve great work such as this. I want to extend my dedication my Spiritual leaders for their prayers and support. I want to continue making you proud.

Acknowledgments

I would like to extend my sincere gratitude to the University of Limpopo, for giving me an opportunity to pursue my studies. I would also like to further my thank the Department of Geography and Environmental Studies under the School of Agriculture and Environmental Sciences, this study would not have been possible without the opportunity that was given to me. I would especially extend my gratitude to the Risk and Vulnerable Science Centre (RVSC) for awarding me a Bursary and logistic support, to pursue my studies at University.

I am very appreciative of my supervisor and promoter, Dr. Timothy Dube, who astonishingly supervised my project and sacrificed his time to assist me in coming with this wonderful dissertation. His professional knowledge, passion, and commitment concerning supervising my work was outstanding. A research project of this kind is not at all the effort on one individual. Hence, I have to thank the following individuals and who, with their diverse and significant contributions, contributed towards the completion of this dissertation: Special thanks go to Mr. Inos Dhau for his knowledge and Skills of research, not forgetting Mr. Mpho Gegana for his technical support; together with Mr Humphrey Kgabo Thamaga and Mrs Paballo Radingwana.

Table of Content

Abstract.....	i
Preface	iii
Declaration.....	iv
Declaration 2: Publications and Manuscripts.....	v
Dedication.....	vi
Acknowledgments.....	vii
Table of Content	viii
List of Figures	xi
List of Tables	xiii
1. Chapter One.....	1
Background of the study.....	1
1.1. Introduction.....	1
1.2. Aim and Specific objectives.....	3
1.3. Description of Study Area	3
1.4. The general structure of the thesis.....	5
2. Chapter Two	6
An appraisal on the progress of remote sensing applications in soil erosion mapping and monitoring.....	6
2.1. Introduction.....	8
2.2. Distribution of soil erosion.....	10
2.3. Available soil erosion modeling techniques.....	11
2.4. Satellite remote sensing of soil erosion	13
2.5. Soil erosion classification strategies: Strength and limitations	19

2.6.	Spectral characteristics and vegetation Indices for mapping soil erosion	21
2.7.	Remote sensing recommendations for soil erosion mapping	24
2.8.	Conclusion	26
3.	Chapter Three	27
	Understanding the spatial distribution of eroded areas in the former rural homelands of South Africa: Comparative evidence from two new non-commercial multispectral sensors..	27
3.1.	Introduction.....	29
3.2.	Materials and Methods.....	32
3.2.1.	Field data collection.....	32
3.2.2.	Remote sensing data acquisition and pre-processing.....	33
3.2.3.	Digital Elevation Model data.....	34
3.2.4.	Landsat 8 OLI and Sentinel-2 derived spectral data and vegetation indices.....	34
3.2.5.	Statistical data analysis.....	36
3.2.6.	Image Classification and Accuracy assessment	37
3.3.	Results	38
3.3.1.	Discrimination of eroded areas from other land cover types	38
3.3.2.	Spectral indices performance	42
3.3.3.	Image classification.....	42
3.4.	Discussion.....	56
3.5.	Conclusions.....	59
4.	Chapter Four	60
	A time-series analysis of soil erosion spatial extent in the former homelands of Sekhukhune, Limpopo using multi-date Landsat series data	60
4.1.	Introduction.....	62
4.2.	Material and methods.....	65
4.2.1.	Field data collection.....	65
4.2.2.	Landsat pre-processing.....	65
4.2.3.	Image classification and accuracy assessment.....	66
4.2.4.	Sekhukhune Geological types.....	67

4.2.5.	Slope and TWI data set derived from DEM	68
4.3.	Results	70
4.3.1.	Changing of spatial land use	70
4.3.2.	Classification Accuracy.....	76
4.3.3.	Analysis of the conversion among specific land covers.....	77
4.3.4.	The relationship between eroded areas and geology	79
4.3.5.	Influence of topographic variables on eroded areas.....	83
4.4.	Discussion.....	87
4.5.	Conclusions.....	89
5.	Chapter Five.....	90
	ASSESSING THE USE OF MULTISPECTRAL REMOTE SENSING IN MAPPING THE SPATIO- TEMPORAL VARIATIONS OF SOIL EROSION: A SYNTHESIS.....	90
5.1.	Introduction.....	90
5.2.	Comparing the effectiveness of Landsat 8 and Sentinel-2 data in mapping soil erosion 90	
5.4.	Conclusions.....	92
5.5.	Recommendations	93
	References.....	94

List of Figures

Figure 1.1 Location of the study site..	4
Figure 2.1 The distribution of global status of human-induced soil degradation (Source: Oldeman et al., 1990).	10
Figure 3.1 Average reflectance of eroded areas in relation to other land cover types derived using Landsat 8 OLI (b. dry season and c, wet season) Sentinel-2 MSI (a dry season and d. wet season) (error bars: signify the level of separability).....	41
Figure 3.2 Overall classification accuracies for three analysis stages. a) dry season; b) wet season.....	45
Figure 3.3 Classified land cover maps derived from Landsat 8 OLI (a. dry and c wet seasons) and Sentinel-2 MSI (b. dry and d. wet season).....	47
Figure 3.4 Derived area per land cover class. a). dry season; b). wet season.....	48
Figure 3.5 Zoomed maps showing eroded areas from classified land cover maps using Landsat 8 OLI (a dry & c wet seasons) and Sentinel-2 MSI (b dry & d wet seasons).....	51
Figure 3.6 Google earth images showing eroded areas in abandoned fields in the former homelands, Sekhukhune, South Africa. (i) Illustrate gully detected in along agricultural field, around steelport town (ii) eroded surface emerging within the villages of Jane Furse (iii) rill forming overabundant substance farms in Mphenama areas and (iv) illustrates erosion imaging from the road of Atok mine.....	51
Figure 3.7 Photographs showing eroded areas taken in the former homelands, Sekhukhune, South Africa. (a) S open eroded areas in abandoned agriculture fields (b) eroded surface imaging all the villages of Jane Furse (c) illustrate a gully forming from a mine waste system channel and (d) illustrate eroded surface within Jane Furse villages.	52
Figure 3.8 Maps showing the relationship between elevation and eroded areas (a. dry & c. wet; b. dry & d. wet season for Landsat 8 and Sentinel 2 respectively).....	54
Figure 3.9. Eroded areas (%) in relation to change in elevation. a). wet & b). dry season; c). dry & d). wet season.....	55
Figure 4.1 Derived soil erosion thematic maps for the year 2002 and 2017. a-b dry and wet season Landsat 7 ETM+ derived soil erosion and (c-d) dry and wet season 2017 Landsat 8 OLI derived.....	72

Figure 4.2 Zoomed maps showing changes amongst land cover within the study area. a), dry season; b) wet season.	74
Figure 4.3 Changes detected between 2002 and 2017 in percentages	76
Figure 4.4 The spatial distribution map of Geology across the study area.....	80
Figure 4.5 Reclassified geology and areas affected by erosion in 2002 (a. dry season b. wet season) and 2017 during (c. dry season d. wet season).	82
Figure 4.6 The spatial distribution map of slope in percentages across the study area	83
Figure 4.7 Slope and areas affected by erosion in 2002 (a. dry season b. wet season) and 2017 during (c. dry season d. wet season).	84
Figure 4.8 The spatial distribution map of topographic wetness index across the study area.....	85

List of Tables

Table 2.1 Summary of remote sensing applications in soil erosion mapping Adopted from Matongera, et al., (2016).....	17
Table 2.2 Remote sensing sensor specifications and cost in soil erosion.....	18
Table 3.1 Landsat 8 OLI and Sentinel-2 MSI spectral characteristics used in this study.....	34
Table 3.2 Selected spectral vegetation indices derived from Landsat-8 OLI and Sentinel-2 images applied in the validation of eroded surface mapping.....	35
Table 3.3 Adopted soil erosion analysis approach.....	36
Table 3.4 Classification accuracies derived using spectral dataset, spectral vegetation dataset as well as combined dataset	44
Table 3.5 Deviation of classification accuracies between Landsat 8 OLI and Sentinel-2 MSI....	46
Table 4.1 Characteristics of the remotely sensed data set selected for this study	66
Table 4.2 detail information on geology (parent) used in the study	67
Table 4.3 Slope Steepness.....	69
Table 4.4 Mapped land covers and their change from 2002 to 2017 (dry season).....	75
Table 4.5 Mapped land covers and their change from 2002 to 2017 (wet season).....	75
Table 4.6 Classification accuracies from error matrix derived using spectral dataset.....	77
Table 4.7 Change in land covers between 2002 and 2017 (unit: ha) dry season.....	78
Table 4.8 Change in land covers between 2002 and 2017 (unit: ha) wet season	79

1. Chapter One

Background of the study

1.1. Introduction

Soil erosion as a major problem, causes the reduction in the capacity of the land to perform ecosystem functions and services that support society and development. Soil erosion is amongst the leading environmental problems in South Africa and the worldover (Le Roux et al., 2007, Wessels et al., 2004). According to Le Roux et al., (2007), soil erosion affects food security, national economic development, and natural resource conservation. For example, the report by Department of Environmental Affairs and Tourism, (2005) indicates that many South African communal areas in the Limpopo, North West, Northern Cape, and Mpumalanga provinces are severely degraded. Greater Sekhukhune District in Limpopo is among some of the areas, which are badly degraded and this impacts on the livelihoods of people living in these areas, due to a decline in the productive capacity of the affected areas (Stronkhors at al., 2009). However, most of these reports were based on routine field surveys and information derived from digitized aerial photographs. This, therefore, calls for the accurate monitoring and mapping of degraded areas to provide essential information on the levels of degradation, as well as prioritization on the areas that require immediate interventions (Le Roux et al., 2007; Wessels et al. 2004). Besides, this information is key in decision-making and in developing possible rehabilitation strategies of the affected and potentially vulnerable areas. Mapping of eroded areas provides valuable spatial information that may benefit operational tasks, such as rehabilitation of affected areas and any other forms of remediation.

Soil erosion is a very complex problem to solve, as a number of factors govern it: ranging from biophysical, climatic and human activities. Human-induced practices, such as overutilization and exploitation of the natural vegetation cover, poor soil, cropland and rangeland management, and overgrazing results in severe soil erosion (Mulibana at al., 2007). Information on the areas affected by soil erosion is central in coming up with management and rehabilitation efforts. In trying to understand soil erosion and its impacts in these areas, researchers have since applied various techniques namely: empirical, conceptual and physically based models (Merritt et al., 2003). However, a major limitation in modelling soil erosion using these techniques is the

restriction in the understanding of the processes involved, particularly in terms of the spatial and temporal distribution (Croke and Mockler, 2001). Previous assessments of the quality and quantity of soil erosion models show that, in general, the spatial aspect and patterns of erosion are poorly predicted (Jetten et al., 2003; Merritt et al., 2003). Furthermore, models can rarely be relied upon to give accurate predictions of absolute amounts of soil erosion. Without adequate input data and calibration, models can only be expected to give a relative ranking of the effects of input variables (Garen et al., 1999). Input data preparation is a difficult task and the mechanics of operating the models is sometimes complicated (Jetten et al., 2003). The large part of the effort goes into the construction of the input data set, often derived from a few basic variables that are available as raw data. In addition, the main limitation of soil erosion models is the fact that they rely on focus on small-scale applications (Nigel and Rughooputh, 2010). Additionally, these models are generally expensive and time-consuming and standard equipment is hardly available.

Regardless of these limitations, several studies (Morgan, 2005; Le Roux et al., 2008; Seutloali et al., 2016; Dube et al., 2017) have identified the applications of satellite remote sensing sensors as the way forward to address soil erosion related environmental problems. However, the major limitation with available remote sensing studies on soil erosion mapping is the use of single-date or images, which limits the generation of meaningful conclusions and recommendations (Sepuru and Dube 2018). Although great strides have also been made in land degradation or soil erosion monitoring, the accuracy of the derived thematic maps remains questionable, especially in developing countries, as the availability of high-resolution data remains a challenge (Luleva et al., 2012). In developing countries, soil erosion monitoring in most communal areas is largely undocumented and this affects food security in these areas. Therefore, the freely available and new crop of sensors, such as Sentinel 2 MSI and Landsat 8 OLI series, with improved spatial, spectral radiometric and temporal resolutions, are perceived to provide the most needed spatial tool for monitoring these areas at low costs. These newly launched sensors, unlike their predecessors, have been highly rated in most of their applications and these include biomass mapping (Yavaşlı, 2016; Zhang et al., 2017), land-surface temperature mapping (Adeyeria, 2017; Avdan and Jovanovska, 2016) and invasive species mapping (Gavier-Pizarro, et al., 2012; Wang et al., 2017). For instance, Sentinel-2 MSI data available at 10m spatial resolution is considered

as one of the most possible solutions to most environmental related challenges in sub-Saharan African, due to its free availability, global footprint, high temporal resolution (± 5 days).

1.2. Aim and Specific objectives

The overall aim of the study was to assess the use of multispectral remote sensing sensors in mapping and monitoring the spatio-temporal variations of soil erosion in the former homelands of Sekhukhune District, South Africa.

The objectives of the study were to:

- i. determine the optimal new generation satellite data that can accurately map the spatial distribution of soil erosion in the former rural homelands of Sekhukhune, South Africa
- ii. To map the seasonal and long term variations in soil erosion in the former homelands of Sekhukhune, Limpopo using multi-date satellite data

1.3. Description of Study Area

The research was conducted in the Greater Sekhukhune District Municipality, Limpopo Province, South Africa (Figure 1.1). The area is located at the coordinates $24^{\circ}23'27.52''\text{S}$ and $29^{\circ}50'06.83''\text{E}$ and lies across the border of Mpumalanga and Limpopo province. The district comprises approximately $13\,528\text{ km}^2$ (1352800 ha) of geographical area, the majority of which is rural. The district lies in the southeastern part of the province, and is comprised of five local municipalities. These include Elias Motsoaledi, Ephraim Mogale, Fetakgomo, Makhuduthamaga, and Tubatse. The district is situated in a semi-arid environment, with average annual rainfall $\pm 560\text{ mm}$ and temperatures showing a moderate fluctuation with average summer temperatures of $\pm 23^{\circ}\text{C}$ (Mpandeli et al., 2015; Stronkhors et al., 2009). The topography of the area is generally rugged ranging from hilly to mountainous with an average altitude of 494 m above sea level. Subsistence or smallholder agriculture accounts for 70% of the farming activities in the district, whilst the other 30% is commercial agriculture (Siambi et al., 2007).

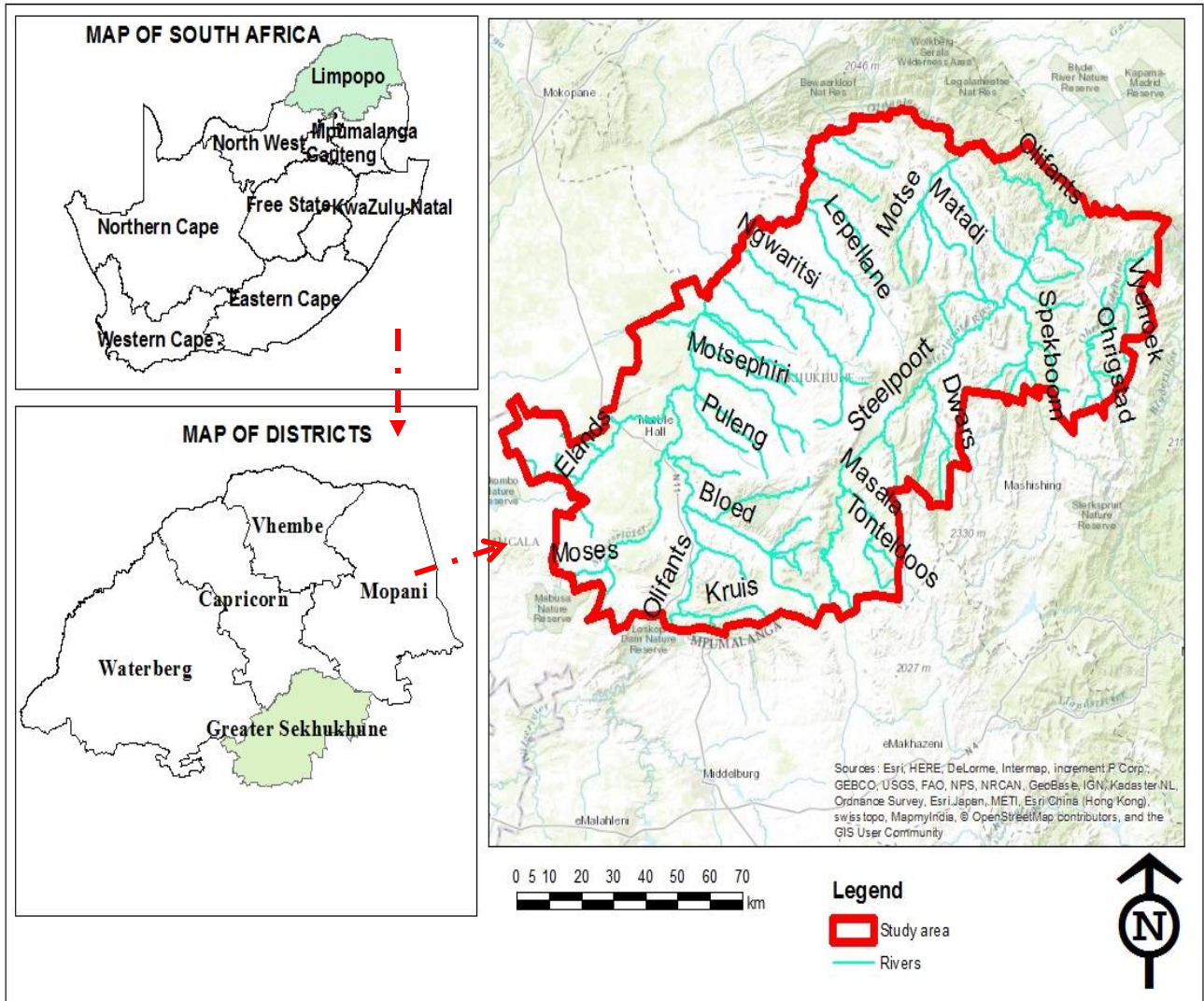


Figure 1.1 Location of the study site.

1.4. The general structure of the thesis

The thesis includes two research papers and one literature paper that answer each of the objectives specified in section 1.2.

Chapter 1

This chapter provides a brief background of the study and highlights the gaps in literature.

Chapter 2

As a paper article reviews the application of remote sensing technology on soil erosion, as a global concern including available methodologies. The review provides information on the levels of erosion and the spatial occurrence. The study outlines available soil erosion models and then highlights the trade-offs between remote sensing applications in mapping and associated image acquisition costs. In addition, included in this review is a discussion on the techniques to classify soil erosion using remotely sensed data.

Chapter 3 and 4

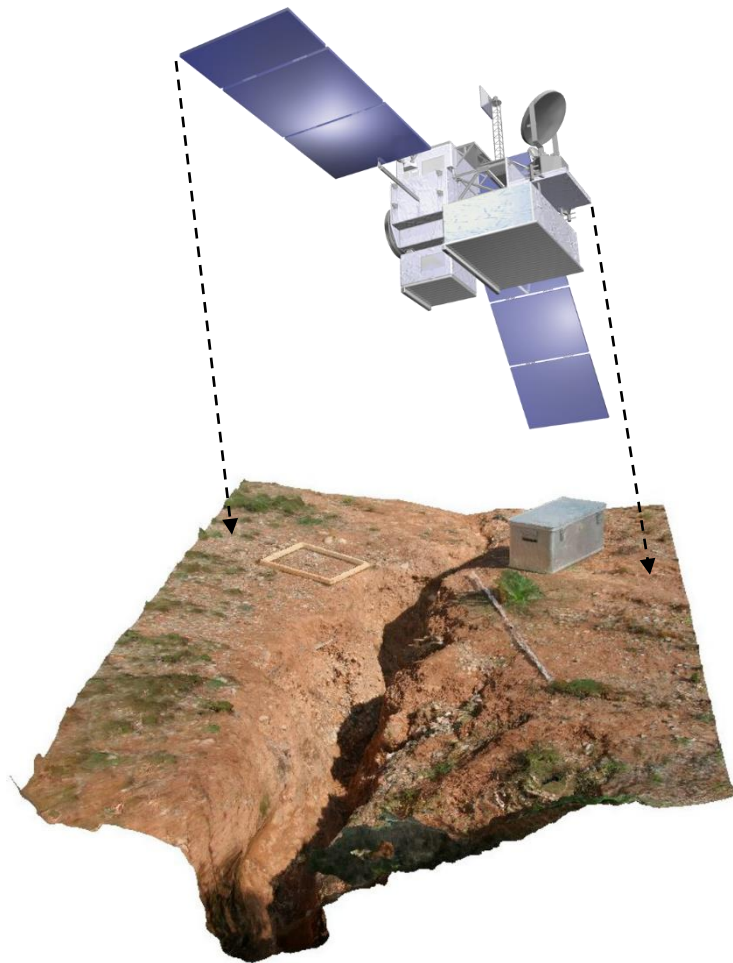
This section focuses on assessing the spatial distribution of eroded areas: Comparative evidence from two new non-commercial multispectral sensors while chapter four conducted a time-series analysis of soil erosion spatial using multi-date Landsat series data. In chapter four, assesses soil erosion in the former homelands of Sekhukhune, South Africa by applying a time-series analysis (2002 and 2017), to track changes of areas affected by varying degrees of erosion. In this chapter the influence of geology, slope and the Topographic Wetness Index (TWI) on the observed erosional trends is further investigated.

Chapter 5

In this chapter, the evaluation and conclusions of the research findings are made. The interpretations made here follow the structure of the dissertation objectives established in the introduction section (Chapter 1). Consequently, this section revisits and provides an evaluation of each research objective. Thereafter, the conclusions of the study are drawn, while the last section offers recommendations and proposals for further research.

2. Chapter Two

An appraisal on the progress of remote sensing applications in soil erosion mapping and monitoring



This chapter is based on a published review paper:

Sepuru, T.K., and Dube, T., 2017. An appraisal on the progress of remote sensing applications in soil erosion mapping and monitoring. *Remote Sensing Applications: Society and Environment* 9 (2018) 1–9

Abstract

Satellite remote sensing applications in soil erosion mapping and modeling has gathered considerable momentum in the last decade, globally. Most importantly, the latest advancements in remote sensing technology and the availability of this data in various resolutions and the immediate demand for up-to-date information on levels of soil loss, soil erosion mapping, and modeling has received renewed attention, particularly to ensure that productive agricultural land remains intact to ensure food security. This work details an overview of the advancements of remote sensing in soil erosion research. The study also, for the first time highlights the strengths and limitations of satellite data in mapping and monitoring soil erosion at various scales. The mostly recommended remotely sensed data in soil erosion modeling were multispectral sensors, such as Landsat data imagery, while high spectral resolution information remained limited, mainly due to acquisition cost. Despite many efforts made to quantify and map the extent of soil erosion, the focus has been restricted to local scale applications. There is, therefore, a need for a more detailed and extensive work to assess the spatial variability and extent of soil erosion at regional scales if sustainable management and effective rehabilitation strategies are to be developed.

Keywords: Erosion modeling, Food security Global changes, Land degradation, Land-based ecosystems, Land management practices, Satellite data, Soil conservation

2.1. Introduction

Soil is a natural resource that provides significant environmental, social, and economic functions. The economies of the world largely dependent on the soil as a natural resource for the provision of goods and services (Blum, 2005). However, due to the high demand of resources or good and services generated from soils, much pressure has been exerted, particularly from underdeveloped countries, which largely depends on primary sectors, such as agriculture and forestry (Wessels et al., 2004). Most of the agricultural practices are largely subsistence, lacking proper soil conservation techniques. Therefore, the pressure generated from these unsustainable human activities results in severe soil erosion (Le Roux et al., 2007) as Figure 1 demonstrates human induced erosion, the world-over. Problems linked to soil erosion, include loss of fertile topsoil for cropping, leading to siltation, eutrophication, damage to infrastructure and loss of aquatic biodiversity that contributes to global change (Morgan, 2005; Nearing et al., 2004; Onyando et al., 2005).

Literature shows that soil erosion, which is a critical component of land degradation, comprising of water and wind erosion, chemical degradation, excessive salts, physical and biological degradation (Luleva et al., 2012), is one of the serious global environmental problem (Wessel et al., 2007) often threatening food security, water resources and biodiversity. For instance, the world loses approximately 75 billion tons of fertile soil from world agricultural systems each year (Eswaran et al., 2001). In Africa for instance, 40% of the land area is degraded, affecting food production and leading to soil erosion, which in turn contributes to desertification (Thompson, 2017). Also, several studies indicate that varying intensities and types of soil erosion have affected over 70% of South Africa's land area (Pretorius, 1998; Garland et al., 2000; Le Roux et al., 2007). This environmental scourge has resulted in international governments, environmental activists, soil scientists and hydrologists embarking on soil conservation training, awareness programs and research across the world, in a bid to curb further losses.

The limitation associated with the above efforts is mainly the lack of the exact information on the areas affected by soil erosion, as well as its magnitude. For instance, most of these efforts are restricted to traditional methods, such as Revised Universal Soil Loss Equation (RUSLE) and whereas conservation programs are deemed a failure because communities from the affected areas do not have a sense of ownership (Merritt et al., 2003). The use of aerial photographs and

satellite data has greatly increased the capacity to quantify and monitor soil erosion at local, national and regional scales (Le Roux et al., 2007). This is because traditional erosion modeling techniques involve manual detection of erosional levels from air photos and fieldwork measurements. The major challenge with these approaches is that they are limited to expert knowledge, besides being time-consuming and costly (Dube et al., 2017). Remote sensing coupled with Geographic Information System (GIS), provides key information on the erosional dynamics and intensity over time and space, which is critical in providing a baseline for soil erosion assessment, control, and prediction (Wang et al., 2013). This is confirmed by numerous studies that have been done to date using satellite technologies.

This thus paper aimed at reviewing the application of remote sensing technology on soil erosion, as a global concern including available methodologies. The paper starts by providing information on the levels of erosion and the spatial occurrence thereof, as well as provide a detailed summary of various land management practices affected by soil erosion. Secondly, the study outlines available soil erosion models and then highlights the trade-offs between remote sensing applications in mapping and associated image acquisition costs. In addition, included in this review is a discussion on the techniques to classify soil erosion using remotely sensed data.

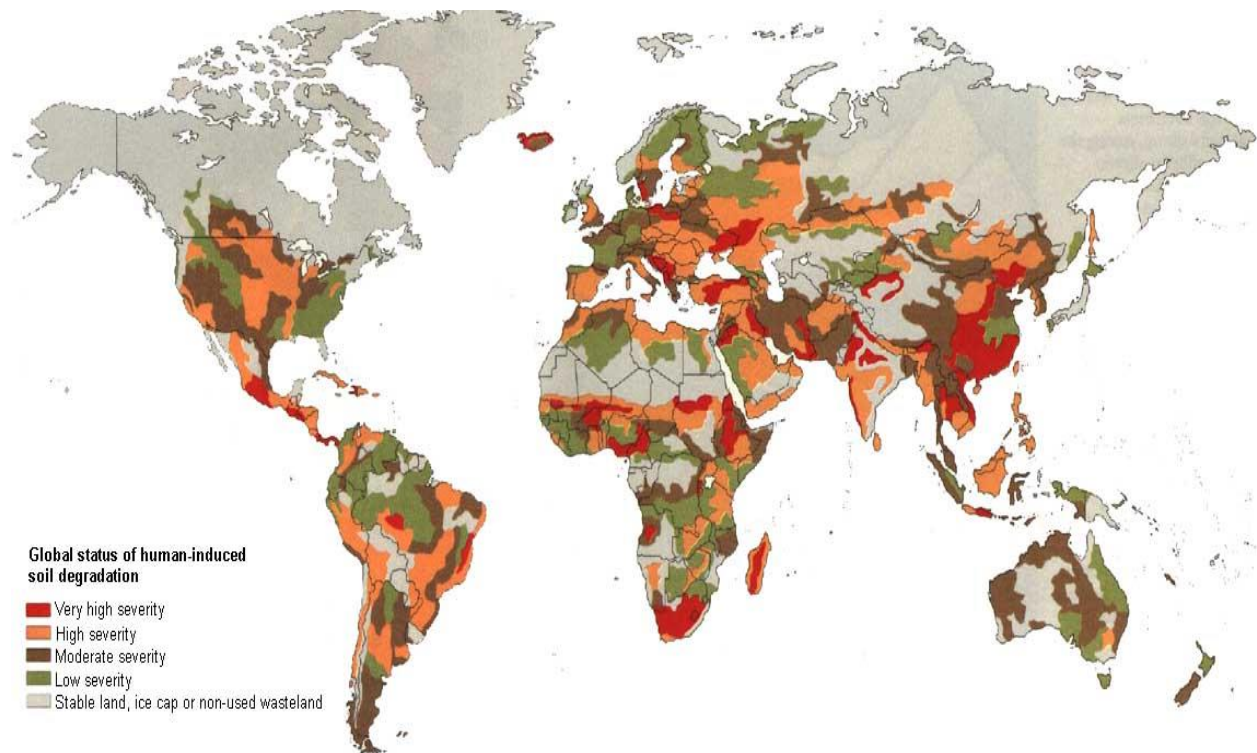


Figure 2.1 The distribution of global status of human-induced soil degradation (Source: Oldeman et al., 1990).

2.2. Distribution of soil erosion

Soil erosion is a worldwide phenomenon, with its magnitude varying extensively across countries depending on the levels of technological advancement, slope/landscape, land use and land cover types and management practices in place (Madikizela, 2000). Several studies have claimed that soil erosion and its related effects severely impact on rural communities since a large number of rural communities' dependent on services derived from land-based ecosystems for their livelihoods (IPCC, 2001; LADA, 2002 and Abbas, 2009). Furthermore, Botha (1996) and Weaver (1991) argued that environmental factors that control soil erosion include bedrock type, soil, climate, topography, vegetation and human activities. Rural communities are, therefore, particularly vulnerable to the consequences of soil erosion. Soil erosion also constitutes towards several socio-economic and environmental threats. As cited by several related studies (Morgan, 2005; Le Roux et al., 2008; Seutloali et al., 2016; Dube et al., 2017).

Soil erosion occurs in the form of a sheet, rill and/or gully erosion of which some of these are difficult to detect using satellite data. To hamper the encroachment of soil erosion and to

formulate the necessary conservation strategies, it is therefore essential to know the phenomenon's spatial distribution and magnitude (Seutloali et al., 2016; Dube et al., 2017). Soil erosion described as a geomorphic process (Lal, 2001)) occur more frequently on shale or dolerite soils (Weaver, 1991), as these rocks develop fine-grained soils once weathered. Additionally, the presence of unconsolidated sediments that are high in silt (colluvial and alluvial sediments) coincides with most of the areas of gully erosion across the world (Botha et al., 1994; Watson, 1997 and Garland et al., 2000), as these sediments generally have higher run-off rates (due to lower permeability) and can easily detach. Sheet erosion, head-cut advance and land sliding suppose major stress factors on vulnerable lands in mountain ranges and other areas in the world (Beguería, 2006). Human activities like land clearing, deforestation, overgrazing, or on the other hand, land abandonment can accelerate the natural rates of these processes, leading to land degradation.

There is a balance between soil erosion and soil formation (Vrieling, 2007) but in many locations, an imbalance currently exists between the two processes. At the global scale, alluvial soil erosion is the most important land degradation problem (Eswaran et al., 2001). Given the unclear nature of soil erosion occurrence, up-to-date information on eroded and potential risky areas is critical for decisions making and implementing preventive measures.

2.3. Available soil erosion modeling techniques

In addressing the soil erosion problems, researchers have since applied various techniques namely; empirical, conceptual and physically based models (Lal, 1994; and Hudson, 1995; Merritt et al., 2003). Empirical models are based on observation/experiment, so it reflects observed facts and helps predict what will happen in the future. The models use a database of set conditions, making them applicable to those conditions. On the other hand, conceptual models had better represent reality, by incorporating the underlying transfer mechanisms of sediment and runoff generation in their structure, representing flow paths in a catchment as a series of storages (Merritt et al., 2003). However, Tesfamichael (2004) states that it is important that each region have a model that matches its own condition and database since there is no universally true model with any given conditions. Conceptual models play an intermediary role between empirical and physically based models. Whilst they tend to be aggregated, they still reflect the hypotheses about the processes governing the system behavior. This is the main feature that

distinguishes conceptual models from empirical models (Beck, 1987). According to Renschler (1996), conceptual models tend to include a general description of catchment processes, without including the specific details of process interactions, which would require detailed catchment information. This allows these models to provide an indication of the qualitative and quantitative effects of land use changes, without requiring a large amount of spatially and temporally distributed input data (Merritt et al., 2003). Empirical models are generally the simplest of these model types. They are based primarily on defining important factors through field observation, measurement, experimentation and statistical techniques relating erosion factors to soil loss (Petter, 1992). In addition, the models are frequently used when compared to more complex models, as they can be implemented in situations with limited data and parameters input (Merritt et al., 2003). The Universal Soil Loss Equation (USLE) and its revised version Revised Universal Soil Loss Equation (Wischmeier and Smith, 1978) are the most widely used and accepted empirical soil erosion models. They were developed for sheet and rill erosion based on a large set of experimental data from agricultural plots. Yet, the equation was derived on single agricultural plots and is only valid when applied to an area up to one hectare (Jahun et al., 2015). Being the most widely used equation in erosion prediction, the USLE still has limitations and weaknesses. In its original form, the model does not provide spatial information on soil erosion distribution; however, this limitation is overcome when integrated with GIS techniques (Fistikoglu and Harmancioglu, 2002).

On the other hand, physically based models are based on the knowledge of the fundamental erosion processes; and incorporate the law of mass conservation and energy (Bennett, 1974). In theory, the parameters used in physical-based models are measurable and therefore known (Merritt et al., 2003). In practice, a large number of parameters involved and the heterogeneity of important characteristics, particularly in catchments, means that these parameters must often be calibrated against observed data (Beck, 1987). Physically based models amongst others include; Soil and Water Assessment Tool (SWAT), Erosion Model for Mediterranean regions (SEMMED) (De Jong et al., 1999) and the Water Erosion Prediction Project (WEPP) (Flanagan and Laflen, 1997). For instance, WEPP has been tested and applied in different geographic locations, across the United States (Huang et al., 1996; Laflen et al., 2004) in Australia

(Rosewell, 2001) and in the United Kingdom (Brazier et al., 2000). However, the application of WEPP in the African context is lacking.

A major limitation in modeling soil erosion in any given area is the restriction in the understanding of the processes involved, particularly in terms of the spatial distribution of soil erosion to those processes and causes (e.g. Croke and Mockler, 2001). Previous assessments of the quality and quantity of soil erosion models show that, in general, the Spatial aspect and patterns of erosion are poorly predicted (Jetten et al., 2003; Merritt et al., 2003). Furthermore, models can rarely be relied upon to give accurate predictions of absolute amounts of soil erosion. Without adequate input data and calibration, models can only be expected to give a relative ranking of the effects of land management (Garen et al., 1999). Input data preparation is a difficult task and the mechanics of operating the models is sometimes complicated (Jetten et al., 2003). The large part of the effort goes into the construction of the input data set, often derived from a few basic variables that are available as raw data. The main limitation of soil erosion models is the fact that they rely on the small-scale application (Nigel and Rughooputh, 2010). Additionally, these models are generally expensive and time-consuming and standard equipment is hardly available. Regardless of these limitations, several studies (Morgan, 2005; Le Roux et al., 2008; Seutloali et al., 2016; Dube et al., 2017) have identified the applications of satellite remote sensing sensor as the way forward to address this kind of environmental problems.

2.4. Satellite remote sensing of soil erosion

Despite the limitation of cost and time consuming of other soil erosion models, remote sensing techniques can map erosion with less expert data, time and cost, and provide the suitable quantitative information necessary for assessing and monitoring the levels of soil erosion. Satellite remote sensing based modeling as both the empirical and physical-based approaches (Shoko et al., 2016), was used and acknowledged by researchers, which widely applied it on land degradation aspect (Bocco and Valenzuela, 1988; Dwivedi et al., 1997; Kiusi and Meadows, 2006). As further highlighted by Seutloali et al. (2016), the increased recognition of remote sensing technologies is associated with its unique strength as it offers a significant potential for a timely, affordable and robust method for investigating soil erosion at a larger spatial scale, particularly in environments where intensive field methods remain a challenge. Recent studies have been made at providing a quantitative estimate of soil erosion (Tanser and Palmer, 1999;

Wessels et al., 2004, 2007; Bai and Dent, 2007; Thompson et al., 2009; Bennett et al., 2012). Table 2.1 provide detailed information on several studies that have utilized remote sensing approaches for estimating soil erosion and their analytical techniques.

Efforts have been put into studying land cover and land-use change (Sobrino and Raissouni, 2000) focusing mainly on vegetation and other ecological parameters, without further going into deep details of environmental problems, such as soil erosion. However, the number of studies decreases (Luleva et al., 2012), when it comes to direct assessment of soil loss and degradation. By using satellite imagery, it is possible to observe only the surface soil characteristics and only when the signal is not covered by the vegetation cover (Vrieling, 2006). According to Luleva et al. (2012) the most commonly used remotely sensed data in soil erosion monitoring come from Landsat data imagery. In developing a map of highly eroded areas in a mountain catchment, Beguería (2006), discriminated soil erosion on bare soil from resistant rock outcrops. To achieve this, he used a supervised classification procedure (multinomial logistic model) over three Landsat thematic mapper (TM) at different months and different datasets. The ability of multi-temporal data (integration of images from different seasons) for discriminating soil erosion features was tested, and compared to the use of single images (Beguería, 2006). Dhakal et al. (2002). Jensen (2005) further highlighted that Landsat TM has a higher spectral resolution of seven bands (two additional mid-IR) making it better suited for mapping eroded landscapes. These seven different bands of Landsat TM record energy in the visible, reflective-infrared, middle-infrared, and thermal infrared regions of the electromagnetic spectrum and are appropriate for mapping soil erosion and peripheral vegetation mapping (Jensen, 2005). Dhakal et al. (2002) found that the visible bands (Red, Green, and Blue) were effective in detecting eroded areas resulting from an extreme rainfall event.

Hochschild et al. (2003) used Landsat 5 TM image of 1996 in their assessment of soil erosion in Mbuluzi river catchment (Kingdom of Swaziland). The study mapped existing erosion types and extents by creating a negative correlation between the erosion levels and the percentage of vegetation cover. Furthermore, Hochschild et al. (2003) outlined soil erosion types ranging from slight rill to deep gullies of which rill to inter-rill erosion and deep linear erosion (gully erosion) are predominant in the Mbuluzi catchment using Landsat satellite data. In Nsikazi, Mpumalanga Province of South Africa, Wentzel (2002) used Indian Remote Sensing satellite (IRS) to derive

bare soil index for likely soil erosion mapping. Randall (1993) delineated gully and sheet erosion areas using Landsat TM images in Olifants River catchment, South Africa to find that gullies could be mapped more accurately. Correspondingly, Liggitt (1988) used remotely sensed data to assess soil erosion in Mfolozi. Liggitt (1988) interpreted orthophotos and aerial photographs taken at different times and scales to estimate the spatial extent of gullies and sheet erosion. The results of this study confirm the importance of geological type on soil erosion, despite the overriding influence of climate and vegetation on soil formation, which has led to similar soil types being distributed over diverse geological formations. Khan and Islam (2003), identified a great deal of riverside retreat, using spatio-temporal analysis of various data sets reveals that very high rates of erosion can occur over periods of 1 year or a few years. However, the same patterns of erosion are not sustained for many years at the same location and they do not occur at all locations simultaneously.

Even though Landsat data is taking over in soil erosion modeling, it is therefore encouraged to compare its effectiveness with other remote sensing datasets. Dwivedi et al. (1997) also found that SPOT image improved the classification of eroded lands than Landsat TM; however, not all the TM bands were utilized in this study. Although SPOT image has proven better at mapping eroded areas, it's a low spectral sampling (4 bands) has proven to be a limitation in mapping gullies (Servenay and Prat, 2003). Servenay and Pratt (2003) found that SPOT was unable to identify outcropping eroded areas even though they had unique spectral signatures. While there is an insufficient amount of literature on SPOT and Landsat TM comparison for mapping of gullies, it can be recognized that spatial resolution and higher spectral resolution Landsat TM may prove to be better at mapping gullies overall because of the spectral sampling capabilities of the sensor (Luleva et al., 2012).

In the past, visual interpretation of aerial photographs together with coarse satellite imagery was applied for mapping gully erosion. Clearly, the combination of both may be the optimal approach. Fadul et al. (1999) monitored and mapped gully erosion over a small area and time, using a dataset of multi-date of aerial photographs data together with Landsat images. The study by Fadul et al. (1999) aimed at to understanding the effects of the environment on gully formation by estimating the rate of annual loss of arable land caused by gully erosion. The results showed that the traditional rainfed agriculture has accelerated gully erosion in the semi-

arid rather than in the arid zone. The progressive rate of gully erosion in the semi-arid zone resulted in the loss of arable land at about 13.4 km² year⁻¹ and 9.8 km² year⁻¹ in the periods 1985–1987 and 1987–1990, correspondingly. Similarly, Fulajtar (2001) utilized high spatial resolution SPOT PAN Image to detect soil erosion patterns and obtained best results in comparison to conventional field survey mapping methods. Recently, Seutloali et al. (2016) assessed and mapped the severity of soil erosion based on soil erosion levels and related to topographic variables (i.e. slope, stream power index and Topographic wetness index). The study identified thresholds of soil erosion classes ranging from sheet erosion to deep gully erosion. For classification and determination of vegetation indices, the study used the 30 m Landsat multispectral satellite data in the former South African homelands of Transkei to map their severity thereof (Seutloali et al., 2016).

Although higher spatial resolution imagery, such as SPOT 5, IKONOS, and Quikbird offer a high-quality data for potential use in erosion mapping (Taruvunga, 2009), their utility remains hindered. Such high-resolution data (IKONOS and QuickBird) are very expensive to acquire for mapping erosion in a large area (Vrieling et al., 2008) and may not be affordable for developing countries. Furthermore, they have low spectral sampling capabilities. More recently, remote sensing has opened new views on inventory, characterization, and monitoring of degraded lands (Tesfamichael, 2004). The value of remote sensing along with GIS for mapping any landscape attribute, such as soil degradation is clear enough, but most of the studies were conducted at a small scale as highlighted in Table 2.1 below. Le Roux (2007) recommended that the remote sensing approaches to soil erosion modeling have to be applied or expanded to a regional scale. Table 2.2 illustrates the sensors used in remote sensing of soil erosion, as well as their cost. Therefore, there is no other techniques offer the promises of spatially exhaustive, objective and repeated measurements at a cost comparable to satellite remote sensing.

Table 2.1 Summary of remote sensing applications in soil erosion mapping Adopted from

Study/Applications	Sensor (s) used	Pixel size	No. of bands	Scale of application	Results	Reference
mapping the spatial distribution of soil erosion in the study area using three Landsat-derived VIs	Landsat8 OLI and SPOT6 /7	30m	Blue, green, red, and NIR Landsat8	Local Municipality	kappa statistical results of 0.64 for SAVI, 0.60 for NDVI, 0.59 for SARVI 0.60	Kwanele and Njoya, (2017)
Assessing and mapping the severity of soil erosion	Landsat TM5	30m	Blue, green, red, and NIR	Local municipality	19.89 percent of Sheet in 1984 and 0.69 percent of Deep gully in 2010	Seutloali, et al., (2016)
Gully Mapping using Remote Sensing	Landsat (TM) SPOT (HRG) and SPOT (Pan)	30m	Blue, green, red, and NIR	Buffalo River (Buffels) sub-catchment	NDVI=0.1, SAVI=0.08, TSAVI=0.45	Taruvinga, (2008)
Identifying erosion areas at basin scale using remote sensing data and GIS	Landsat TM/ETM+	30m	Blue, green, red, and NIR	Catchment of the Yesa reservoir	0.02 AUR.	Beguería, (2006)
Gully erosion mapping using object-based and pixel-based image classification methods	IRS-P6	23.5m IRS-P6 and a Panchromatic band of 5.8m	Blue, green, red, and NIR bands	Local catchment	OBIA kappa coefficient of 0.82, PBC kappa coefficient (0.62)	Karami et al., (2015)
Delineation of erosion classes in semi-arid grasslands	Landsat-TM5	25m.	Red, and NIR bands	Local catchment	small erosion factor, C-factor 0– 0.1 gullies, C-factor > 0.4	Hochschild et al., (2003)

Matongera, et al., (2016).

Table 2.2 Remote sensing sensor specifications and cost in soil erosion

Sensor	Spectral bands	Spatial resolution (m)		Swath-width (Km)	Revisit time (days)	Cost of image acquisition (US \$/km ²)
Landsat Thematic Mapper (TM)	7	30 120	Band (1-5 and 7) Band 6	185	26	Free
Landsat Enhanced Thematic Mapper plus (ETM+)	8	30 15	Band (1-7) Band 8	185	18	Free
Landsat Operation Land Imager (OLI)	9	30 120	Band (1-9)	185	16	Free
Moderate Resolution Imaging Spectrometer (MODIS)	36	250 500 1000	Band (1-2) Band (3-7) Band (8-36)	2330	1-2	Free
RapidEye	5	5	All bands	77	1 (off nadir) / 5.5 (nadir)	US \$1.28
Système Pour l'Observation de la Terre 5 (SPOT 5), High-Resolution Stereoscopic (HRS), High-Resolution Geometric (HRG) and Vegetation (VGT)	5	10 20	Band (1-3) Band 4	60	2.5	US \$5.15
Quickbird	5	2.40 0.60	All multispectral bands Panchromatic band	16.8	1-3.5	US \$24
World View-2	8	2 0.46	All multispectral bands Panchromatic band	16.4	1.1	US \$28.5
World View-3	8	1.24 0.31	All multispectral bands Panchromatic band	13.1	1	US \$29
Indian Remote Sensing Satellite (IRS-P6)	4		Band (2-5)	23.9-740	5	US \$20

2.5. Soil erosion classification strategies: Strength and limitations

Classification algorithms can be parametric or non-parametric. Both require user input, in the form of training data, to guide the image processing software through the classification. Parametric algorithms use parameters, such as mean and variance-covariance matrices for each of the classes to determine its decision boundary between classes; whereas non-parametric algorithms do not make any assumptions about the distribution of the data used (Tsfamichael, 2004). Identification and mapping of soil erosion features have been performed by the classification algorithms in the extraction of digital information based on spectral and/or structural pattern recognition (Alatorre and Beguería, 2009). Several approaches to classification exist, for example, supervised, unsupervised or hybrid (combination of supervised and unsupervised classifications) methods (Vrieling, 2006). These classification methods are normally in hand with mathematical algorithms which include: Interactive Self-Organizing Data Analysis Technique (ISODATA), Maximum Likelihood Classification (MLC), Support Vector Machines (SVM), Fuzzy set classification logic and Mahalanobis distance classifier (MDC). Classifiers based on statistical probability functions commonly use the spectral signature of a single pixel (pixel-based classifiers) and spatial context around a pixel to aid in its classification (object-based classifiers).

Unsupervised classification (e.g. ISODATA algorithm) is normally carried out to gain an idea about spectral variability. In this method, the separation of clusters of pixels is carried out based on statistically similar spectral response patterns, to gain information categories by determining classes that are spectrally different, and then define their information value (Lillesand and Kiefer, 1994). Many studies created maps for preliminary assessment using unsupervised classification (Naseer and Puneet, 2017). Even though it does not require much of human attention to have knowledge of the classes, the ability to come up with correct land classes becomes the weakness when mapping soil erosions.

Unlike unsupervised classifiers, the supervised classification allows image analyzers to use specific pixels (training sites) to specify the various pixel values that should be associated with each class. The most commonly used classification method is based on MLC; a per-pixel based classification (Taruvunga, 2008). Floras and Sgouras (1999) used the MLC of Landsat TM imagery to separate soil erosion classes. The Gaussian maximum likelihood classifier had an

overall accuracy of 83.94% in identifying and mapping land cover, sloping and eroded areas (Floras and Sgouras, 1999). Bocco and Valenzuela (1988) applied the similar classifier for multispectral Landsat TM and SPOT HRV images to distinguish between several erosion and vegetation classes. They found that the higher resolution SPOT data achieved better in classifying eroded areas. Metternicht and Zinck (1998) performed a maximum likelihood classification on Landsat TM, and also on the combination of Landsat TM with JERS-1 SAR data, and the combination yielded highest classification accuracy. This approach of classification has limitations in resolving complex classes that are not normally distributed. Since erosion levels and their surrounding areas are spectrally complex, application of this traditional parametric algorithm may be challenging for soil erosion mapping. MDC is similar to MLC, however, its decision boundaries assume all class covariances are equal (Richards and Jia, 2006) and simply measures the maximum distance of an unknown pixel as opposed to MLC which calculates the probability density function of each class.

Literature has given particular attention to the SVM approach, which was tested to produce higher classification accuracies (Gualtieri et al., 1999). SVM classifiers have been applied to multi-spectral remote sensing data (Hermes et al., 1999; Roli and Fumera, 2001; Huang et al., 2002). SVM classifiers represent a promising non-parametric classification method for identifying soil erosion from other land cover types (Taruvunga, 2008). SVM's potential lies in its ability to separate classes by locating a hyperplane that maximizes the distance from the members of each class to the optimal hyperplane. There is a lack of information on the parameters used and the level of accuracy obtained from using SVM for one-class classifications. SVM has been used for forest fire detection and urban area extraction in SPOT 5 satellite imagery (Lafarge et al., 2005). The focus of their study was on the kernel parameters based on textual information and radiometric information, and their ability to separate in one case forest smoke and in other urban areas. Furthermore, Congcong et al. (2014) they compared SVM with other algorithm using Landsat TM and come up with 88.5% accuracy.

For the validity and reliability of the results based on the classification of soil erosion maps, accuracy assessment has to be performed for each class. Furthermore, accuracy assessment is done to validate the classification using ground reference data collected using tools such as global position system (GPS) (Mhangara, 2011). The Kappa Analysis technique is widely used

in remote sensing for accuracy assessments as a powerful method used to measure the agreement between predicted and observed phenomena (Jenness and Wynnes, 2005). Assessment of classification accuracy is controlled with the help of error matrix reference test pixel data (Mustafa et al., 2012). In comparing object-based image analysis (OBIA) and pixel-based image classification (PBC) Karami et al. (2015) used multi-spectral data sets of an Indian Remote Sensing Satellite (IRS-P6) for mapping gully erosion features. Karami et al. (2015) utilized IRS-P6 in mapping gullies in the local catchment of Lamerd Township in the southwestern region of Iran. The results showed OBIA at model 6 reached an overall accuracy of 89.6% and a kappa coefficient of 82%, which was the highest among all models. The most accurate PBC model was supervised model 2, which had an overall accuracy (82%) and kappa coefficient (62%) but was significantly lower than that of model 6.

2.6. Spectral characteristics and vegetation Indices for mapping soil erosion

Besides classification techniques, there is a direct relationship between soil and spectral reflectance, which allows the detection of disturbed soil and the mapping of its spatial occurrence (Price, 1993). Thus, the complexity of mapping soil erosion from its levels of the formation such as sheets, rills or gullies using remote sensing satellite data lies in their spectral differences (King et al., 2005). Therefore, it is important to understand the spectral response and reflectance of the erosion features characteristics, and whether the levels of erosion are to be mapped as a discrete feature in a landscape using remote sensing. The bare soil spectral signature of levels of erosion is influenced by mineral composition, soil texture, moisture and organic matter (Irons et al., 1989; Barnes and Baker, 2000; Sujatha et al., 2000).

In addition to the spectral reflectance of soils, the spectral separability of other surface features, such as vegetation cover, built-up areas, cultivated lands, water bodies etc. also contribute to the spectral distinction of the eroded soil due to that vegetation and cultivated lands has more complex spectral properties than soil (De Asis and Omasa, 2007). The spectral response of the characteristics in the near-IR makes it easy to distinguish vegetation from a non-living feature. A study made by Price (1993), there is a correlation between reflectance values of single Landsat TM bands, especially band 4 (NIR), and erosion rates. In supporting this findings Pickup and Nelson (1984) successfully distinguished eroding, stable, and depositional areas using the

satellite data defined by the 4/6 and 5/6 band ratios of Landsat MSS imagery (corresponding to green/NIR and red/NIR respectively) for arid rangelands in Australia.

Vegetation indices (VIs) derived from satellite images are one of the primary remote sensing approaches for obtaining information about the Earth's surfaces reflectance and have been used as a simple and quick feature extraction technique for soil erosion mapping (Singh et al., 2004; King et al., 2005). VIs, in particular, have gained recognition in soil erosion research (Mathieu et al., 1997; Singh et al., 2004). Normalized Difference Vegetation Index (NDVI), since its initiation by Rouse et al. (1973), it has been used quite widely in soil erosion related research (Vaidyanathan et al., 2002; Taruvinga, 2008; Seutloali et al., 2016; Kwanele and Njoya, 2017). Moreover, various modifications have been proposed to address the sensitivity of NDVI to non-vegetation factors (Lawrence and Ripple, 1998; Kwanele and Njoya, 2017). The Soil Adjusted Vegetation Index (SAVI) proposed by Huete (1988), and Soil and Atmospherically Resistant Vegetation Index (SARVI) developed by Huete and Liu (1994) are amongst the most widely used modifications of NDVI in soil erosion research (Kwanele and Njoya, 2017). In mapping, the spatial distribution of soil erosion Kwanele and Njoya (2017) used the three Landsat-derived VIs (NDVI, SAVI, and SARVI,) and they assess the accuracy of VI derived soil erosion maps and determined the best VI for detecting soil erosion features at a catchment level. In the discussion of their results, SAVI-derived erosion map yielded good results across all levels of accuracy, including the PA and UA of 77.5% and 79.5% for the erosion class, respectively, together with kappa statistical results of 64%.

NDVI can easily be derived from data acquired by a variety of satellites and low-value thresholds can be selected to extract eroded areas (Mathieu et al., 1997; Vaidyanathan et al., 2002; Thiam, 2003; Symeonakis and Drake, 2004). Using SPOT imagery, Mathieu et al. (1997) mapped gully erosion in northern France by calculating NDVI and doing a maximum similarity with a brightness index and masking out vegetation, limestone outcrops, and built-up areas. Thiam (2003) also used NDVI to produce a three-class (low, moderate, and high) land degradation risk map using multi-temporal NOAA/AVHRR and averaged NDVI values to specific soil types which allowed for the evaluation of the spatial extent of land degradation risk in southern Mauritius. Symeonakis and Drake (2004) used NDVI as an indicator of vegetation cover to determine areas of desertification over sub-Saharan Africa, using AVHRR. Using

imagery from the Indian satellite sensor IRS-1B LISS-II, Vaidyanathan et al. (2002) used NDVI thresholds to identify classes for an erosion intensity map in Garhwal. This technique allowed the separation of four different classes, namely: snow, vegetation, barren and water (Vaidyanathan et al., 2002). However, the extensive use of NDVI has also presented significant weaknesses. Govaerts and Verhulst (2010) noted that satellite-based NDVI results are subject to interference by non-vegetation factors including, but not limited to atmospheric conditions and soil background. One of the weakness to NDVI is that it is sensitive to the effects of soil brightness, soil color, atmosphere, cloud and cloud shadow, and leaf canopy shadow and requires remote sensing calibration (Xue and Su, 2017).

VI's are developed to minimize the effect of soil, such as the SAVI which had been attempted to improve the detection of erosion features, in open vegetated areas (Botha and Fouche, 2000) and TSAVI (Hochschild et al., 2003). SAVI was originally developed using ground-based data, but it was later found useful in minimizing soil background effects using satellite imagery (Jackson and Huete, 1991). SAVI has been used in land degradation studies in southern Africa (Botha and Fouche, 2000). Using Landsat TM and MSS, Botha (2000) used SAVI to detect land degradation change whereas Dang et al. (2003) used Landsat ETM to calculate SAVI for a soil erosion model for Miyun County in China. SAVI and TSAVI are based on the assumption that bare soil reflectance lies on a single line in the feature space of the red and NIR bands (soil line) (Baret et al., 1993). The red and NIR bands have proven to be very useful for identifying soil erosion through the use of the 'soil line' concept (Mathieu et al., 1997) which is a linear relationship between bare soil reflectance observed in the red and near-IR bands (Richardson and Wiegand, 1977).

Satellite image-derived NDVI, SAVI, and SARVI are considered mainly because they are some of the simplest, cheapest, and quickest feature extraction techniques (Singh et al., 2004; Gandhi et al., 2015; Alhawiti and Mitsova, 2016; Sonawane and Bhagat, 2017) that can be used to map soil erosion events. Soil erosion is a dynamic process requiring constant monitoring while keeping up-to-date information on its spatial distribution. Besides the discussed Vegetation related parameters in soil erosion mapping, other parameters have been investigated such includes; Topography, Soil moisture, Chemical properties of soils etc. for the assessment of remote sensing of soil erosion. Luleva et al. (2012) summarized parameters regarding gaps and

opportunities in the use of remote sensing for soil erosion assessment of which they include; Modified Temperature - Vegetation Dryness Index (MTVDI) (Kimura, 2007), Normalized Difference Water Index (NDWI) (Dasgupta et al., 2007), Leaf Area Index (LAI) and Land Surface Temperature (LST), Normalized Soil Moisture Index (NSMI) (Haubrock et al., 2008).

2.7. Remote sensing recommendations for soil erosion mapping

Application of remote sensing to natural resources inventory has become fundamental for natural resources management as it is deemed environmental friendly (Lillesand and Kiefer, 1994). The remote sensing approach is the only practical method for mapping soil erosion features because of the large area and complexity of the size, shape, and occurrence of the eroded features (Knight et al., 2007). So far, the most commonly used remotely sensed data in soil erosion modeling is the Landsat series data dating back to 1972. Availability and low cost of the images scenes allow long-term monitoring of the affected areas. The main benefit of Landsat sensor is the multi-temporal aspect (de Jonget al., 1999), although the low spectral resolution of the sensor presents a serious limitation. Soil erosion parameters estimated from this imagery, are limited to the assessments of vegetation cover, outlining of bare surfaces, calculation of vegetation indices and rarely, changes in topography (Alatorre and Beguería (2009). It is, however, important to note that information provided by such remote sensors is limited to the mapping of surface characteristics that cannot be linked to soil erosion except through inference techniques (Vrieling, 2006). Monitoring visible signs of degradation, such as sheets, rills or gullies, as well as physical deteriorations, such as crusting, hard setting, and compaction, total erosion can be estimated over time is hindered by sensor resolution (Boardman, 2006; Omuto and Shrestha, 2007).

However, the newly launched Landsat 8 sensor has improved spectral and radiometric characteristics making it suitable for both regional and local soil erosion mapping (Pickup and Nelson, 1984; Dwivedi et al., 1997; and Dhakal et al., 2002). The previous Landsat TM series provided higher spectral resolution of seven bands (two additional mid IR) better suited for eroded landscapes and these bands record energy in the visible, reflective-infrared, middle-infrared, and thermal infrared regions of the electromagnetic spectrum and are appropriate for erosion and peripheral vegetation mapping (Dhakal et al., 2002; Jensen, 2005). Dhakal (2002) found that the visible bands were effective in detecting eroded areas resulting from an extreme

event. The SPOT series satellites provide a higher spatial resolution sensors called High Resolution Visible (HRV) and High Resolution Visible and Infrared (HRVIR), which are capable of measuring reflected radiance in three bands at a spatial resolution of 20 m, and have proven better at distinguishing eroded areas compared to Landsat TM observations (Bocco and Valenzuela, 1988; Dwivedi et al., 1997). Although important, these sensors cannot be used to detect and map erosion fine characteristics such as rills or sheet erosion.

Furthermore, the literature shows that satellites such as SPOT-5, and QuickBird offer high-quality data for potential use in soil erosion mapping (Vrieling, 2006); but even these have their limitations in soil erosion studies. Such high-resolution data (IKONOS and QuickBird) are very expensive to acquire for mapping erosion in a large area (Vrieling et al., 2008) and may not be affordable for developing countries. Besides, they have low spectral sampling capabilities. Other studies have found the high-resolution IKONOS sensor as offering little advantage over lower resolution air photographs in terms of financial resources as compared to the mapping aspect (Nichol et al., 2006). SPOT 5 is more affordable than IKONOS and QuickBird and has already been acquired for many studies (Lu and Weng, 2007) but its low spectral resolution, limits its application in soil erosion monitoring due to limited spectral observations. However, the recent introduction of the freely and readily available Sentinel 2 sensor by the European Space Agency, with an average spatial resolution of 10 m and its 5 day-repeated coverage. This makes it one of the most possible and lucrative alternatives for soil erosion after Landsat series data, especially in developing countries where the acquisition of high resolution sensors remains a daunting task. Its application in vegetation (Shoko et al., 2016; Sibanda et al., 2016), water resources mapping has so far demonstrated its potential in helping solve key environmental as well as ecological questions. There is, therefore, a need for future studies to embrace this new sensor and even comparing its performance with that of Landsat 8 sensor. Although the two sensors have been compared in vegetation and grass biomass estimation (Shoko and Mutanga 2017; Sibanda et al., 2016), the possibility of drawing similar conclusions in soil erosion modeling cannot be confirmed at this stage unless tested. Based on a review of studies that compared the two sensors, one can hypothetically conclude that the two sensors can achieve almost similar results when applied in soil erosion modeling.

2.8. Conclusion

Although many researchers have studied various aspects of soil erosion, the temporal soil degradation paths and landscape developments have received little attention. The current study provides an overview of the progress of remote sensing applications in soil erosion over time and space. Despite many efforts made to quantify the extent of soil erosion, most of the focus was on the small-scale application, such as sub-catchment and municipal levels. Therefore, more detailed and extensive work is required to assess the spatial variability and extent of soil erosion within given regions. Furthermore, the discrimination of soil erosion over different land management practices is required if sustainable and effective soil erosion control, remedial and preventive strategies are to be developed. In developing countries, soil erosion monitoring in most communal areas is largely undocumented and this affects food security in these areas. Therefore, the new crop of sensors, such as Sentinel 2 and Landsat 8 series, with improved spatial, spectral radiometric and temporal resolutions provide the most needed spatial tool for monitoring these areas at low costs.

3. Chapter Three

Understanding the spatial distribution of eroded areas in the former rural homelands of South Africa: Comparative evidence from two new non-commercial multispectral sensors



Source: Google Earth 2018.

This chapter is based on:

Sepuru, T.K., and Dube, T., 2018. Understanding the spatial distribution of eroded areas in the former rural homelands of South Africa: Comparative evidence from two new non-commercial multispectral sensors. *International Journal of Applied Earth Observation and Geoinformation*, 69, pp.119-132.

Abstract

In this study, the most suitable multispectral sensor that can accurately detect and map eroded areas from other land cover types in Sekhukhune rural district, Limpopo Province, South Africa is determined. Specifically, the study tested the ability of multi-date (wet and dry season) Landsat 8 OLI and Sentinel-2 MSI images in detecting and mapping eroded areas. The implementation was done, using a robust non-parametric classification ensemble: Discriminant Analysis (DA). Three sets of analysis were applied (Analysis 1: Spectral bands as independent dataset; Analysis 2: Spectral vegetation indices as independent and Analysis 3: Combined spectral bands and spectral vegetation indices). Overall classification accuracies ranging between 80% to 81.90% for MSI and 75.71% to 80.95% for OLI were derived for the wet and dry season, respectively. The integration of spectral bands and spectral vegetation indices showed that Sentinel-2 (OA = 83, 81%), slightly performed better than Landsat 8, with 82, 86%. The use of bands and vegetation indices as independent dataset resulted in slightly weaker results for both sensors. Sentinel-2 MSI bands located in the NIR (0.785-0.900 μm), red edge (0.698-0.785 μm) and SWIR (1.565-2.280 μm) regions were selected as the most optimal for discriminating degraded soils from other land cover types. However, for Landsat 8 OLI, only the SWIR (1.560-2.300 μm), NIR (0.845-0.885 μm) region were selected as the best regions. Of the eighteen spectral vegetation indices computed, NDVI, SAVI, SAVI, and Global Environmental Monitoring Index (GEMI) were ranked selected as the most suitable for detecting and mapping soil erosion. Additionally, SRTM DEM derived information illustrates that for both sensors eroded areas occur on sites that are 600m and 900m of altitude with similar trends observed in both dry and wet season maps. Findings of this work emphasize the importance of free and readily available new generation sensors in continuous landscape-scale soil erosion monitoring. Besides, such information can help to identify hotspots and potentially vulnerable areas, as well as aid in developing possible control and mitigation measures.

Keywords: mapping accuracy; multispectral sensors; rural areas; soil erosion; subsistence agriculture.

3.1. Introduction

Soil plays a vital role in many economies of the world, particularly in developing countries, such as South Africa, agriculture, and forestry form the backbone of the economy (Department Of Agriculture Forestry and Fisheries, 2015). A review on the outlook of Agriculture in South Africa by the Department of Agriculture, Forestry and Fisheries (2010) shows that agriculture accounts for approximately 15.2% of the country's Gross Domestic Product (GDP). Currently, the sector consisting of 82% (100 million hectares) of the South African land area whereas, in developed countries like Scotland, Europe, 79% of the land area is attributed to agriculture, accounting for 1.8% of the GDP and directly employing over 25,000 people (Scottish Environment Protection Agency, 2001). Despite their economic importance, soils in most developing countries are subject to continuous deterioration due to poor land management practices in place (Ighodaro et al., 2013), leading to severe soil degradation at a phenomenal rate (Pretorius, 1998; Garland et al., 2000; Le Roux, et al., 007). For example, in South Africa over 70% of the land is affected by soil erosion (Le Roux 2007), with an estimated occurrence rate of 8 to 30 times faster than the rate of regeneration (Baade et al., 2012, Seutloali et al., 2016). Human activities like land clearing for farming, deforestation, overgrazing, or land abandonment coupled with climate change, accelerate the rate of land degradation (Alatorre and Beguería, 2009). In addition, the negative effects of land degradation are not limited to agriculture; they extend to other hydraulic structures, including reservoir sedimentation, which is associated with water treatment costs. This complicates water availability, which is already a problem, especially in the developing world of Africa. For example, South Africa alone losses approximately two billion rands annually including off-site costs for purification of water whose poor quality is caused by the siltation of dams in eroded surfaces rehabilitation (Department of Environmental Affairs and Tourism, 2006). Whereas, other countries like Malawi and Kenya lost about US\$2 billion and US\$11 billion between 2001-2009 periods from land degradation, respectively (Kirui and Mirzabaev, 2015; Voortman 2003; Nkonya et al., 2013). Additionally, Dube et al., (2017) indicated that pressure, due to these processes, has caused serious implications on rural economies; as most of them rely on agriculture as a source of living. Therefore, the need for reliable information on degraded areas and possible vulnerable areas has increased in order to understand the level of degradation and to come up with possible control measures. It is thus important to provide an accurate and update, as well as detailed soil erosion maps for the former

homelands of South Africa as baseline information for monitoring, rehabilitation and control purposes.

Soil erosion, which is considered to be the most critical environmental problems leading to land degradation (Seutloali et al., 2016, Le Roux et al., 2007; Le Roux et al., 2008), has put a burden on national economies. Although great strides have been made in land degradation or soil erosion monitoring, the accuracy of the derived thematic maps remains questionable, especially in developing countries, as the availability of high-resolution data remains a challenge (Luleva et al., 2012). The Landsat series data have so far been the most commonly used remotely sensed data in soil erosion modeling and monitoring. For instance, Dube et al., (2017) assessed the potential of using freely available Landsat series in mapping degradation levels in Eastern Cape, South Africa. They found out that degraded areas could be detected from the Landsat series data. Additionally, the main benefit of Landsat sensor is the multi-temporal aspect (de Jong et al., 1999), although the medium spectral resolution of the scenes presents a limitation. In addition, Lo Curzio and Magliulo (2010), by means of Landsat data series assessed the spatial distribution of degraded areas, with a good spatial accuracy of 97,48% Overall Accuracy (OA) and limited cost in southern Italy. Moreover, Seutloali et al., (2016) mapped the severity of soil erosion, using the 30m Landsat multispectral satellite data in the former South African homelands of Transkei and the results of the study have indicated that a variety of soil erosion levels (i.e. sheet, slight rills, deep rills, medium gullies to deep gullies) could be detected and mapped.

Even though Landsat data is viewed and appraised as the most reliable and appropriate dataset for soil erosion modeling, especially when compared with other multispectral sensors, such as MODIS or AVHRR that are provided at coarse spatial resolution, its applications remain largely restricted. This dataset's associated slightly poor spatial resolution largely compromises its fullness in erosion-related studies, especially where farm or catchment level monitoring is required. For example, fine-scale erosional problems remain difficult to document from Landsat ETM+7 which has since experienced scanline errors resulting in approximately 22% data loss. Most studies that have tested the utility of historical Landsat archival data concluded that the sensor has an outstanding performance in mapping soil erosion at a larger scale. However, the performance of Landsat ETM+7 remains compromised for farm level monitoring, due to 22% data loss from the scanline errors.

The newly launched Landsat 8 unlike its predecessors, has been highly rated in most of its applications and these include biomass mapping (Yavaşlı, 2016; Zhang et al., 2017), land surface temperature mapping (Adeyeria, 2017; Avdan and Jovanovska, 2016), and invasive species mapping (Gavier-Pizarro, et al., 2012; Wang et al., 2017). For instance, studies by Vågen et al., (2013) demonstrated that land degradation and soil health in Ethiopia at scales appropriate for management can be assessed, using Landsat-8 bands. Most of the studies associated the successful performance of the sensor to its improved sensing characteristics (Wulder et al., 2008). Landsat 8 OLI also occupies a unique spatial-temporal position in the sense that its bands can better detect and monitor human changes in land cover, whereas at the same time having an imaging footprint that is sufficiently large to enable wide-area applications (Wulder et al., 2012). Given the sensor's recommended performance we, therefore, assume its improved sensing characteristics can aid in determining and mapping, as well as monitoring eroded areas in the former homelands of South Africa – a previous challenging task with broadband sensors like MODIS.

Similar to Landsat 8, Sentinel-2 MSI (Multi-Spectral Instrument) data available at 10m spatial resolution is considered as one of the most possible solutions to most environmental related challenges in sub-Saharan African, due to its free availability, global footprint, high temporal resolution (± 5 days), and presence of new multiple bands. These has previously missing from the previous batch of broadband multispectral sensors, such as ASTER, Landsat 4, 5 and 7, MODIS etc. Studies that have used sentinel 2, for instance in forest mapping, Korhonen et al. (2017) indicated that the sensor's addition red edge (RE1, RE2, RE3) spectral bands have the capability to improve the accuracy of estimating key plant biophysical variables. They have also shown that the sensor provides the most unique and robust datasets required for understanding environmental problems. For example, Korhonen et al. (2017) have shown that the specific information content of a batch of the broadband multispectral Sentinel-2 sensor may be useful in the monitoring of canopy properties.

Testing the ability of this free-and-readily available remotely sensed datasets in soil erosion monitoring is, therefore critical. So far, the rich information contained in these sensors has not yet been fully exploited in mapping and monitoring eroded areas. This is primarily due to the fact that these sensors were launched recently. Among the different types of the readily-available

multispectral remote sensing sensors, archive digital dataset with a wider swath-width (185-km Landsat 8 OLI; 290 km Sentinel-2 MSI) and a 16 (OLI) and 5 (MSI) day temporal resolution. This makes the two sensors to be perceived as the key primary data sources highly suitable for providing practical or operational regional or district level analysis of eroded areas. This study for the first time sought to assess soil erosion mapping abilities of two new non-commercial multispectral remote sensing data: Landsat 8 OLI and Sentinel-2 MSI in the Sekhukhune district, Limpopo Province of South Africa. To determine the most optimal bands and vegetation indices that can accurately detect and map soil erosion regardless of form. Further, the study wanted to determine whether the areas identified as degraded in the dry season could be as well be detected during the wet season or it was a dry season phenomenon associated with the non-cropping. The study also establishes if the observed soil erosion patterns are a function of elevation or land use.

3.2. Materials and Methods

3.2.1. Field data collection

The field survey was conducted from the 26th to 28th of June 2017, coinciding with the dates of remotely sensed data acquired for the study area. Data collection was done by recording coordinates at sub-meter accuracy using GPS device, to validate satellite remote sensing data. Eroded areas were identified during field surveys using random walks and google earth maps of the area. A similar approach was used in collecting data on other major land cover classes in the area, and these included built-up areas, cultivated areas, eroded areas forest-woodland, and grass-shrubland, vegetation covers and water bodies. Land cover classes were identified using visual observation. The vector maps of the study, courtesy of Sekhukhune District together with the aid of google earth were used to navigate to areas affected within the study area. During the field operation, a total of 300 (50 per class) points were recorded, using a Trimble GeoXH 6000 series handheld Global Position System (GPS) at sub-meter accuracy. These GPS points were used in extracting spectral data from the two satellite data sets. Furthermore, photographs of eroded areas and other land cover types were taken, using a handheld camera. During the collection of photographs, GPS coordinates were also recorded and these were used to verify the classified maps.

3.2.2. Remote sensing data acquisition and pre-processing

Landsat-8 and Sentinel-2 satellite images were used in mapping eroded areas across two seasons (dry and wet season) in the Greater Sekhukhune District Municipality (Table 3.1). Landsat-8 acquires global moderate-resolution measurements of the Earth's surface in the visible, near-infrared, shortwave, and thermal infrared. The sensor was launched on the 11th of February 2013, with a combination of two push broom instruments: The Operational Land Imager (OLI) consisting of nine spectral bands (refer to Table 3.1) and (ii) the Thermal Infrared Sensor (TIRS) which encompasses thermal bands 10 and 11 at a 100 m spatial resolution. Sentinel-2 mission, launched on the 23rd of June 2015, is a land monitoring constellation of two satellites (Sentinel-2a and Sentinel-2b) providing global optical imagery with 13 spectral bands at a 5-day interval, using MSI (Multispectral Imager) instrument.

In this study, cloudless Landsat 8 OLI and Sentinel 2 MSI images were acquired respectively during the 1st of June 2017 and 31st July 2017 for the dry season and between 1st of December 2016 and 31st January 2017 accessed from the USGS Earth Resources Observation and Science (EROS) Centre archive (<http://earthexplorer.usgs.gov/>). Subsequently, the images were re-projected and mosaicked. Both images were atmospherically corrected, using the dark object subtraction (DOS1) model in QGIS version 2.1.8 software.

Table 3.1 Landsat 8 OLI and Sentinel-2 MSI spectral characteristics used in this study

Landsat 8 OLI spectral bands			Sentinel-2 multispectral bands		
Band#	Bandwidth (um)	GSD (m)	Band#	Bandwidth (um)	GSD (m)
1 (Ultra Blue (coastal aerosol))	0.43-0.45	30	1 (costal aerosol)	0.433-0.453	60
2 (Blue)	0.450-0.515	30	2 (blue)	0.458-0.52	10
3 (Green)	0.525-0.600	30	3 (green)	0.543-0.578	10
4 (Red)	0.630-0.680	30	4 (red)	0.650-0.698	10
5 (NIR)	0.845-0.885	30	5 (vegetation red edge)	0.698-0.713	20
6 (SWIR)	1.560-1.660	30	6 (vegetation red edge)	0.733-0.748	20
7 (SWIR)	2.100-2.300	30	7 (vegetation red edge)	0.765-0.785	20
8 (Panchromatic)	0.500-0.680	15	8 (NIR)	0.785-0.900	10
9 (Cirrus)	1.36-1.38	30	8a (vegetation red edge)	0.855-0.815	20
10 (TIRS)	10.60-11.19	100	9 (water vapour)	0.930-0.950	60
11 (TIRS)	11.50-12051	100	10 (SWIR-Cirrus)	1.365-1.385	60
			11 (SWIR)	1.565-1.655	20
			12 (SWIR)	2.100-2.280	20

*Bold represents the bands used in this study

3.2.3. Digital Elevation Model data

The Shuttle Radar Topography Mission (SRTM)-derived digital elevation model (DEM) was used to generate information on the elevation of the area and this data was used to determine whether the occurrence eroded areas can be explained as a function elevation (slope). This study used SRTM DEM because of its higher spatial resolution (30 m/pixel) corresponding to that of the two sensors and accessibility. The DEM was converted to meters (m) and the elevation of the area under study ranged between 495 m and 2101m. DEM preprocessing was done using ArcGIS tools 10.4.1 software.

3.2.4. Landsat 8 OLI and Sentinel-2 derived spectral data and vegetation indices

Spectral reflectance values (Table 3.2) along with selected simple spectral band ratios were applied in this study. The choice of vegetation indices was based on their performance as demonstrated from previous studies (Vaidyanathan et al., 2002; Taruvinga, 2009; Singh, et al., 2004) were retrieved from Landsat-8 OLI and Sentinel-2 data sets. The spectral reflectance was extracted from the images, using points collected during field surveys. The extraction was done, using the Hawth's spatial analysis tool embedded in ArcGIS 10.4.1 software. Eighteen vegetation

indices were computed (Table 3.2). The indices were selected based on their successful application in the classification and analysis of degraded surface mapping from the highlights made by previous studies and remotely sensed variables for validation (Seutloali et al., 2016; Kwanele and Njoya, 2017; King et al., 2005).

Table 3.2 Selected spectral vegetation indices derived from Landsat-8 OLI and Sentinel-2 images applied in the validation of eroded surface mapping

Parameters	Computation	Reference
Normalized Difference Vegetation Index (NDVI)	$\frac{\text{NIR} - \text{RED}}{\text{NIR} + \text{RED}}$	Rouse <i>et al.</i> , (1974)
Soil Adjusted Vegetation Index (SAVI)	$\frac{(\text{NIR} - \text{RED})}{\text{NIR} + \text{RED} + 0.5} * (0.5 + 1)$	(Huete, 1988)
Simple Ratio Index (SRI)	$\frac{\text{NIR}}{\text{RED}}$	(Rouse <i>et al.</i> , 1974)
Ratio Vegetation Index (RVI)	$\frac{\text{RED}}{\text{NIR}}$	(Richardson and Wiegand, 1977)
Transformed Vegetation Index (TVI)	$\sqrt{\frac{\text{NIR} - \text{RED}}{\text{NIR} + \text{RED}} + 0.5}$	(Deering <i>et al.</i> , 1975)
Modified Soil-adjusted Vegetation Index (MSAVI) ²	$((2*(\text{NIR}+1)) - (((2*\text{NIR}+1)^2 - 8(\text{NIR}-\text{RED}))^{0.5}))*0.5$	(Qi <i>et al.</i> , 1994)
Enhanced Vegetation Index (EVI)	$\frac{\text{NIR} - \text{RED}}{\text{NIR} + 6 * \text{RED} - 7.5 * \text{BLUE} + 1}$	Huete, (1999)
Normalized Difference Water Index (NDWI)	$\frac{(\text{GREEN} - \text{NIR})}{(\text{GREEN} + \text{NIR})}$	(McFeeters, 1996)
Normalized Difference Water Index (NDWI)	$\frac{(\text{NIR} - \text{SWIR2})}{(\text{NIR} + \text{SWIR2})}$	(Gao, 1996)
Renormalized Difference Index (RDI)	$\frac{(\text{NIR} * 1 - \text{RED})}{(\text{NIR} * 1 + \text{RED})^{0.5}}$	(Roujean and Breon, 1995)
Normalized Ratio Vegetation Index (NRVI)	$\frac{\left(\frac{\text{RED}}{\text{NIR}} - 1\right)}{\left(\frac{\text{RED}}{\text{NIR}} + 1\right)}$	(Baret and Guyot 1991)
Visible Atmospherically Resistant Index (VARI)	$\frac{(\text{GREEN} - \text{RED})}{(\text{GREEN} + \text{RED} - \text{BLUE})}$	(Gitelson <i>et al.</i> , 2002)

Visible Green Index (VGI)	$\frac{(\text{GREEN} - \text{RED})}{(\text{GREEN} + \text{RED})}$	(Gitelson <i>et al.</i> , 2002)
Green Difference Index (GNDVI)	$\frac{(\text{NIR} - \text{GREEN})}{(\text{NIR} + \text{GREEN})}$	(Gitelson <i>et al.</i> , 1996)
Global Environmental Monitoring Index (GEMI)	$\left(\frac{[2(\text{NIR}^2 - \text{RED}^2) + 1.5\text{NIR} + 0.5\text{RED}]}{(\text{NIR} + \text{RED} + 0.5)} \right) * \left(\frac{(1 - 0.25 \left(\frac{[2(\text{NIR}^2 - \text{RED}^2) + 1.5\text{NIR} + 0.5\text{RED}]}{(\text{NIR} + \text{RED} + 0.5)} \right)) - (\text{RED} - 0.125)}{(1 - \text{RED})} \right)$	(Pinty and Verstraete, 1992)
Pigment Specific Ratio (Chlorophyll b) (PSSRb)	$\frac{\text{NIR} * 1}{\text{RED}}$	(Blackburn, 1998)
Green Index (GI)	$\frac{\text{NIR}}{\text{GREEN}} - 1$	Gitelson <i>et al.</i> , 2005)
Red Index (RI)	$\frac{\text{NIR}}{\text{RED}} - 1$	Gitelson <i>et al.</i> , 2005)

3.2.5. Statistical data analysis

One-way analysis of variance (ANOVA) was used to test whether there were significant differences between the mean reflectance of the six identified classes. Also, the variable ranking was performed to test the significant performance ($\alpha = 0.05$) of spectral indices. These six classes we tested for a significant difference ($\alpha = 0.05$) using reflected multivariate extracted values. The variable ranking was performed to identify the optimal spectral indices that can detect and discriminate eroded areas from other land cover types. To map eroded areas, three stages of analysis (presented in Table 3.3) were implemented based on the two sets of variables (bands and indices) derived from the two sensors.

Table 3.3 Adopted soil erosion analysis approach

Analysis stage	Data type	Data source	Details
1	Image spectral information (ISI)	Landsat 8	6 bands (blue, green, red, NIR, SWIR I & II)
		Sentinel-2 MSI	10 bands (2 (blue, green, red vegetation red edge (I,II & III), NIR, vegetation red edge, SWIR(I & II)
2	Spectral indices (SIs)	OLI	18 Indices (NDVI, SAVI, SRI, RVI, TVI, MSAVI, EVI, NDWI 1, NDWI 2, RDI, NRVI, VARI, VGI, GNDVI, GEMI, PSSRb, GI, RI)
		MSI	18 indices (NDVI, SAVI, SRI, RVI, TVI, MSAVI, EVI, NDWI 1, NDWI 2, RDI, NRVI, VARI, VGI, GNDVI, GEMI, PSSRb, GI, RI)
3	ISI + SIs	OLI	(6 bands) + (18 indices)
		MSI	(10 bands) + (18 indices)

3.2.6. Image Classification and Accuracy assessment

The Discriminant Analysis (DA) classification ensemble was used to discriminate eroded lands from other land cover types. DA is a nonparametric classification ensemble, which searches for a linear combination that best discriminates amongst land cover types (Sibanda et al., 2015). Sibanda et al., (2015) and Dube et al., (2017), indicated that this non-parametric classification, converts the reflectance data of land covers at each waveband into several components that account for the difference in reflectance amongst the land cover types. The DA algorithm assumes that the samples are random (Dube et al., 2017), which is the case with land management unit's samples that were used, hence appropriate for this kind of study. This algorithm provides cross-validated results with variable scores (Eigenvalues) that indicated the strength of a specific function in discriminating eroded surfaces under different land management units.

Eigenvectors also knew as variable scores were produced by DA and used to evaluate the relative contribution of each waveband and vegetation indices to the DA function that optimally discriminated eroded surfaces under different management practices. The DA algorithm applies the Box test (Chi-square asymptotic approximation), Box test (Fisher's F asymptotic approximation), Mahalanobis distances, Wilks's Lambda test (Rao's approximation), and

Kullback's test to test whether within-class covariance matrices were equal. These tests exhibited significant classification power ($P < 0.05$). The classification was conducted using XLSTAT for Microsoft Excel 2013 software and confusion matrices were derived. In each confusion matrix, the columns represented the test data, while the rows represented the classes to which each sample was allocated to by the DA classifier.

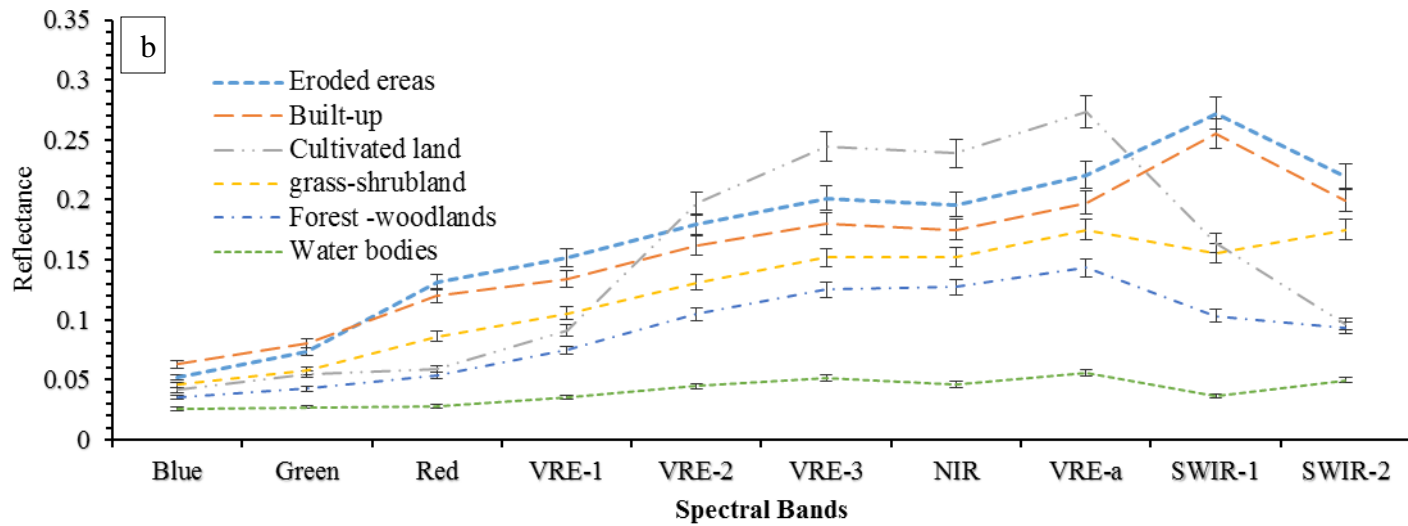
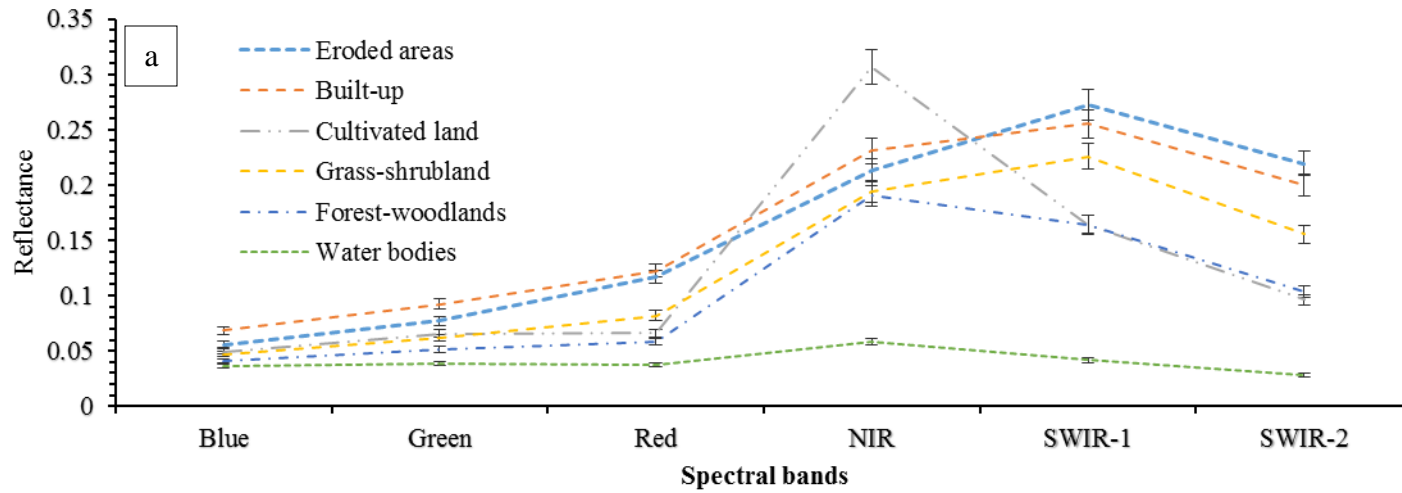
To assess the classification accuracy of the results, quantity disagreement, and allocation disagreement was used following its best application from Sibanda et al., (2016) as a way of separating data into training tested data also recommended by Pontius Jr. and Millones, (2011) as the successor of Kapa Statistic. Quantity disagreement is a sum of least perfect matches between the training (70%) and the testing (30%) reflectance datasets of each land management practice. Precisely, the quantity disagreement follows when the column total of a management practice class deviates from the row total of that class in a confusion matrix. To estimate the extent of the difference between Landsat 8 OLI data accuracy and that of Sentinel-2 MSI agreement between classification results and ground truth data was measured using the producer accuracy (PA), user accuracy (UA) and overall accuracy (OA) generated from the confusion matrices. These two parameters were used in accuracy assessment, as suggested by Pontius Jr. and Millones, (2011).

3.3. Results

3.3.1. Discrimination of eroded areas from other land cover types

Figure 3.1 shows the differences amongst averaged spectral bands values or curves of eroded areas and other land cover types for the wet and dry seasons. ANOVA results reveal significant differences ($p < 0.05$), which implies eroded areas can be discriminated from other land cover types. It can be observed that sentinel-2 MSI could optimally discriminate eroded areas from other land cover types, using bands located in the NIR (0.785-0.900 μm), and red edge (0.698-0.785 μm) and SWIR (1.565-2.280 μm) regions for both dry and wet season (Figure 3.1, b & d). Similarly, Landsat 8 OLI illustrated the ability of SWIR (1.560-2.300 μm) region, followed by NIR (0.845-0.885 μm) region to optimal in discriminate eroded areas eroded areas. However, the visible regions (from 0.433-0.578 μm) from both sensors show close or inseparable reflectance curves, which implies weaker discrimination capabilities for both dry and wet season. But the visible (0.450-0.680 μm) region of Landsat 8 still became worse than that of Sentinel-2. Moreover, it can be observed that when using Landsat 8 OLI data, eroded areas could be

discriminated from the built-up and grass-shrublands in the SWIR region, when compared with the red and green region of the visible range on the electromagnetic (EM) spectrum. However, when using Sentinel 2 MSI data, more eroded areas were discriminated from the built-up and grass-shrublands in the red edge region as compared with the SWIR region in the wet season than dry season. When using Landsat 8 OLI data, the dry season shows that most of the eroded areas were discriminated from the woodland-forest in the SWIR region of the EM spectrum but there were some overlaps in the visible region and NIR of EM spectrum (Figure.3.1). On the other hand, when using Sentinel 2 MSI, most of the woodland-forest unit was differentiated from the eroded areas in the SWIR, VRE, NIR and visible (red, green) regions of the EM spectrum except for the blue region of the spectrum (Figure. 3.1).



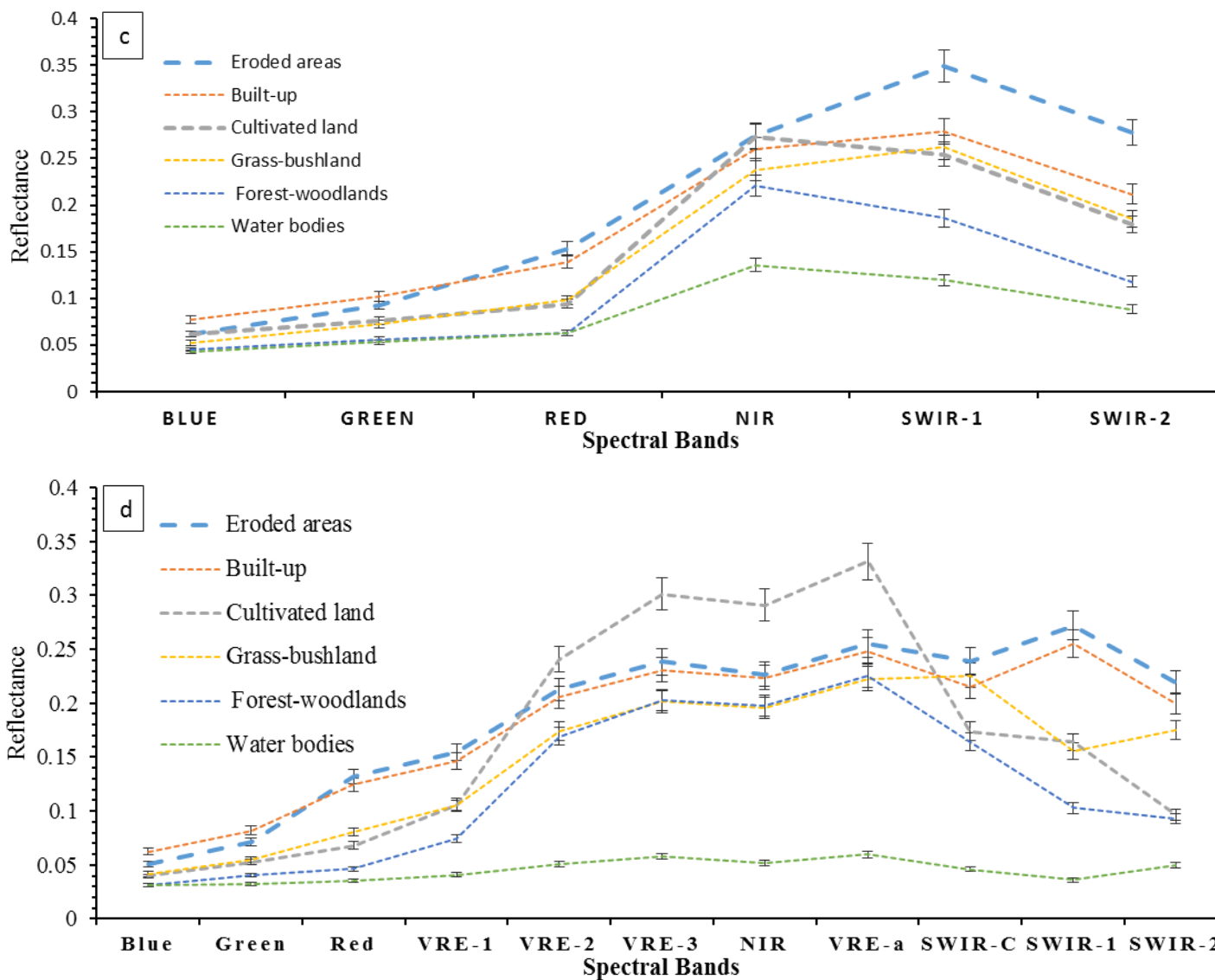


Figure 3.1 Average reflectance of eroded areas in relation to other land cover types derived using Landsat 8 OLI (b. dry season and c, wet season) Sentinel-2 MSI (a dry season and d. wet season) (error bars: signify the level of separability)

3.3.2. Spectral indices performance

Variable ranking ($P < 0.05$) was performed and of eighteen spectral indices used, results reveal that Landsat 8 derived NDVI and SAVI had the highest ranking in discriminating eroded areas from other land cover types. Using Sentinel-2, SAVI and GEMI had the highest ranking.

3.3.3. Image classification

3.3.3.1. Analysis 1: Soil erosion classification using spectral bands as an independent dataset

Table 4 illustrates overall classification accuracies derived from Landsat 8 OLI and Sentinel 2 as an independent data set for two seasons (dry and wet seasons). The results indicated that the spectral reflectance information of Landsat 8 OLI alone produced slightly good classification results, with an overall accuracy (OA) of 80.95% over Sentinel-2 in the dry season but Sentinel outperformed Landsat 8 with ± 0.48 OA in the wet season. The results showed the superiority of Landsat 8 over Sentinel-2 in the dry season by achieving an overall classification accuracy of ± 80 while Sentinel performed better in the wet season (Table 3.4). Both sensors yielded good user and producer accuracies of above 50% in all land cover types of the study area for both dry and wet season. In agreement to this, eroded areas had user accuracy (UA) of 79.31%, using Sentinel-2, higher than that of Landsat 8 (magnitude of 5.63%) in the dry season (Figure, 3.2). In the wet season, eroded areas specifically produced UA of 76% (Sentinel) and 66% using Landsat 8. Over the six classes, better soil erosion PA and UA were achieved from both sensors for the dry season data, whereas in the wet season, a UA of 96.30% using Landsat 8 OLI.

3.3.3.2. Analysis 2: Soil erosion mapping classification using vegetation indices as an independent data.

For the dry season, Landsat 8 OLI derived vegetation indices performed slightly less in detecting and mapping eroded areas with an OA of 75.71%. On the other hand, Sentinel-2 derived spectral indices had a considerably high OA of 81.90% (Table 3.4). For the wet season, derived vegetation indices performed slightly less in detecting and mapping eroded areas with an OA of less than 75.71% when compared with the dry season. When compared to classification results based on spectral bands (analysis I), the OA decreased by $\pm 5.24\%$ for Landsat 8 OLI datasets

and increased by $\pm 5.9\%$ for Sentinel-2 MSI datasets in the wet season (Table 3.4). Furthermore, user and producer accuracies for Landsat 8 OLI also slightly decreased with most of the classes ranging from $\pm 2.78\%$ - $\pm 18.92\%$ whereas Sentinel-2 maintained an increase of $\pm 2.58\%$ - $\pm 14.70\%$ in most of the classes (table 3.5). The results attained using Landsat 8 OLI and Sentinel-2 derived vegetation indices separately produced slightly high classification accuracies when compared to the use of spectral bands as an independent dataset. Sentinel-2 achieved better accuracy results than Landsat 8 with user accuracy of 79.31% in validating eroded areas and whilst Landsat 8 OLI scored 78.13% of user accuracy, respectively. The difference with regards to the magnitude of performance using vegetation indices as a separate data set for detecting and mapping eroded areas was $\pm 6.19\%$ between the two sensors. Landsat 8 OLI thus had slightly lower accuracies when compared to the 10-m Sentinel 2 data.

3.3.3.3. Analysis 3: Soil erosion classification using a combination of spectral bands and spectral vegetation indices.

As illustrated in Table 3.4 the combined dataset (i.e. spectral bands and vegetation indices) achieved high classification results, when compared to analysis 1 and analysis 2. For instance, in the dry season using the combined data set, Landsat 8 OLI and Sentinel-2 produced high overall accuracies of 82.86% and 83.81%, respectively. Landsat 8 OLI sensor performed slight less than the Sentinel-2 sensor. Eroded areas were classified as a producer and user accuracy results of about 80% demonstrating an increase of more than 10% for both sensors, particularly in dry season. Furthermore, during the wet season eroded areas were classified with high UA and PA accuracies of $\pm 70\%$ for both the sensors (table 3.4), although less than that of the dry season. The results obtained from combined dataset significantly improved classification accuracies, although Sentinel-2 produced slightly good classification accuracy of 85% when compared Landsat 8. In general, both sensors yielded the best performance in classifying eroded areas based on combined spectral bands and spectral vegetation indices (Figure 3.2).

Table 3.4 Classification accuracies derived using spectral dataset, spectral vegetation dataset as well as a combined dataset

a	LANDSAT 8						SENTINEL 2					
	Analysis 1		Analysis 2		Analysis 3		Analysis 1		Analysis 2		Analysis 3	
	PA	UA	PA	UA	PA	UA	PA	UA	PA	UA	PA	UA
Eroded areas	84.85	73.68	75.76	78.13	78.79	83.87	79.31	79.31	79.31	79.31	86.21	80.65
built-up	63.89	85.19	63.89	74.19	80.56	76.32	53.33	66.67	56.67	77.27	56.67	85.00
cultivated land	76.47	96.30	76.47	86.67	73.53	96.15	83.33	90.91	80.56	85.29	86.11	91.18
Grass-Shrubland	80.56	78.38	77.78	70.00	83.33	81.08	70.59	64.86	85.29	67.44	85.29	65.91
forest-woodland	82.35	66.67	82.35	60.87	88.24	71.43	85.00	77.27	85.00	80.95	87.50	83.33
water bodies	97.30	92.31	78.38	93.55	91.89	94.44	100.00	95.35	97.56	100.00	95.12	100.00
OA	80.95		75.71		82.86		80.00		81.90		83.81	
b	LANDSAT 8						SENTINEL 2					
	Analysis 1		Analysis 2		Analysis 3		Analysis 1		Analysis 2		Analysis 3	
	PA	UA	PA	UA	PA	UA	PA	UA	PA	UA	PA	UA
Eroded areas	78.79	76.47	84.85	80.00	87.88	90.63	68.97	71.43	68.97	64.52	72.41	65.63
Build-up	75.00	81.82	75.00	62.79	88.89	86.49	63.33	61.29	63.33	65.52	60.00	66.67
Cultivated land	32.35	84.62	50.00	80.95	64.71	88.00	69.44	86.21	63.89	76.67	72.22	92.86
Grass-shrubland	90.00	57.69	82.00	65.08	92.00	70.77	55.88	54.29	73.53	52.08	64.71	47.83
Woodland	65.00	76.47	75.00	83.33	75.00	88.24	82.50	71.74	80.00	88.89	82.50	80.49
Water bodies	89.19	94.29	59.46	73.33	89.19	97.06	97.56	97.56	87.80	100.00	87.80	100.00
OA	73.81		71.43		84.29		74.29		73.81		74.29	

(PA= Producer Accuracy, UA= User Accuracy, and OA =Overall Accuracy. a) dry season b) wet season

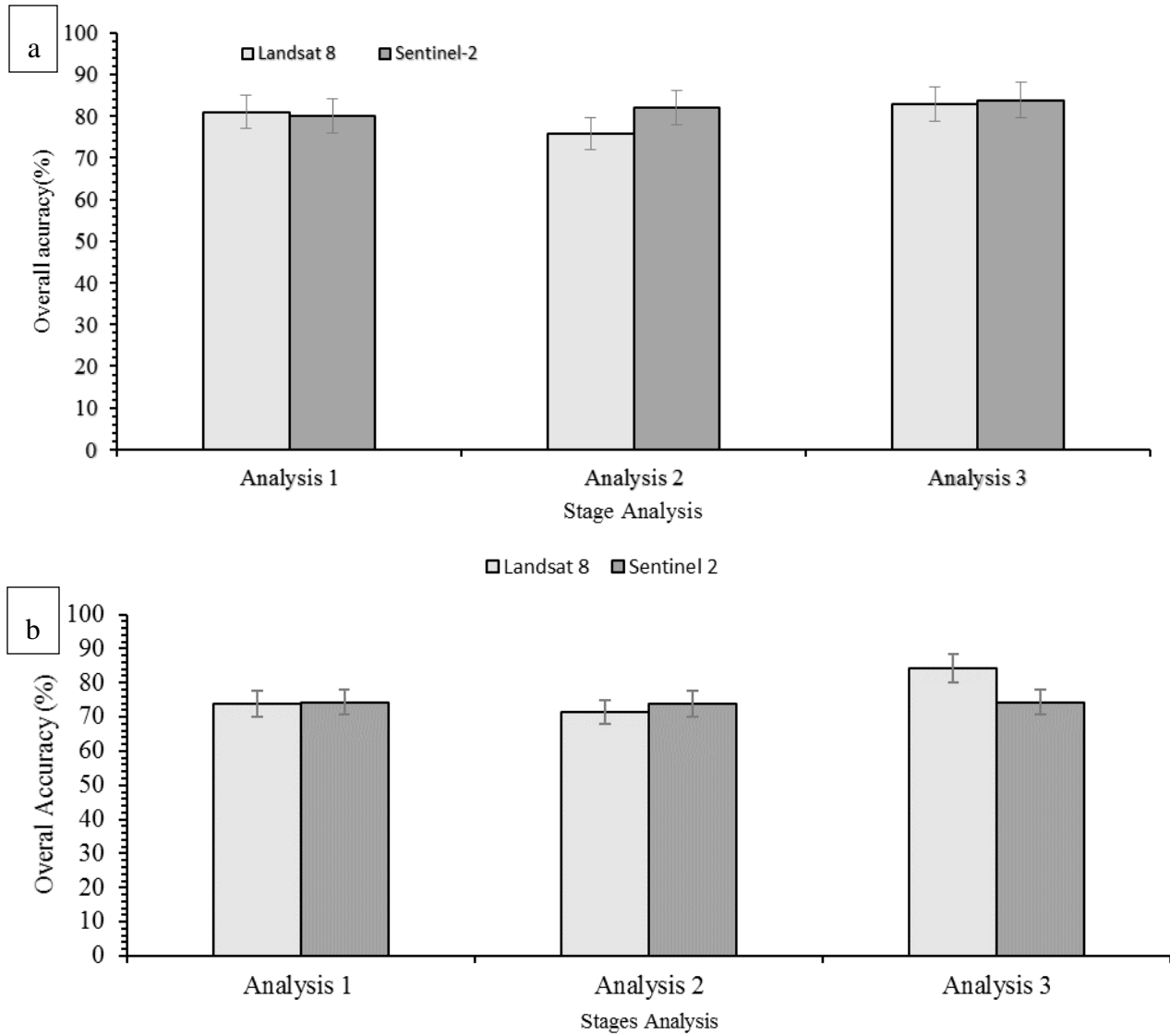


Figure 3.2 Overall classification accuracies for three analysis stages. a) dry season; b) wet season.

Table 3.5 Deviation of classification accuracies between Landsat 8 OLI and Sentinel-2 MSI

	Sensor	Parameter	Overall accuracy	Deviation in terms of accuracy (%)		
				1	2	3
Dry season	Landsat 8 OLI	Image spectral information (ISI)	80.95%	-	+5.24	-1.91
		Spectral indices (SIs)	75.71%	-5.24	-	-7.15
		ISI + SIs	82.86%	+1.91	+7.15	-
	Sentinel-2 MSI	Image spectral information (ISI)	80.00%	-	-1.9	-3.81
		Spectral indices (SIs)	81.90%	+1.9	-	-1.91
		ISI + SIs	83.81%	+3.81	+1.91	-
Wet season	Landsat 8 OLI	Image spectral information (ISI)	73.81	-	+2.38	-10.48
		Spectral indices (SIs)	71.43	-2.38	-	-12.86
		ISI + SIs	84.29	+10.48	+12.86	-
	Sentinel-2 MSI	Image spectral information (ISI)	74.29	-	+0.48	-
		Spectral indices (SIs)	73.81	-0.48	-	-0.48
		ISI + SIs	74.29	-	+0.48	-

3.3.3.4. Derived soil erosion maps

Figure 3.3 shows the derived maps of the eroded areas. Overall it can be observed that both Landsat 8 and Sentinel-2 sensors have depicted a similar pattern in the distribution of eroded areas and the trend is identical across the wet and dry seasons. The derived maps indicate that the central part of Sekhukhune is more eroded when compared to other areas. However, comparatively, Landsat 8 (Figure 3.3 a and c) demonstrate high levels of erosion when compared to Sentinel 2 (Figure 3.3 b and d). For instance, Figure 3.4 demonstrates the area in percentage of each classified land cover class in comparison of the two sensors. Landsat 8 showed that most classes are more than 5% when compared to Sentinel-2 in dry season while with more than 6% in a wet season (Figure 3.4).

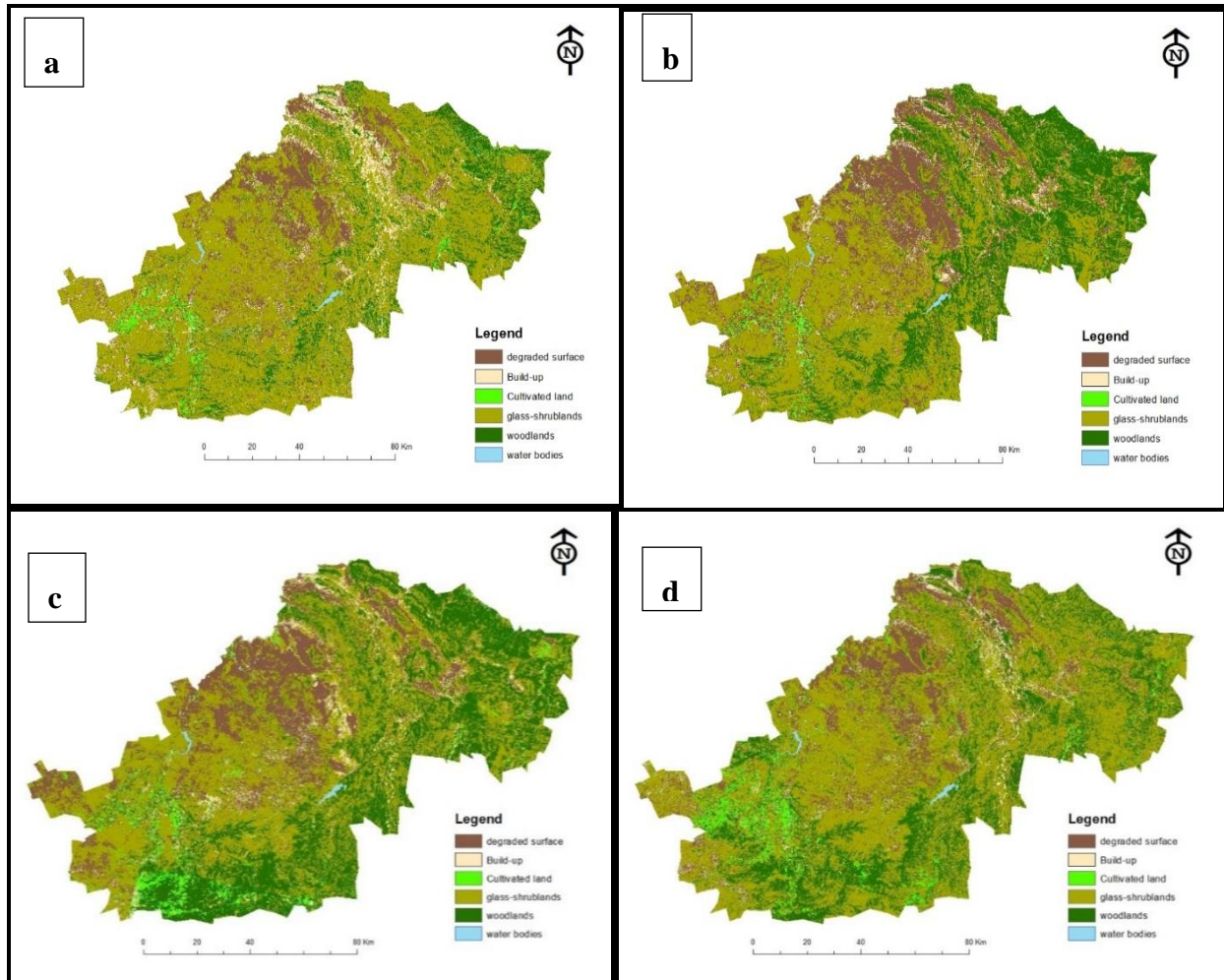


Figure 3.3 Classified land cover maps derived from Landsat 8 OLI (a. dry and c wet seasons) and Sentinel-2 MSI (b. dry and d. wet season).

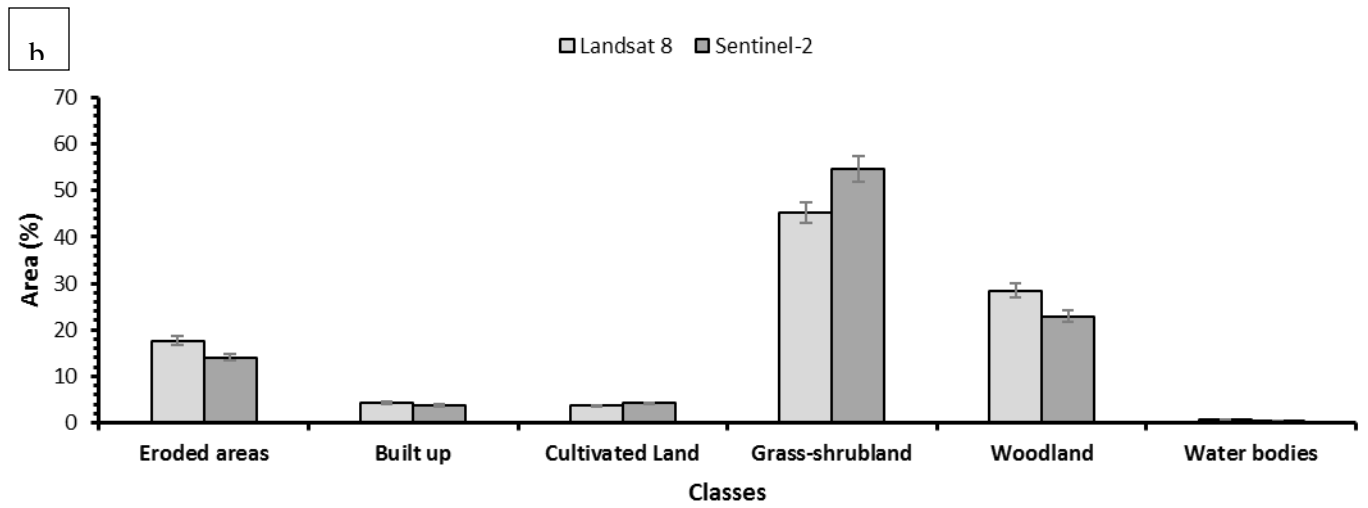


Figure 3.4 Derived area per land cover class. a). dry season; b). wet season

Figure 3.5 illustrates eroded areas as detected by the two sensors. Figure 3.5 further shows the zoomed areas for clear visualization of the eroded areas. Extensive levels of eroded areas can be observed in Fig. 3.5 (a) to (f). It can be observed that the majority of the land disturbances through erosion are concentrated along villages and agricultural fields. Figure 3.6 as it also compares the two sensors; it can be perceived that sentinel-2 managed to detect eroded surfaces than Landsat 8 from the classified images. Moreover, it can be observed that the major disturbances in Sekhukhune are mainly related to croplands. Figure 3.6 (b) shows evidence of disturbed areas along agricultural farms. In addition, photographs were taken during field, observation indicates that some of the eroded surfaces are detected along villages (figure 3.7 b and d). From the observation, it is noticed that some of the eroded surfaces were detected along mines as one anthropogenic activity (figure 3.7 (d) and figure 7 (c)) and also some of the open areas like abandoned croplands appear to experience severe erosion.

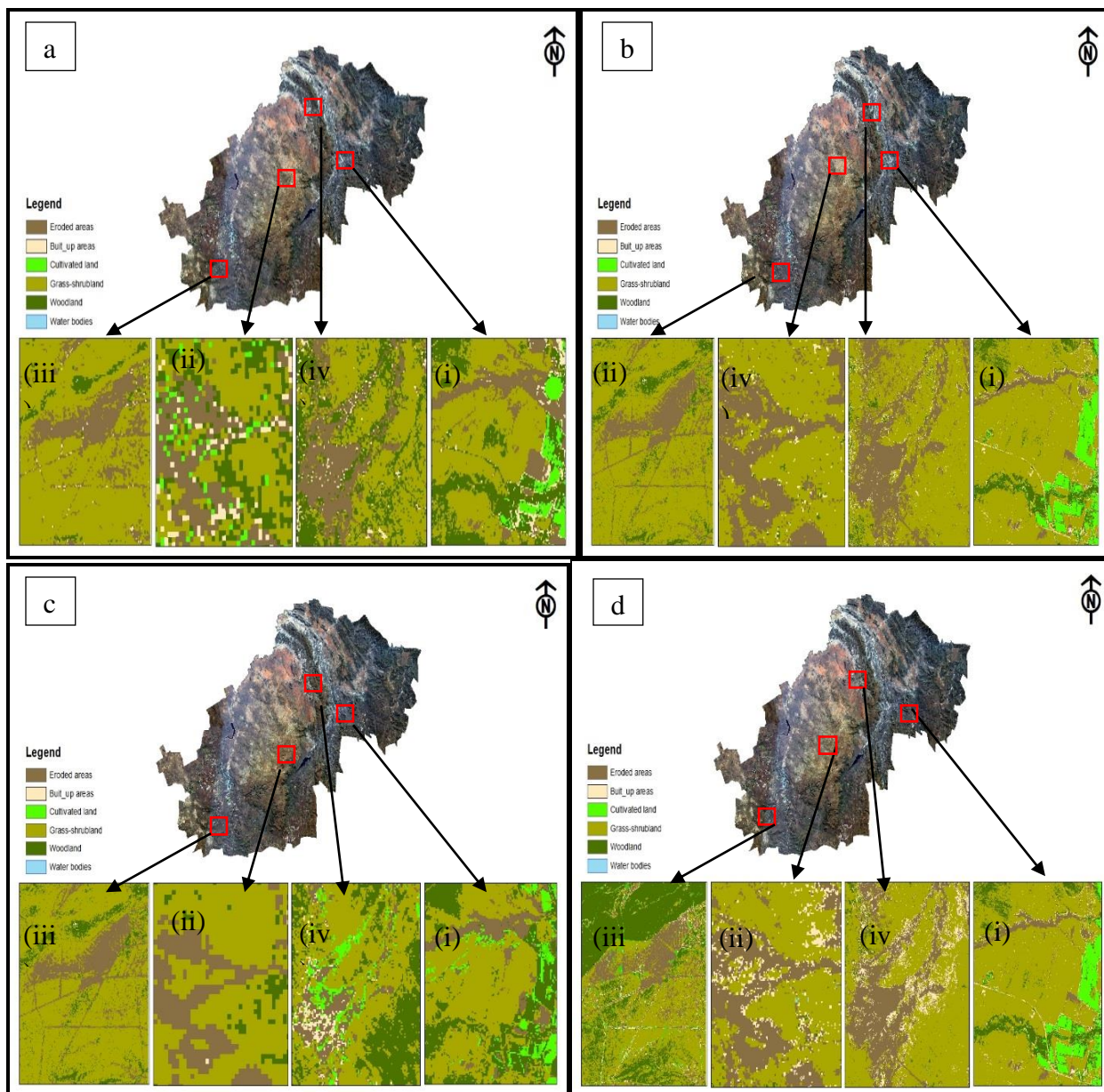


Figure 3.5 Zoomed maps showing eroded areas from classified land cover maps using Landsat 8 OLI (a dry & c wet seasons) and Sentinel-2 MSI (b dry & d wet seasons).

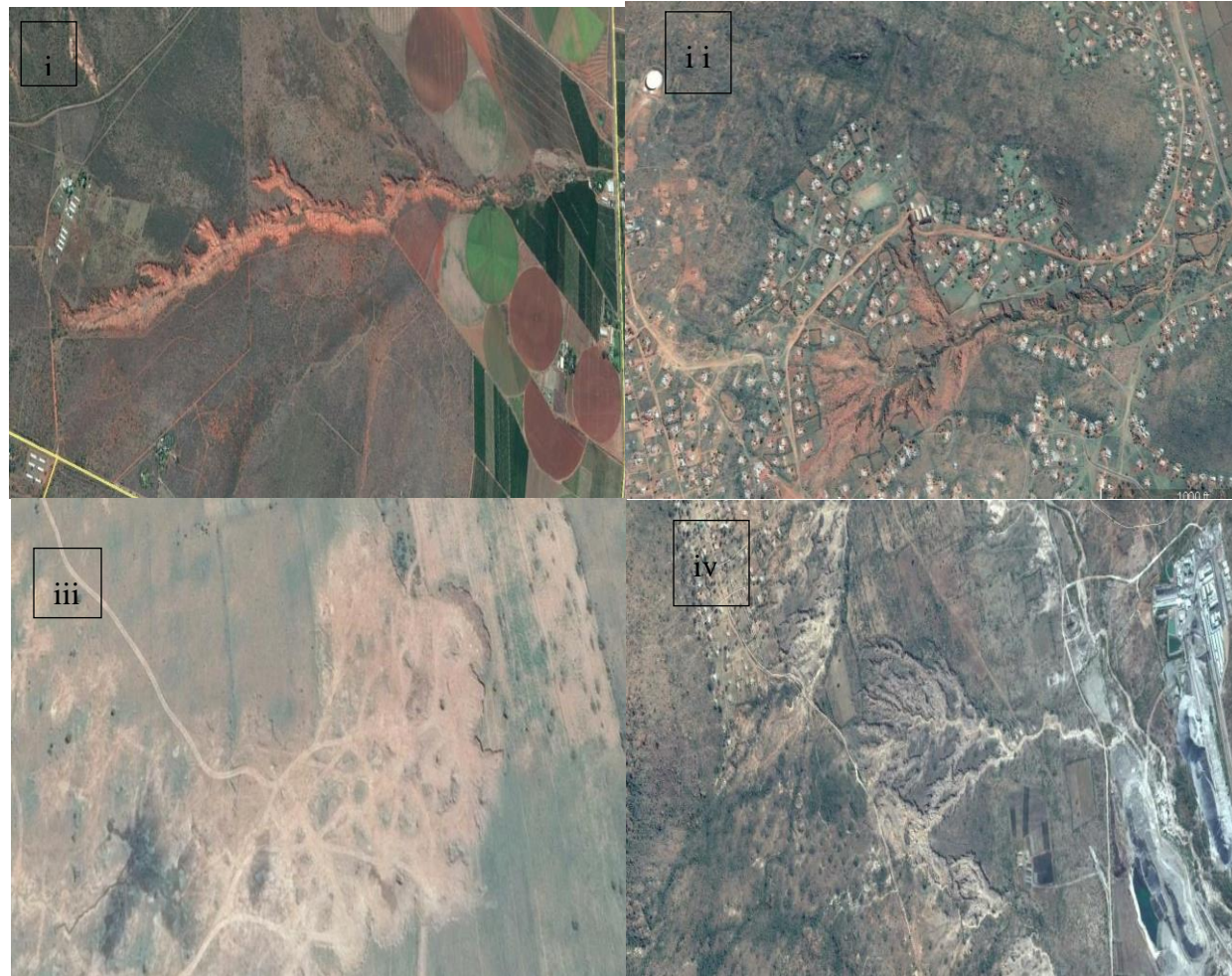


Figure 3.6 Google earth images showing eroded areas in abandoned fields in the former homelands, Sekhukhune, South Africa. (i) Illustrate gully detected in along agricultural field, around steelpoort town (ii) eroded surface emerging within the villages of Jane Furse (iii) rill forming overabundant substance farms in Mphenama areas and (iv) illustrates erosion imaging from the road of Atok mine.



Figure 3.7 Photographs showing eroded areas taken in the former homelands, Sekhukhune, South Africa. (a) S open eroded areas in abandoned agriculture fields (b) eroded surface imaging all the villages of Jane Furse (c) illustrate a gully forming from a mine waste system channel and (d) illustrate eroded surface within Jane Furse village.

3.3.3.5. The relationship between eroded areas and elevation

Derived erosion layers were extracted and overlaid on the elevation map (Figure 3.8). It can be observed that much of the area between 600m and 900m exhibited high levels of erosion when compared to low-lying and mountainous areas (Figure 3.9). From the map, it can as well be noted that high proportions of eroded areas occurred in areas with an elevation between 600 and 1500m. Moreover, areas in the extremes (495m to 600 and 1800m to 2101m) areas show less rate of soil erosion (figure 3.9).

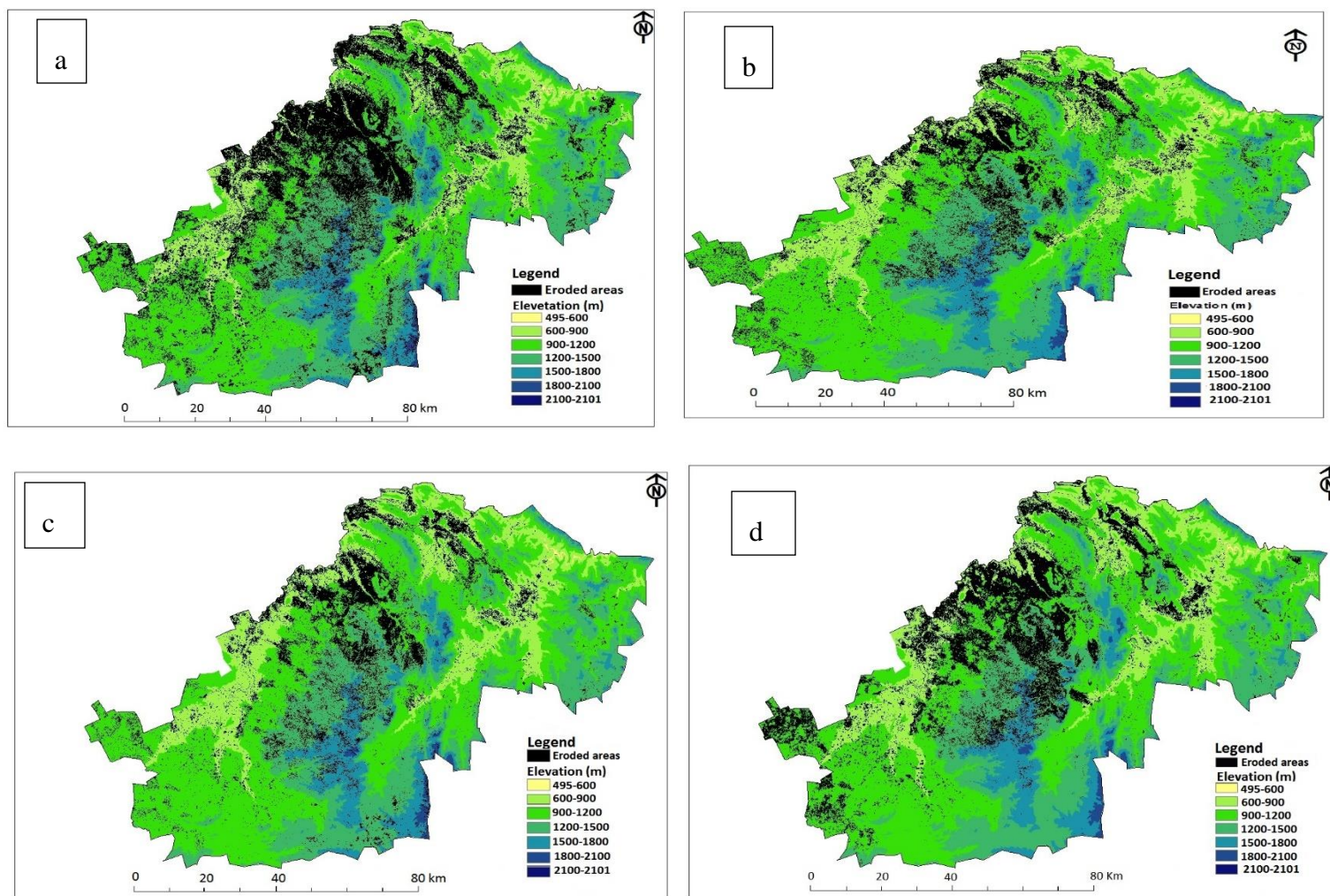


Figure 3.8 Maps showing the relationship between elevation and eroded areas (a. dry & c. wet; b. dry & d. wet season for Landsat 8 and Sentinel 2 respectively).

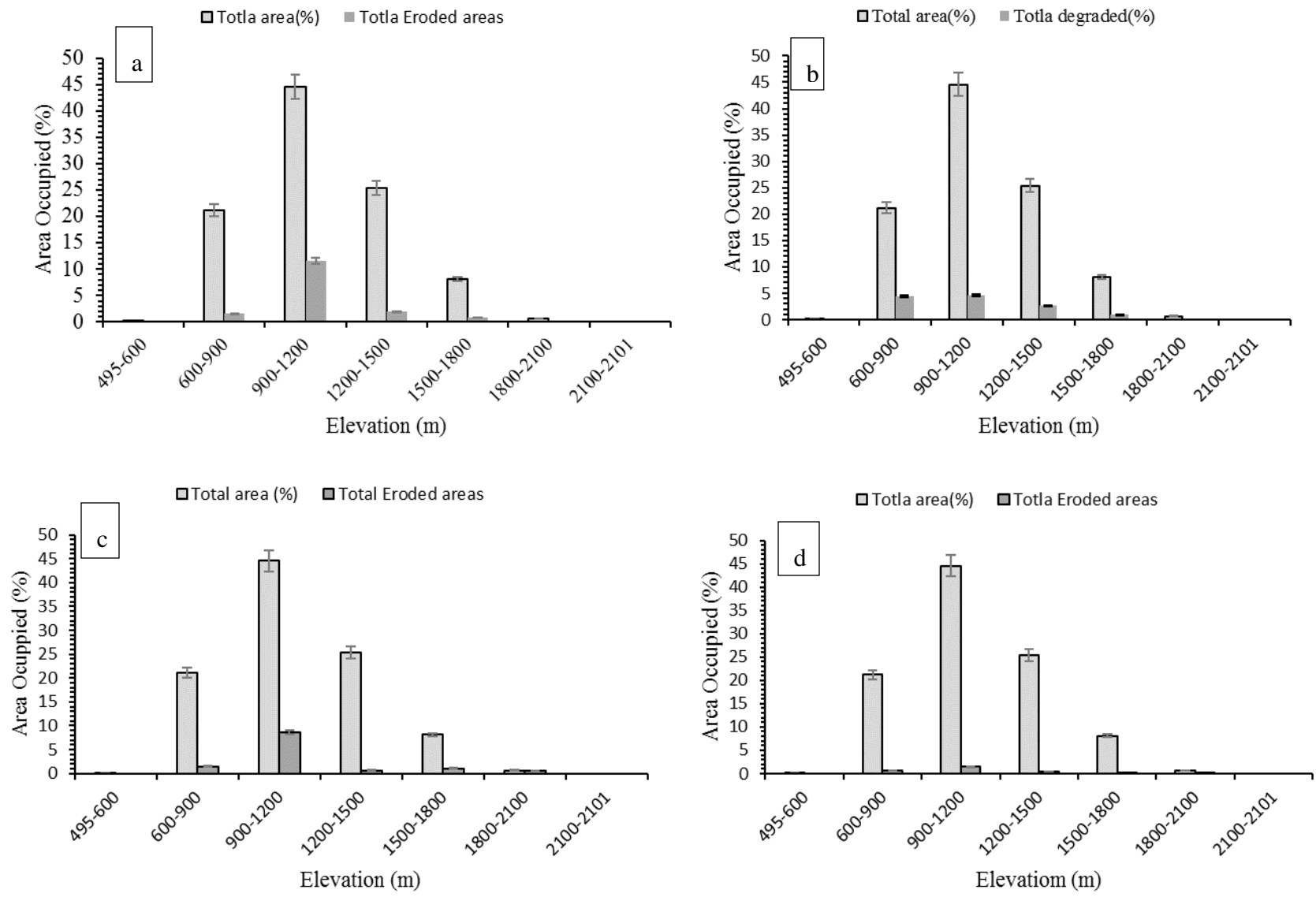


Figure 3.9. Eroded areas (%) in relation to change in elevation. a). wet & b). dry season; c). dry & d). wet season.

3.4. Discussion

The main essence of this study was to test the effectiveness of two new generation sensors in detecting and mapping the spatial distribution of eroded areas amongst other land cover types in the former homelands of Sekhukhune, South Africa. Accurate mapping of eroded areas provides a critical input dataset required for soil conservation strategies. Specifically, the study aimed at assessing soil erosion mapping abilities of two new non-commercial multispectral remote sensing data: Landsat 8 OLI and Sentinel-2, as well as determine the optimal bands and indices that can detect and map soil erosion in former homelands. Also, the study sought to find out if the variations in terms of soil erosion can be explained using variations in elevation.

Although the provision of remote sensing multispectral sensors provides an attractive alternative for mapping and monitoring eroded areas, one of their primary challenges is the inability to reduce the mapping error. Results of this study demonstrated the potential of the newly launched Sentinel-2 MSI in detecting and mapping eroded areas with overall accuracy results that are slightly higher than that of Landsat 8 OLI. Combined spectral vegetation indices and extracted Sentinel-2 MSI spectral reflectance information were used to accurately discriminate eroded surfaces from other land cover types and high classification accuracies in terms of percentages (OA, PA, and UA) were observed as compared to Landsat 8 OLI. The same results were also observed when only extracted spectral information were used with Sentinel-2 MSI slightly outcompeting Landsat 8 OLI. However, when spectral vegetation indices were used, Landsat 8 OLI performed slightly better than Sentinel-2 MSI. Overall, Sentinel-2 MSI outperformed Landsat 8 OLI.

It can be observed that the use of the combined dataset improved the classification accuracies, were Sentinel-2 outperformed Landsat 8. The unique performance of the Sentinel 2 imagery can be attributed to the uniqueness of sensor design. For instance, Sentinel 2 is a pushbroom scanner, with numerous new and strategically positioned bands that provide unique information about the earth's surface (Clark and Kilham, 2016; Guidici and Clark, 2017). For example, Sentinel-2's NIR (0.785-0.900 μm), red edge (0.698-0.785 μm) and SWIR (1.565-2.280 μm) region of the EM spectrum have been depicted as the most important bands providing separability windows for discriminating eroded surfaces from other land cover types. On the other hand, Landsat 8

OLI does not cover the red edge portion of the EM spectrum, hence slightly weaker performance. In that regard, the lack of information from the red edge region could also explain the unsatisfactory performance of Landsat 8 OLI in this study. The study by, Korhonen et al. (2017) have shown that the lack of red edge bands in most multispectral sensors downplays their potential in mapping environmental properties. Moreover, since accuracies increased in both sensors after combining spectral bands and vegetation indices, the results of the current study, therefore, clearly indicate the importance of combining vegetation indices with spectral bands in the discrimination of eroded areas from other land cover types. This combination agrees with the result from the study made by Sibanda et al., (2016) where they demonstrated that the high classification accuracies exhibited using vegetation indices and wavebands in spectrally discriminating grasses grown under different management practices. Similarly, Matongera et al., (2017) integrated the spectral bands and derived vegetation indices yielding the best overall classification accuracy (80.08% and 87.80% for Landsat 8 OLI and Worldview-2 respectively) in detection and mapping the spatial configuration of bracken fern weeds.

The results of this study show significant variations of the spatial distribution of eroded areas derived using the two sensors (Landsat 8 and Sentinel-2). For example, it can be observed from the results that the Sentinel-2 sensor with high spectral bands can depict eroded surfaces from other land cover types as when compared to the Landsat 8. Furthermore, spectral separability results indicated slight weaknesses of Landsat 8 when compared to Sentinel-2. However, this can be linked to the fact that images with low spectral reflectance have a challenge of mixed pixels. Although Landsat 8 demonstrated moderately poor quality (i.e. poor radiometric, spatial, spectral characteristics), particularly for detecting spatial occurrence of soil erosion, it holds a good record, especially large-scale mapping, as it is acknowledged by researcher on similar studies (Millington and Townshend, 1984; Whitlow, 1986; Vrieling, 2006; Zhou et al., 2008; Taruvinga, 2009, Seutloali et al., 2016, Dube et al., 2017). Based on the digital classification of Landsat thematic mapper and JERS-1 data, the study by Metternicht and Zinck (1998) detected and mapped different soil erosion feature in Bolivia and concluded that the synergy of Landsat TM provides a unique combination that allows more accurate identification of eroded areas. Furthermore, the study by Seutloali et al., (2016), in the former South African homelands of Transkei has indicated the effectiveness of utilizing Landsat data as a free and readily available multispectral remote sensing in mapping soil erosion levels. Even though Landsat 8 seems to

yield comparatively good results than Sentinel-2 its spatial resolution makes it difficult to map eroded areas or vulnerable areas especially at plot or farm level due to mixed pixels.

The plausible classification results can also be attributed to Discriminant Analysis (DA) algorithm applied in mapping eroded areas, performed best results. The studies made by Sibanda et al., (2015) and Dube et al., (2017) indicated the potential of using this algorithm over other classification techniques. Unlike the traditional classification approaches, such as the maximum likelihood classification algorithms, Sibanda et al., (2015) have shown that the DA classification ensemble has the potential to spectrally detect and discriminate complex classes. Furthermore, Dube et al., (2017) stated that this classification ensemble is repeatable and simple to use and it is illustrated by its usefulness across a wide range of research areas, including natural resources management, electronics, finance, and accounting. The major hindrance of this algorithm, however, is that it requires data sets that are normally distributed of which according to Dube et al., (2017), is not usually the case.

The study further showed that soil erosion varies with a change in elevation. It can be observed that most of the mapped eroded areas are found within areas that are not in slightly higher elevation. For example, the results showed that much of the eroded areas occurred in highly elevated areas i.e. between 600m and 900m when compared to low-lying or flat areas. Slightly elevated areas are likely to experience soil erosion due to runoff during the rainy season (Balaguer-Puig et al. 2017). Rainwater has limited time to infiltrate into the soil as the areas will be a slope, hence more runoff and vice-versa. This observation is also confirmed by previous studies that have found out that highly elevated experience more runoff and consequently due to high gravitational force. For example, the study by Mondal et al. (2017) used open source DEMs of different resolution and ascertained their effects on soil erosion which mostly were detected in less steeped areas and reports that the DEMs gives better results with less uncertainty.

Future research studies should, therefore, focus on using Sentinel 2 MSI, as it provides a better alternative for mapping and monitoring at various scales given it's the high resolution and other related sensing characteristics. Also, the free and readily available nature of the sensors makes it the most optimal solution for mapping soil erosion problems in sub-Saharan Africa, which is currently characterized with limited resources for accurate mapping of soil erosion for management and monitoring of environmental problems. In a nutshell from a land management

side, the results of this study are vital and relevant to related stakeholders, i.e. environmental managers, soil scientists, and agriculturalists, as well as policymakers. The findings provide significant information on location and extent of the affected areas, and this will help in decision-making, rehabilitation or remedial purposes.

3.5. Conclusions

The main aim of the study was to assess the effectiveness of Landsat 8 OLI and Sentinel-2 in mapping the spatial distribution of eroded areas in Sekhukhune district, Limpopo Province of South Africa. The findings of this work have shown that Sentinel 2 offers free, effective and time efficient of acquiring information on the spatial distribution of eroded areas. Sentinel 2 produced an overall classification accuracy of more than 80% whilst Landsat 8 with more than 75% of all tested analytical stages. The integration of Landsat 8 and Sentinel 2 derived raw spectral bands and vegetation indices significantly ($\alpha = 0.005$) improved the detection and mapping accuracies. The study further showed that soil erosion varies with a change in elevation. For example, much of the eroded areas were occur in elevated areas when compared to low-lying or flat surfaces. In summary, the findings of this study have shown that the new generation of readily available multispectral remote sensors together with discriminant analysis classification ensemble presents a potential for mapping and monitoring the spatial occurrence of eroded areas in resources constraints areas across different scales.

4. Chapter Four

A time-series analysis of soil erosion spatial extent in the former homelands of Sekhukhune, Limpopo using multi-date Landsat series data



This chapter is based on a manuscript under review

Sepuru, T.K., and Dube, T., “A time-series analysis of soil erosion spatial extent in the former homelands of Sekhukhune, Limpopo using multi-date Landsat series data” at International Journal of Remote Sensing

Manuscript ID is TRES-PAP-2018-0529.

Abstract

In this study, a time-series analysis (2002 and 2017) of soil erosion in the former homelands of Sekhukhune, South Africa was done, using wet and dry season satellite data. To achieve this task, dry and wet season satellite Landsat series data (Landsat products 8 Operational Land Imager (OLI) and 7 Enhanced Thematic Mapper plus (ETM+)) acquired over the Sekhukhune rural district, Limpopo Province, South Africa were classified to assess and map changes in eroded areas, using the robust classification algorithm: Discriminant Analysis. Additionally, derived eroded areas were extracted and an overlay analysis was performed to assess whether and to what extent the observed erosional trends can be explained, using geology, slope and the Topographic Wetness Index (TWI). The results indicated that the dry season of 2002, 16.61 % (224733 ha) of the area was eroded whereas in 2017, 19.71% this increased to 3.1%. A similar trend was also observed in the wet season. Also, seasonal assessment demonstrated that about 16.61% (224733 ha) was affected in the dry season whereas 14.86% (201077 ha) for the wet season. Statistical analysis shows that the erosional extent did not significantly ($p < 0.05$) vary across the two seasons. The findings of this work also indicate that the dominant geology type (Lebowa granite: Red and Granite, Fine- to medium-grained; and Rustenburg layered its lithology strata: Pyroxenite, norite, anorthosite, chromitite, Gabbro, norite, anorthosite, Black magnetite gabbro) experienced more erosional disturbances than other geological types. Slope steepness had a significant influence on the magnitude of soil erosion. For instance, slopes ranging between 2-5% (Nearly level) experienced more erosion and vice-versa. On the hand, the relationship between TWI and eroded areas showed that much erosion occurred between 3 and 6 TWI values in all the seasons for the two different years. We, therefore, recommend that those severely overgrazed areas should be protected and monitored from overgrazing to allow grass and vegetation growth.

Keywords: Eroded areas; geology; Landsat data-set; slope; Sustainable Development; Time series analysis; Topographic Wetness Index.

4.1. Introduction

Severely eroded areas are a major global problem in South Africa, as well as elsewhere in the world, the effects of which are most strongly felt in developing countries where large proportions of the population directly depend on the soil for their livelihoods (Tully et al., 2015; Sanchez and Swaminathan, 2005; Sanchez, 2002). The Global Assessment of Soil Degradation (GLASOD) study estimated that nearly 2 billion ha (22.5%) of agricultural land, pasture, forest, and woodland has been degraded since the mid-twentieth century (Oldeman et al., 1990; Gibbs and Salmon, 2015). Moreover, Oldeman et al. (1990) estimated that roughly two percent of the soils are so severely degraded that the damage is likely to be irreversible, and another seven percent was moderately degraded such that huge on-farm investments would be required. The development of relevant area specific and consistent soil erosion monitoring spatial tools is, therefore, increasingly important to identified eroded and potentially vulnerable areas to put control or rehabilitation measures in place.

The Sustainable Development Goal 15 of the 2030 (SDG 15) Agenda emphasizes on the need to “protect, restore and promote sustainable use of terrestrial ecosystems, sustainably manage forests, combat desertification, and halt or reverse land degradation, as well as halt biodiversity loss” (Keesstra, et al. 2016). This, therefore, paves a way for studies on understanding changes in eroded areas as one of the global impact (Le Roux, et al., 2007). Linking to this, the research conducted by Hoffman (2014) in South Africa stated that any study on land use and land cover change cannot be considered in isolation of a native's Land Act of 1913 because natural environments have all changed fundamentally, since its inception. Most of the areas in South Africa have been shaped by the political history of the country, with its successive colonial and apartheid governments who divided the land into separate areas of very different sizes reserved for different race groups (Kakembo and Rowntree, 2003; Giannecchini, et al. 2007; Coetzer, et al. 2013). The former black ‘bantustan’ or homeland areas under the communal tenure possess a fundamentally different environmental history from the state-owned conservation areas and white-owned farmland under freehold tenure, which surrounds the former homelands (Hoffman, 2014). Therefore, the way in which land is used, and altered as a result of the successive colonial and apartheid governments, it has further affected the production of the land, leading to more eroded areas. Therefore, to reach a sustainable situation as described in SDG 15, there is an

urgent need to understand the spatial-temporal patterns or trends of the eroded areas, particularly in former homelands/farmlands.

Soil erosion greatly affects the livelihoods of many poor rural communities (former homeland settlers) who depend on farming for food production and survival (Le Roux, et al., 2007). The vast majority of them need to share grazing areas and arable lands, since they live under a common setup and soil degradation occurs because of the high demand and pressure that is put on the soil for production in view of population growth and the high level of poverty which requires that they use the soil for food production (Maskey, et al. 2003). As stated by Davaasuren (2001), people in many affected regions who are driven by poverty and greed have a desire to derive as much benefit as possible from the land in a short period of time, and this leads to the initiation and progression of erosional processes. Although poor communities are seen as the perpetrators of soil erosion, it is also evident in other areas where it is a result of intense land use and land cover change driven by modern developmental pressures (Davaasuren, 2001). Xulu (2014) detailed that United Nations Economic Commission for Africa lists the causes of soil erosion, among others, as clearance of vegetation for agricultural, industrial and residential development, overgrazing and inappropriate land use. Several land degradation studies (Deeks, et al. 2012; Zimdahl, 2012; Finch, et al. 2014) have linked the occurrence of soil erosion to intense land cover change. On this basis, there are several mitigation and rehabilitation strategies that have been developed to combat the severity of soil erosion, but as stated by Gibbs and Salmon (2015), the lack of understanding of the location, area, and condition of the degraded land is a significant limiting factor to a more reality-based rehabilitation or mitigation strategy.

In addressing the problems of soil erosion researchers have since applied various techniques namely; empirical, conceptual and physically based models (Lal, 1994; and Hudson, 1995; Merritt et al., 2003). The majority of these approaches or models used to quantify eroded lands have shown some limitations. For instance, most of them are restricted in understanding processes involved, particularly in terms of the spatial and temporal distribution of eroded surfaces (e.g. Croke and Mockler, 2001). Despite the cost and time-consuming nature of other soil erosion models, remote sensing techniques have been observed as the most lucrative alternative technique that can map erosion with less expert data. Also, this technique is timely and less cost and provides the most suitable quantitative information necessary for assessing and

monitoring the levels of soil erosion. Satellite remote sensing-based modeling embraces both the empirical and physical-based approaches (Shoko et al., 2016). As such this approach has been successfully used and acknowledged by researchers (Bocco and Valenzuela, 1988; Dwivedi et al., 1997; Kiusi and Meadows, 2006). No other techniques offer the promise of spatially exhaustivity, objectivity and repeated measurements at a cost comparable to satellite remote sensing (Muttitanon and Tripathi, 2005; Sepuru and Dube 2017).

The major challenge with remotely sensed studies on soil erosion using remotely sensed data is that they used single-date or images collected over a period of one year (Sepuru and Dube 2018). Although the results are good, they are not enough for policy development. This has been largely attributed to the lack of appropriate spatial data, with a resolution that can capture these variations. According to Geymen and Baz, (2008), accurate understanding of soil erosion requires the long-term trend analysis of land degradation by comparing multiple land cover maps derived from remotely sensed data at different times and seasons, which are co-registered with one another to determine spatial changes. This is a clear indication that long-term (multi-year images) analysis is therefore key if soil conservation is to be achieved. Such information can provide an in-depth understanding of the rates of change or spread, as well as help point areas that need immediate attention. In areas where some erosional features are dominant i.e. do not change over time, single date images cannot capture such detail hence the need for a long-term monitoring. More recently, remote sensing has opened new vistas in inventory, characterization, and monitoring of eroded areas, which is critical for understanding the spatiotemporal changes of eroded areas and to come up with appropriate soil conservation strategies. Thus, the freely available Landsat series data and Sentinel 2 data makes them suitable for both regional and local scale mapping of the spatial occurrence of eroded areas (Pickup and Nelson, 1984; Dwivedi et al., 1997; and Dhakal et al., 2002). However, the challenge with the latter is that it was only launched recently, hence does not have considerable archival data required for long-term monitoring. Despite having a high spatial resolution of 10m, Sentinel 2 was only launched in 23rd of June 2015 (Sentinel- 2a and Sentinel- 2b) and this makes it only suitable for snapshot applications (Korhonen et al. 2017; Sepuru and Dube 2018). In this study, we, therefore, assess soil erosion in the former homelands of Sekhukhune, South Africa by applying a time-series analysis (2002 and 2017), to track changes of areas affected by varying degrees of erosion. Specifically, the study assessed and mapped changes of eroded areas (wet and dry season), using

multi-date Landsat products 8 Operational Land Imager (OLI) and 7 Enhanced Thematic Mapper (ETM+). Additionally, the derived eroded areas were extracted and an overlay analysis was performed to assess whether and to what extent the observed erosional trends can be explained using geology, Topographic Wetness Index (TWI) and the slope of the area under study.

4.2. Material and methods

4.2.1. Field data collection

The most common method of validating the results of erosion models is through erosion surveys in which a visual estimation of erosion risk is conducted based on observed features (e.g. Dwivedi et al., 1997; Metternicht and Zinck, 1998). Data collection was done by recording coordinates at sub-meter accuracy using GPS device, to validate satellite remote sensing data. Eroded areas were identified during field surveys using random walks and google earth maps of the area. A similar approach was used in collecting data on other major land cover classes in the area, and these included built-up areas, cultivated areas, eroded areas forest-woodland, and grass-shrubland, vegetation covers and water bodies. Land cover classes were identified using visual observation. The vector maps of the study, courtesy of Sekhukhune District together, with the aid of google earth, were used to navigate to areas affected within the study area. During the field operation, a total of 300 (50 per class) points were recorded, using a Trimble GeoXH 6000 series handheld Global Position System (GPS) at sub-meter accuracy. These GPS points were used in extracting spectral data from the multi-date Landsat series data sets. Furthermore, photographs of eroded areas and other land cover types were taken, using a handheld camera. During the collection of photographs, GPS coordinates were also recorded and these were used to verify the classified maps.

4.2.2. Landsat pre-processing

The proposed methodology uses Landsat satellite time-series composites data to detect eroded areas over other land cover types, using the image classification approach. In this study, cloudless Landsat 8 OLI and Landsat 7 ETM+ images acquired respectively during the 1st of June 2017 and 31st July 2017 for the dry season and between the 1st of December 2016 and 31st January 2017 (table 1) were used. The images were accessed from the USGS Earth Resources Observation and Science (EROS) Centre archive (<http://earthexplorer.usgs.gov/>). Subsequently,

the images were re-projected and mosaicked. Both images were atmospherically corrected, using the dark object subtraction (DOS1) model in QGIS version 2.1.8 software.

Table 4.1 Characteristics of the remotely sensed data set selected for this study

Satellite	Sensor	Resolution (m)	Season
Landsat 7	ETM+ Multispectral	30	Dry
Landsat 8 Operational Land Imager (OLI)	Operational Land Imager (OLI)	30	
Landsat 7	ETM+ Multispectral	30	Wet
Landsat 8 Operational Land Imager (OLI)	Operational Land Imager (OLI)	30	

4.2.3. Image classification and accuracy assessment

Image classification was carried out using Maximum likelihood classification algorithm embedded in ArcGIS software 10.4. Using the training samples as described in Field data collection subheading, the spectral bands for Landsat 7 ETM+ and Landsat 8 OLI images separately were classified into six classes using pixels of the data sets. To assess the classification accuracy of the results, quantity disagreement, and allocation disagreement was used following its best application as demonstrated in the literature (Sibanda et al. 2016). The method was applied as a way of separating data into training and tested data also recommended by Pontius and Millones (2011) as the successor of Kapa Statistic. Quantity disagreement is a sum of least perfect matches between the training (70%) and the testing (30%) reflectance datasets of each land management practice. Precisely, the quantity disagreement follows when the column total of a management practice class deviates from the row total of that class in a confusion matrix. To estimate the extent of the difference between Landsat 8 OLI data accuracy and that of Landsat 8 ETM+ agreement between classification results and ground truth data was measured using the producer accuracy (PA), user accuracy (UA) and overall accuracy (OA) generated from the confusion matrices. These two parameters were used in accuracy assessment, as suggested by Pontius and Millones (2011).

4.2.4. Sekhukhune Geological types

According to Mousazadeh and Salleh (2014), for one to understand soil erosion, there is a need for studies to integrate lithology (geology type) on the analysis. There are clear connections and associations between areas that are eroded with the parent material. Table 4.2 below illustrates geological data of the area under study corresponding to the information presented in figure 4.4, which shows spatial information of this dataset. This secondary data set was used to check the relationship between geology covering the study area with eroded areas. The data set was accessed from South African Institute of Geoscience.

Table 4.2 detail information on geology (parent) used in the study

PARENT	LITHSTRAT	DESCRIPTION
Bushveld	Rustenburg Layered, Rashoop Granophyre	Norite, Diallage pegmatoid, Pyroxenite, Granite granophyre, Quartz-feldspar porphyry, granophyre
Chuniespoort	Penge, Duitschland, Malmani	Iron-formation, Dolomite/limestone (+ chert), shale, subordinate quartzite, conglomerate and diamictite, Dolomite, subordinate chert, minor carbonaceous shale, limestone and quartzite, Chert, Shale
Karoo	Ecca, Irrigasie, Clarens	Shale, with sandstone-rich units present towards the basin margins in the south, west and northeast and coal seams in the northeast, Predominantly red mudstone containing one or more sandstone units towards the base, Fine-grained sandstone, siltstone
Lebowa Granite	Nebo Granite, Klipkloof Granite, Makhutso Granite	Coarse-grained granite, Red, medium-grained near top, Fine- to medium-grained, generally porphyritic granite, Fine-grained porphyritic biotite granite, Porphyritic biotite granite
Other Parent	Dennilton, Makhutswi Bushveld, Karoo Dolerite	Spitskop, Gneiss, Diabase, Carbonatite, Water, Carbonatite, Surface deposits, Alluvium and scree, Granophyric Gneiss, Schist and granulite, Rhyolite, Granite-gneiss, Gneiss and amphibolite, Fenite, Ijolite, nepheline syenite, pyroxenite, carbonatite, Homogeneous, light grey (leucocratic) medium-grained granodioritic/tonalitic biotite gneiss, Network of dolerite sills, sheets and dykes, mainly intrusive into the Karoo Supergroup, Diallagite pegmatite, Network of dolerite sills, sheets and dykes, mainly intrusive into the Karoo Supergroup

Pretoria	Timeball Hill, Nederhorst, Daspoort, Dwaalheuwel, Hekpoort, Magaliesberg, Strubenkop, Silverton, Vermont, Makeckaan, Lakenvalei, Steenkampsberg, Boshhoek, Dullstroom	Mudrock, quartzite, minor diamictite, Flagstone and brownish to grey shale at top, Quartzite, minor shale, Shale, Shale, subordinate siltstone, minor quartzite, Metamorphosed mudstone and shale with minor quartzite, dolomite and chert, Siltstone and sandstone, Feldspathic arenite, quartz arenite, subordinate wacke, micaceous siltstone, shale and conglomerate, Quartzite, feldspathic quartzite, arkose, Quartzite, minor shale, Arkosic quartzite, subgreywacke, siltstone, shale, conglomerate (in places), Shale/hornfels and minor carbonate rocks overlain in the south by argillaceous quartzite and arkose Quartzite with minor shale and siltstone, Quartzitic sandstone, mudrock and (in the west) conglomerate, Andesitic lava, subordinate pyroclastic rocks, minor quartzite, shale and conglomerate Pyroxene hornfels, Basaltic andesite, minor felsite, pyroclastic rocks, arenite and hornfels,
Rooiberg	Damwal, Kwaggasnek, Schrikklouf	Rhyolite with subordinate pyroclastic rocks and minor sandstone, Black rhyolite, leptite, Red granophyric rhyolite, Fine-grained, flow-banded, porphyritic and spherulitic felsite, Massive, generally red, porphyritic felsite, minor pyroclastic rocks and sandstone/quartzite
Rustenburg Layered	Shelter Norite, Dsjate, Dwars River, Croydon, Roosenekal	Norite, feldspathic pyroxenite, quartz norite, Magnetite layer, Olivine diorite, magnetite gabbro, gabbro, gabbro, norite, Chromite layer - upper zone, Pyroxenite, norite, anorthosite, chromitite, Gabbro, norite, anorthosite, Black magnetite gabbro,
Silverton	Boven Shale, Lydenburg Shale, Machadodorp	Shale, minor carbonate, and chert, Hornfels, Mudrock, Tuff, and agglomerate overlain by pillow basalt, Calcareous with dolomitic limestone lenses
Timeball Hill	Klapperkop Quartzite	Quartzite (ferruginous in places), wacke, siltstone, shale, magnetic ironstone
Transvaal	Pretoria, Rooiberg, Bloempoort, Wolkberg, Black Reef	Quartzite, shale and andesitic-basaltic lava, Quartzite, Quartzite, subordinate conglomerate and shale, mpure quartzite and conglomerate, Basic lava, tuff, agglomerate and shale, Dolomitic limestone and shale, Fine to medium grained quartzite, feldspathic quartzite, lava, Andesite, Blue and yellow banded slate, quartzite, Felsite, basaltic andesite (lower part), minor shale and agglomerate.
Waterberg	Wilge River	Reddish-brown and purple, medium- to coarse-grained sandstone, subordinate conglomerate, minor shale
Wolkberg	Selati, Sadowa, Abel Erasmus	Mudrock, sandstone, Basaltic lava, subordinate dolomitic shale, chert, quartzite, arkose, subgraywacke and pyroclastic rocks, Mudrock, quartzitic sandstone

4.2.5. Slope and TWI data set derived from DEM

The Shuttle Radar Topography Mission (SRTM)-derived (DEM) was used to generate information on the slope of the area and this data was used to determine whether the occurrence

of eroded areas could be explained in terms of terrain characteristics. This study used SRTM DEM because of its higher spatial resolution (30m/pixel) corresponding to that of the two sensors and its accessibility. In this study, topographic variables (slope and Topographic Wetness Index (TWI) were derived from the DEM. The slope is a vital surface characteristic that affects surface runoff and soil erosion rates (Seutloali and Beckedahl, 2015). It has been found that soil erosion rises with an increase in slope, due to the increase in rubbing ability of concentrated runoff (Jordan and Martínez-Zavala, 2008). Thus, the slope can provide an indication of the potential of an area to generate concentrated runoff and hence soil erosion. In this study, the slope was therefore calculated so as to determine its effects on soil erosion development and the observed trends. The slope was generated in ArcGIS tools 10.4.1 software following equation 1. Table 4.3 shows the steepness of slope that was adopted from Barcelona Field Studies Centre, (2017). TWI is one of the most important topographic variables in predicting soil erosion. It indicates soil water variability over a land surface (Iqbal et al., 2005). TWI was calculated in ArcGIS software as shown in equation 2 (Beven and Kirkby, 1979).

$$\text{Slope} = \frac{(\text{slope(DEM)} \times 1.570796)}{90} \quad \text{Equation.....1}$$

$$TWI = \ln\left(\frac{a}{\tan B}\right) \quad \text{Equation.....2}$$

a = Upstream contributing area in m² (flow accumulation)

B = Slope raster map

TWI = Topographic wetness index

Table 4.3 Slope Steepness

Slope (%)	Approximate degrees	Steepness
0-0.5	0	Level
0.5-2	0.3-1.1	Nearly level
2-5	1.1-3	Very Gentle Slope
5-9	3-5	Gentle Slope
9-15	5-8.5	Moderate slope
15-30	8.5-16.5	Strong slope
30-45	16.5-24	Very strong slope
45-70	24-35	Extreme slope
70-100	35-45	Steep slope
>100	>45	Very steep slope

4.3. Results

4.3.1. Changing of spatial land use

Soil erosion maps were derived for the dry and wet seasons for the year 2002 and 2017 (Figure 4.1). During the dry season of 2002, 16.61 % (224733 ha) of the area was eroded whereas in 2017, 19.71% this increased to 3.1% (table 4.4, Figure 4.3). A similar trend was also observed in the wet season. For example, in the year 2002, 14.86% of the area was eroded whereas in 2017, 17.70% this increased by 2.84% (table 5, Figure 4.3). Eroded areas covered 224733 ha (16.61%) of the study area in dry season, while in the wet season it accounted for 201077 ha (14.86%). In 2002 grass-shrub land class, covered the most area from other land cover type for both seasons by 72047 ha, accounting for 53.26% of the total area (Table 4.4) for the dry season and 523979 ha (38.73%) for wet season (Table 5.5).

There were 224733 ha (16.61 %) eroded areas in 2002 and 266596 ha (19.71%) in 2017 which had a positive change of 41863 ha for the dry season, some of which had been added from other

land covers. Moreover, there were 201077ha (14.86%) eroded areas in 2002 and 239428 ha (17.70%) 2017, which had a positive, change of 38351 ha for the wet season. Therefore, nearly a quarter of the study area had been affected by soil erosion for all the seasons and years. Spatially, such eroded areas are distributed throughout the study area, but with a higher concentration in the Northern part of the study area (Figure 4.2). Figure 4.3 (a and b) illustrated randomly selected area between the seasons (dry and wet) of 2002 and 2017 to show changes amongst farms and land cover classes within the area under study and the impact of soil erosion in the former homelands of Sekhukhune district.

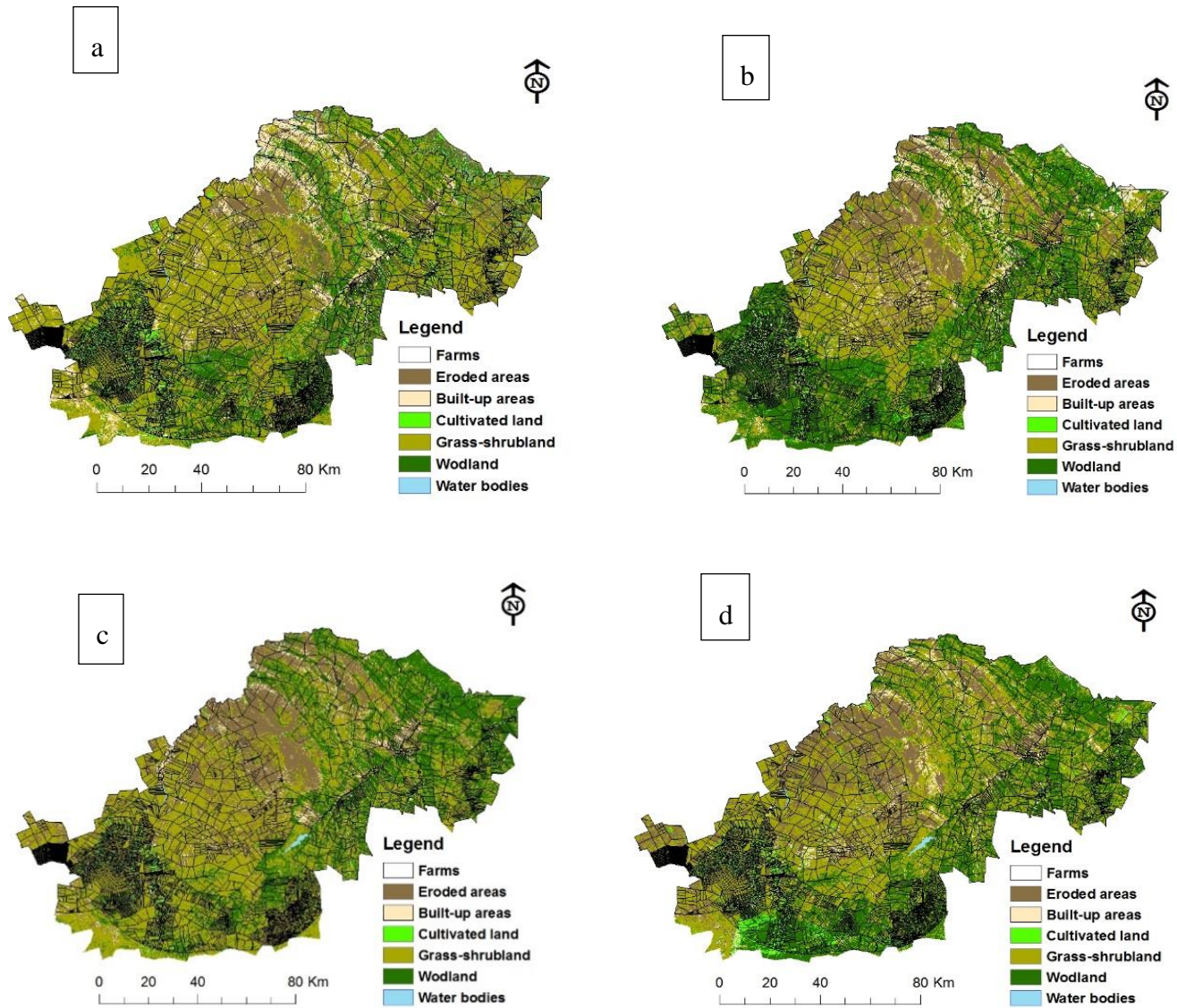
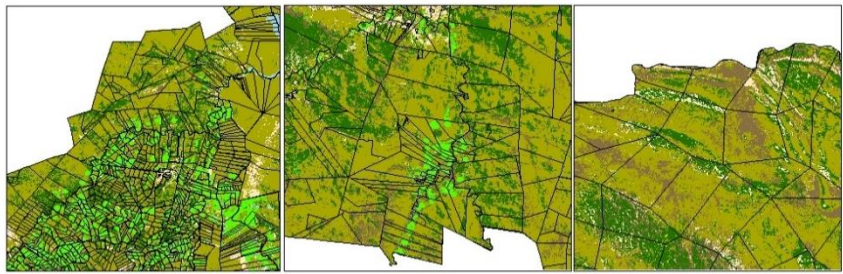
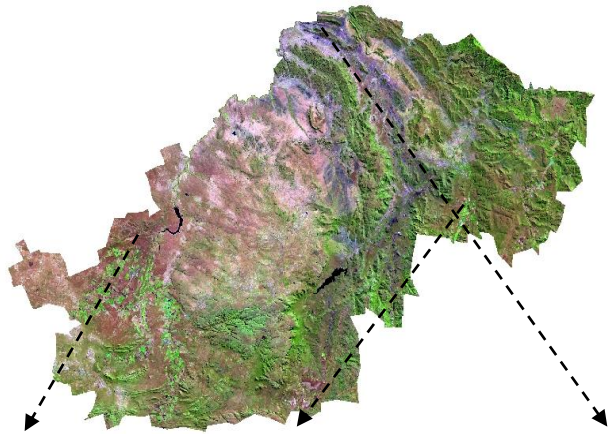
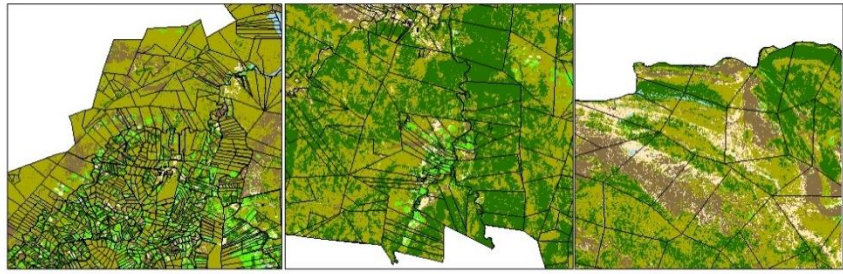


Figure 4.1 Derived soil erosion thematic maps for the year 2002 and 2017. a-b dry and wet season Landsat 7 ETM+ derived soil erosion and (c-d) dry and wet season 2017 Landsat 8 OLI derived.

a



2000
(Landsat 7)



2017
(Landsat 8)

Legend
Farms Built-up areas Grass-shrubland Water bodies
Eroded areas Cultivated land Wadland

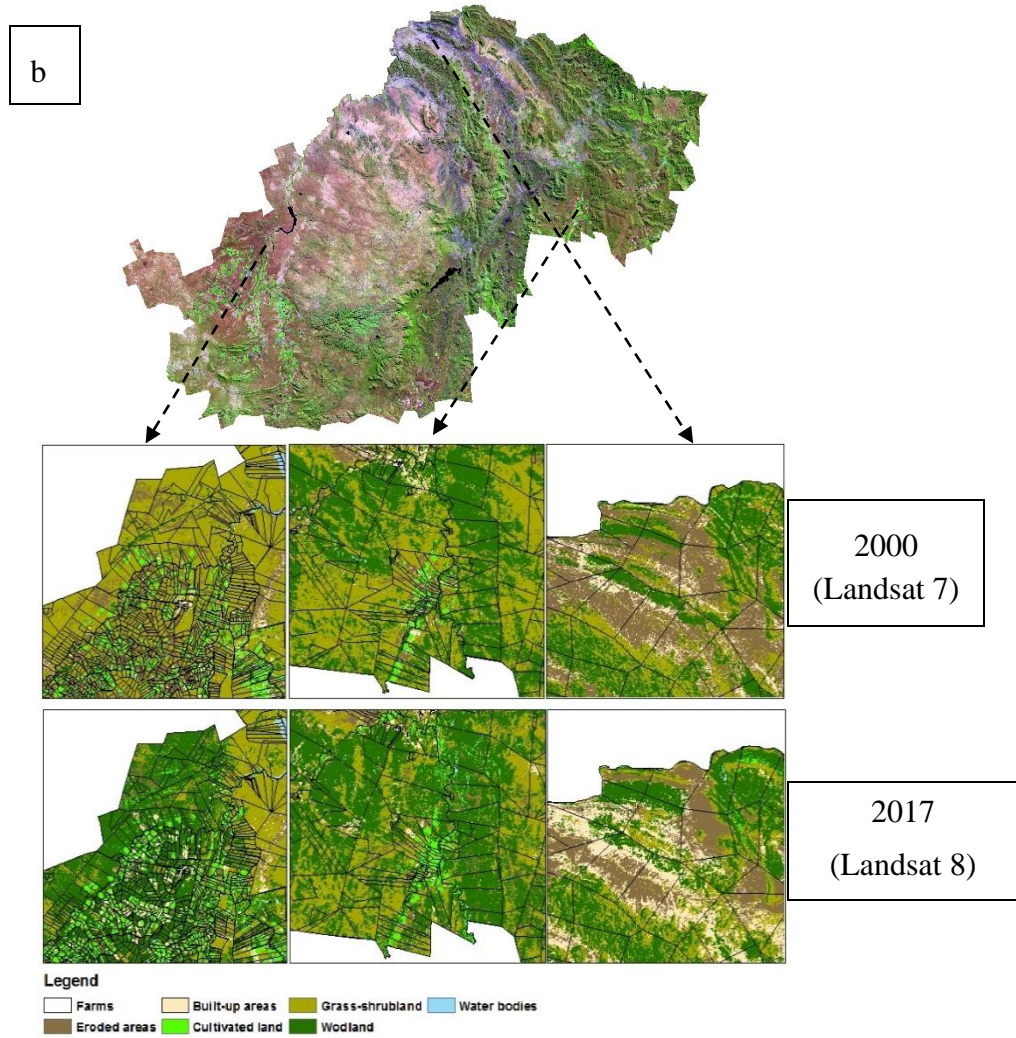


Figure 4.2 Zoomed maps showing changes amongst land cover within the study area. a), dry season; b) wet season.

Table 4.4 Mapped land covers and their change from 2002 to 2017 (dry season)

Classes	2002		2017		Changes	
	ha	%	ha	%	ha	%
Eroded Areas	224733	16.61	266596	19.71	41863	3.1
Built-up	56914	4.21	104391	7.72	47477	3.51
Cultivated Land	59215	4.38	19377	1.43	-39838	-2.78
Grass-shrubland	720475	53.26	665503	49.19	-54972	-4.07
Woodland	285995	21.14	294051	21.74	8057	0.6
Water bodies	5469	0.40	8082	0.60	2613	0.2
total	1352800	100	1352800	100		

Table 4.5 Mapped land covers and their change from 2002 to 2017 (wet season)

Classes	2002		2017		Changes	
	ha	%	ha	%	ha	%
Eroded Areas	201077	14.86	239428	17.70	38351	2.84
Built-up	58323	4.31	94652	7.00	36329	2.69
Cultivated Land	43762	3.23	48650	3.60	4888	0.37
Grass-shrubland	523979	38.73	575675	42.55	51696	3.82
Woodland	519799	38.42	385029	28.46	-134770	-9.96
Water bodies	5861	0.43	9366	0.69	3506	0.26
total	1352800	100	1352800	100		

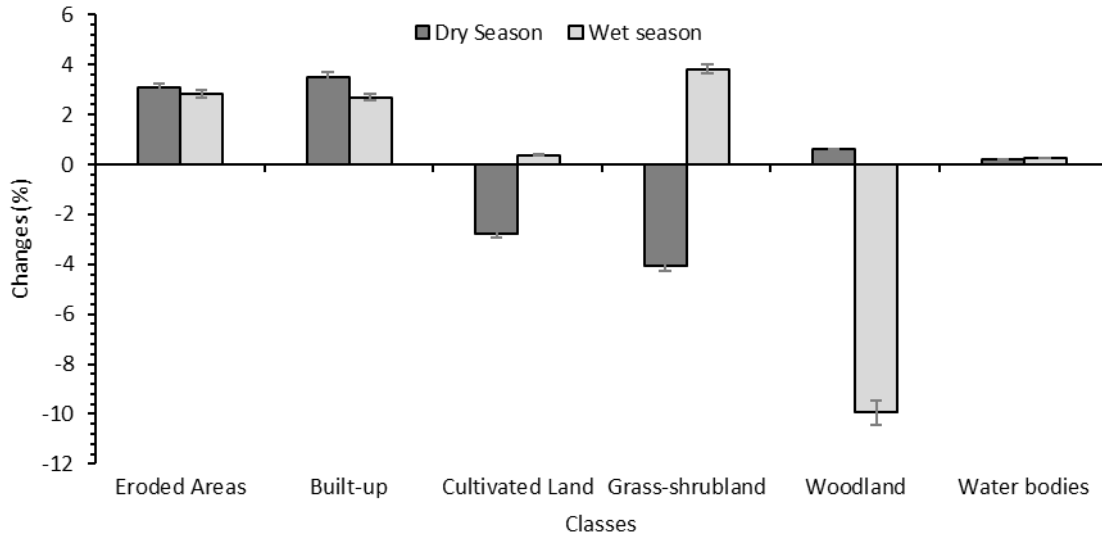


Figure 4.3 Changes detected between 2002 and 2017 in percentages.

4.3.2. Classification Accuracy

In this study, accuracy assessment was carried out for the land cover maps in Figure. 4.1 and 4.2 to validate the results of the classification algorithm. Presented in Table 4.6 is an accurate assessment for a Landsat TM image of 2002 (wet and dry season) and Landsat 8 2017 (wet and dry season) of the study area. According to this error matrix, the degraded land was mapped at an Overall Accuracy (OA) of 67.66% and 80.95% in the dry season the year 2002 and 2017, respectively.

Table 4.6 Classification accuracies from error matrix derived using spectral dataset.

	Landsat 7 (2002)				Landsat 8 (2017)			
	Dry Season		Wet Season		Dry Season		Wet Season	
	PA	UA	PA	UA	PA	UA	PA	UA
Eroded areas	65	82	81.25	78	84.85	73.68	78.79	76.47
built-up	74	74	85	68	63.89	85.19	75	81.82
cultivated land	60	68	100	86	76.47	96.3	32.35	84.62
Grass-Shrubland	89	62	79.55	70	80.56	78.38	90	57.69
forest-woodland	64	50	59.26	96	82.35	66.67	65	76.47
water bodies	71	70	90.91	80	97.3	92.31	89.19	94.29
OA	67.66		79.67		80.95		73.81	

*(PA= Producer Accuracy, UA= User Accuracy, and OA =Overall Accuracy)

4.3.3. Analysis of the conversion among specific land covers

Analysis of the changes amongst land cover types (figure 4.1) is helpful in determining possible explanations behind the observed changes. Moreover, this spatial comparison is more conducive to the revelation of specific changes in the actual degraded area than the net figures in Table 4.7 and Table 4.8. Representing the breakdown of their complements in Table 4.7, figures in Table 4.8 illustrate all the possible changes between any two covers. Some of these results have low values most probably due to misclassifications. They, therefore, do not reveal the general trend of eroded areas. In order to reveal this trend, this section concentrates on the critical changes. For instance, 9264 ha of cultivated land and 5514 ha of grass-shrub land became eroded during 2002–2017. These changes indicate that over cultivation of crops in this vulnerable environment has contributed towards soil erosion. Furthermore, 46800 ha of woodland was also eroded during the study period. Similar to grassland and woodland class, the cultivated area is also vulnerable to erosion if its carrying capacity is exceeded as it has changed from 2002 to 2017. The decrease in woodland by 14980 ha is due to conversion to farmland (e.g., land reclamation through

deforestation) and urbanization. These changes are indicative of an increasing degradation that may worsen in the future.

Table 4.7 Change in land covers between 2002 and 2017 (unit: ha) dry season

	1.Eroded Areas	2.Built-up	3.Cultivated Land	4.Grass-shrubland	5. Woodland	6. Water bodies	Sum
1. Eroded Areas	83116 (6.14 %)	14109 (1.04%)	1143 (0.04%)	70120 (5.18%)	59343 (4.38)	312 (0.02)	228144 (16.87%)
2. Built-up	46135 (3.41%)	18423 (1.36%)	1349 (0.10%)	14960 (1.10%)	14833 (1.10%)	524 (0.04%)	96224 (7.11%)
3. Cultivated Land	9264 (0.7%)	3554 (0.26%)	6982 (0.51%)	14272 (1.06)	11992 (0.89%)	094 (0%)	46158 (3.41%)
4. Grass-shrubland	114222 (8.44%)	19081 (1.41%)	5066 (0.37%)	442779 (32.73%)	93345 (6.90%)	532 (0.04%)	675025(49.90%)
5. Woodland	15851 (1.17%)	1537 (0.11%)	1225 (0.09%)	119866 (8.86%)	148221(10.95%)	1755(0.13%)	288454 (%)
6. Water bodies	179 (0.13%)	117 (0.008%)	072 (0.005%)	325 (0.02%)	16936 (1.25%)	1165 (0.09%)	18796 (1.39%)
Sum	268766 (19.86%)	56822 (4.20%)	15837 (1.17%)	662322 (48.99%)	344671 (25.48%)	4382 (0.32%)	1352800 (100%)

*Bold numbers: main classes converted to erosion

Table 4.8 Change in land covers between 2002 and 2017 (unit: ha) wet season

	1. Eroded Areas	2. Built-up	3. Cultivated Land	4. Grass-shrubland	5. Woodland	6. Water bodies	Sum
1. Eroded Areas	123355 (9.12%)	14921 (1.10%)	1645 (0.12%)	45863 (3.39%)	15096 (1.12%)	232 (0.02%)	201111(14.87%)
2. Built-up	38066 (2.81%)	14493 (1.07%)	2187 (0.16%)	26121 (1.93%)	13330 (0.99%)	398 (0.03%)	94595 (6.99%)
3. Cultivated Land	8401 (0.62%)	2013 (0.15%)	4884 (0.36%)	15363 (1.14%)	12969 (0.96%)	152 (0.01%)	43782 (3.24%)
4. Grass-shrubland	72756 (5.38%)	17713 (1.31%)	3064 (0.23%)	320832 (23.72%)	73001 (5.40%)	362 (0.03%)	487728 (36.05%)
5. Woodland	23867 (1.76%)	7672 (0.57%)	4920 (0.36%)	256822 (18.09%)	223864 (16.55%)	2591 (0.19%)	519734 (38.42%)
6. Water bodies	134 (0.01%)	083 (0.006%)	068 (0.005%)	536 (0.04%)	3311 (0.25%)	1718 (0.13%)	5850 (0.43%)
Sum	266578 (19.71%)	56895 (4.21%)	16768 (1.24%)	665538 (49.20%)	341570 (25.25%)	5452 (0.40%)	1352800 (100%)

*Bold numbers: main classes converted to erosion

4.3.4. The relationship between eroded areas and geology

It can be observed that much of the areas on the Rustenburg geological layer exhibited high levels of erosion, followed by Lebowa granite when compared to other geological types. This was also observed across the two seasons for the year 2002 and 2017 (Figure 4.5). Lebowa granite is mainly made by the Red and Granite, Fine- to the medium-grained material as described in Table 4.2, while Rustenburg layered its lithology strata is Pyroxenite, norite, anorthosite, chromitite, Gabbro, norite, anorthosite, Black magnetite gabbro etc.

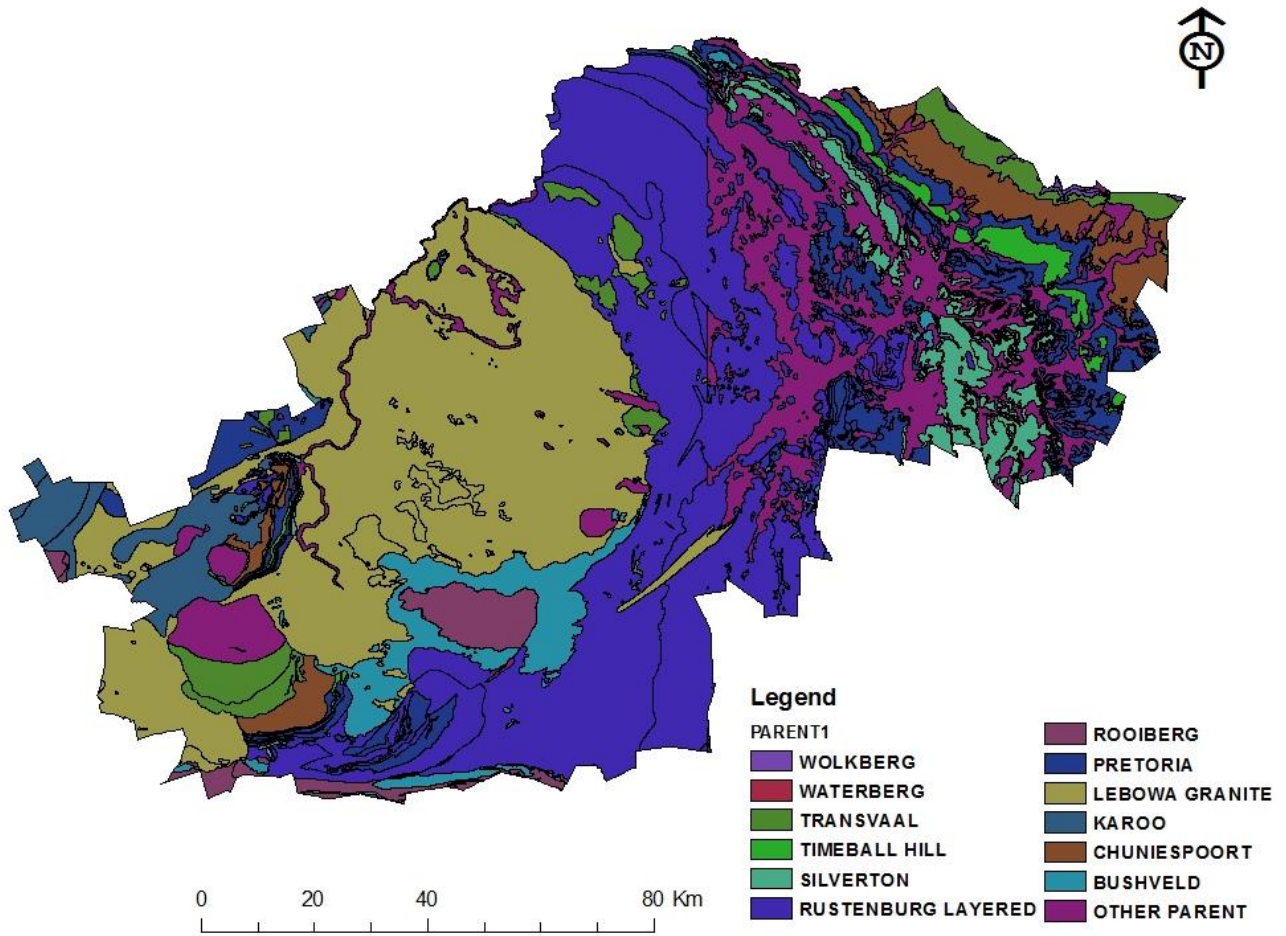
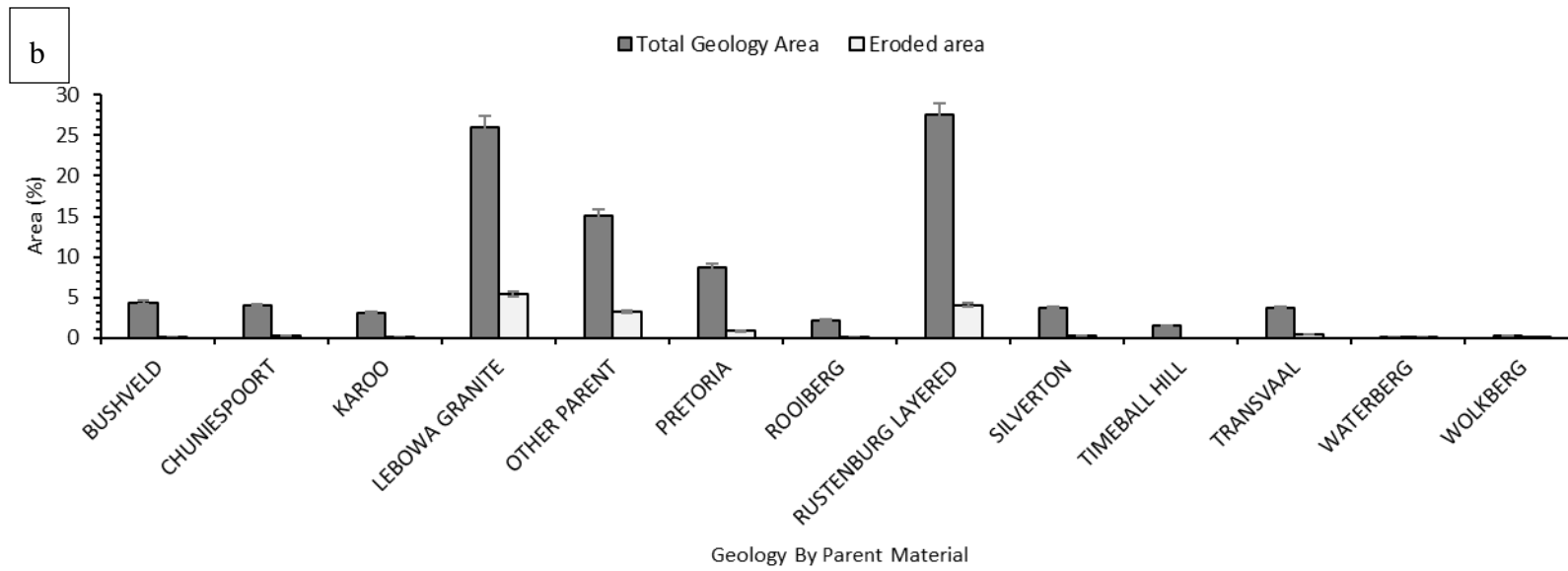
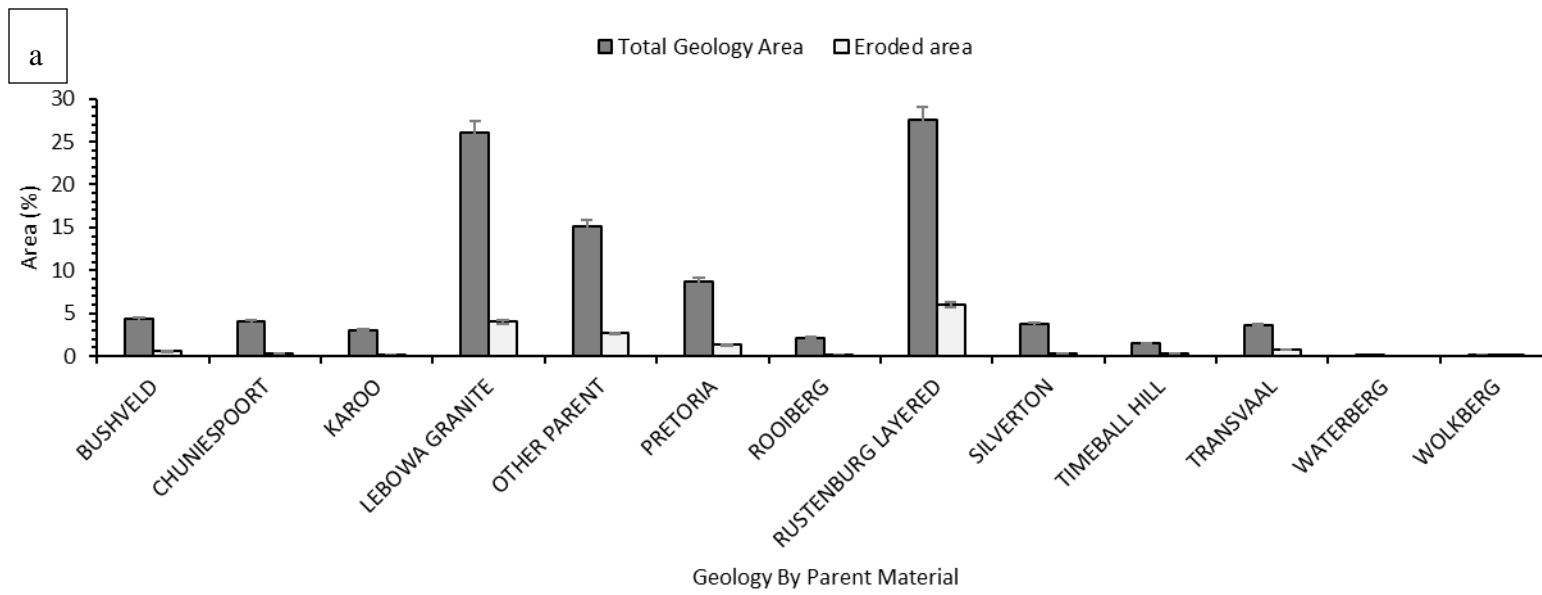


Figure 4.4 The spatial distribution map of Geology across the study area



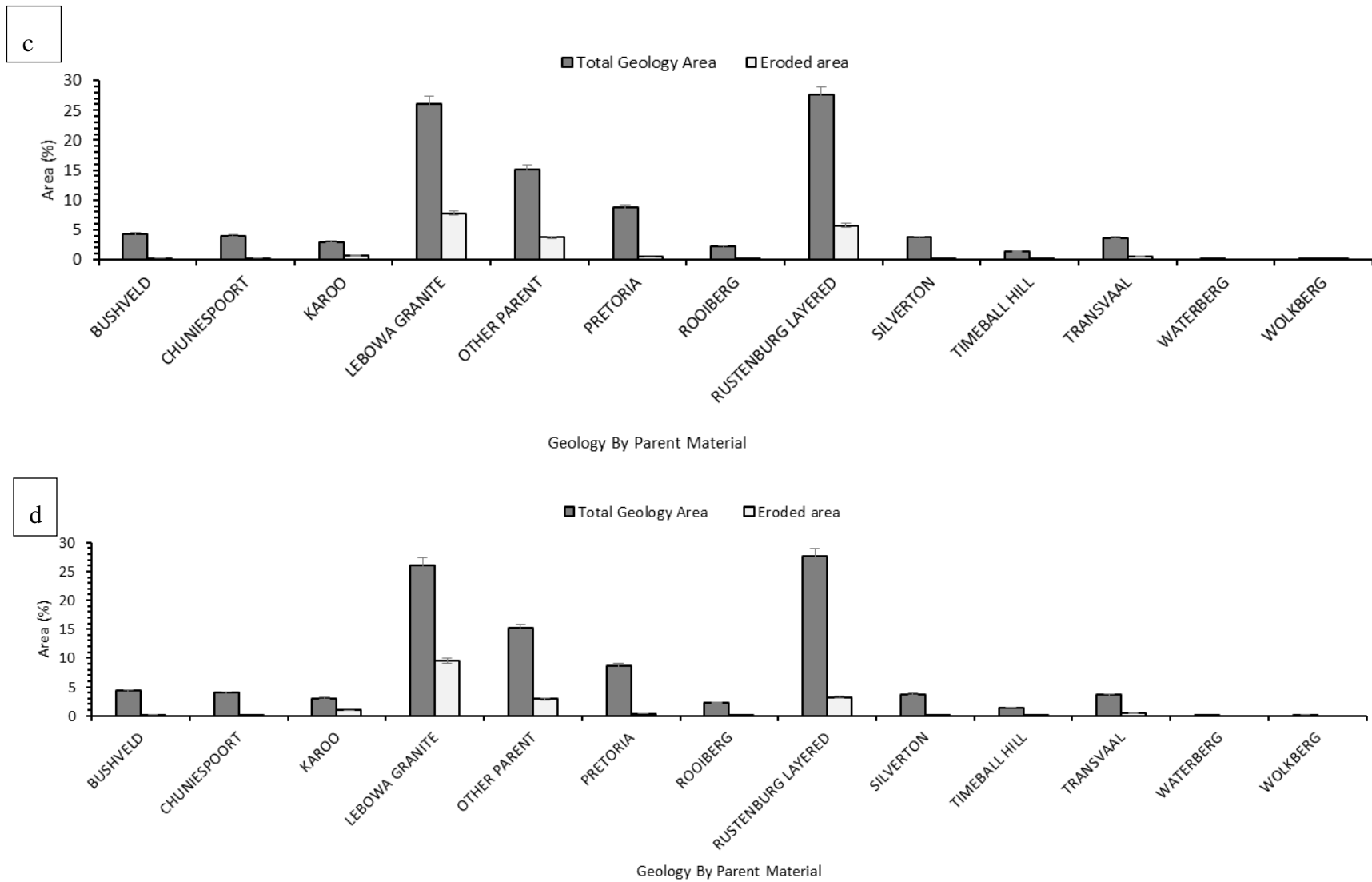


Figure 4.5 Reclassified geology and areas affected by erosion in 2002 (a. dry season b. wet season) and 2017 during (c. dry season d. wet season).

4.3.5. Influence of topographic variables on eroded areas

4.3.5.1. The relationship between eroded areas and the steepness of the slope (topography)

Figure 4.6 provides a map showing the spatial distribution of slope cover in percentage across the area under study. The relationship between topographic variables i.e. slope (steepness) and soil erosion is evaluated in figure 4.7. To obtain slope information at areas of different soil erosion extent obtained soil erosion maps were overlaid with slope map. The results in figure 4.7 show that the extent of eroded areas occurs mostly in less steep slopes. For example, slopes between 2-5% (1.10-30: slope very gentle), particularly in the dry season of 2017 experienced less erosion. (Table 3). Furthermore, erosion was observed on slope steepness between 0.5%-2% particularly in the wet season of 2017 and this level symbolize that the slope is nearly level.

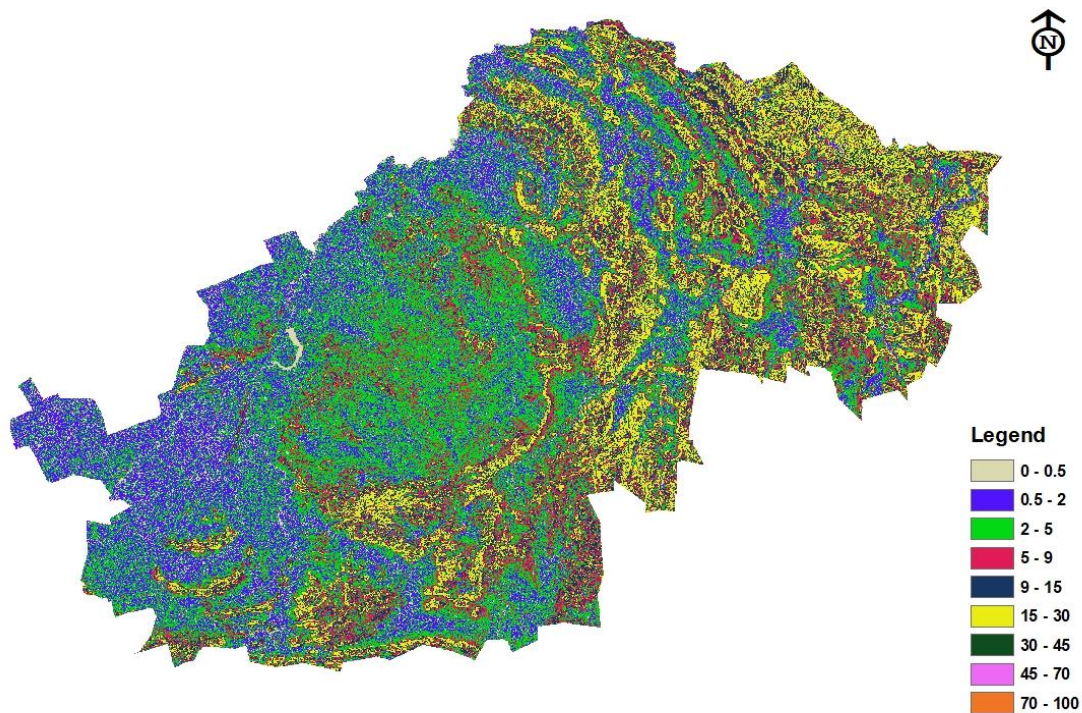


Figure 4.6 The spatial distribution map of slope in percentages across the study area

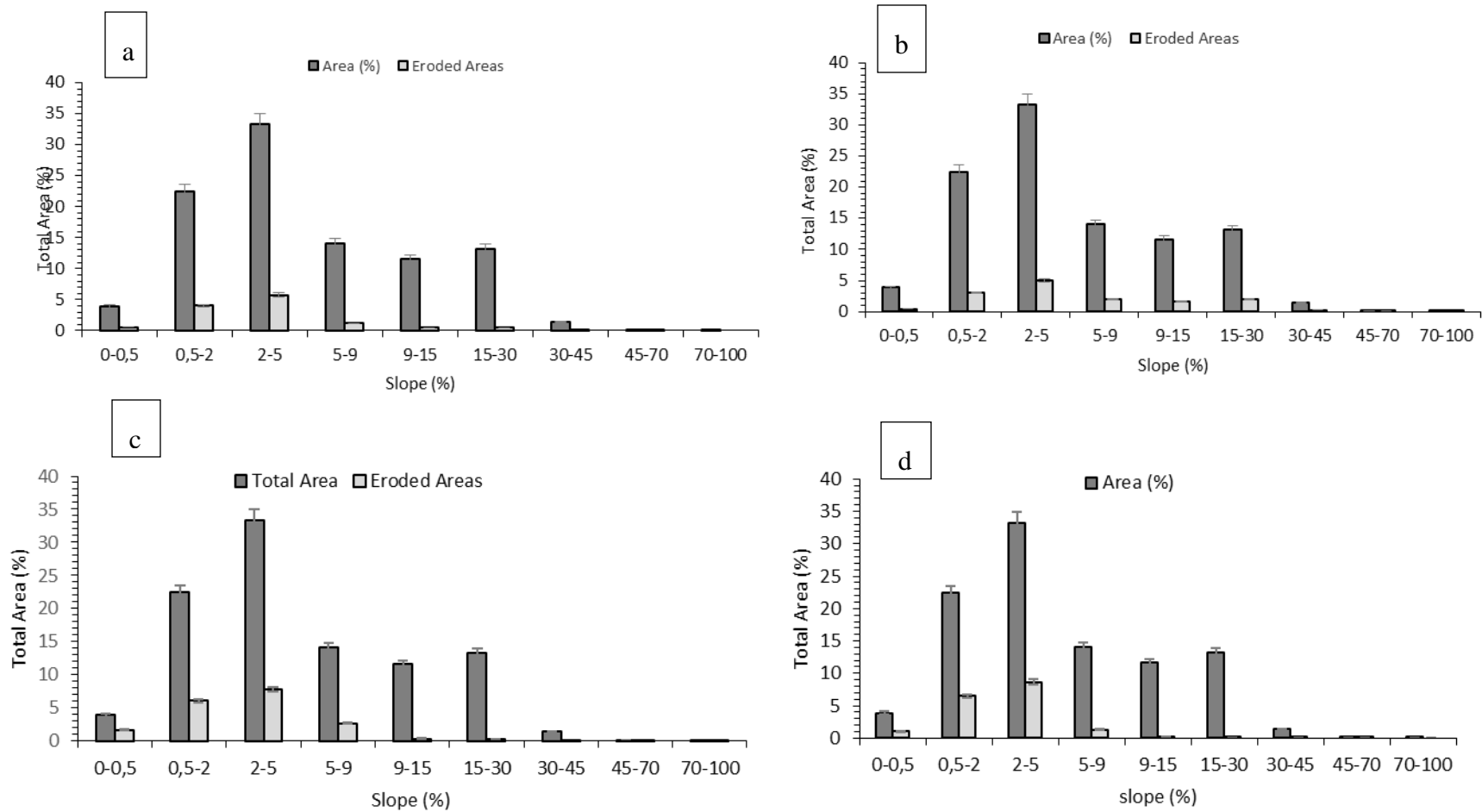


Figure 4.7 Slope and areas affected by erosion in 2002 (a. dry season b. wet season) and 2017 during (c. dry season d. wet season)

4.3.5.2. Effects of soil moisture influence erosivity on eroded areas

Figure 4.8 provides map illustrating the spatial distribution of cover in percentage across the area under the study with Figure 4.9 showing this relationship between two seasons (wet and dry) of 2002 and 2017. To obtain effects of soil moisture influence information at areas of soil erosion, the obtained soil erosion data were overlaid with TWI. The results in figure 4.9 show the relationship between soil moisture availability and soil erosion occurrence. The results show those areas with TWI values between 3 and 12 and less experienced high erosion whereas those with higher TWI values of 12 and 21 experienced less erosion. For example, in 2002 the highest TWI values that experienced much of erosion are between 3 and 6 in all the seasons but the dry season influenced the most (figure 4.9, a) followed by 2017 dry season (figure 4.9, c).

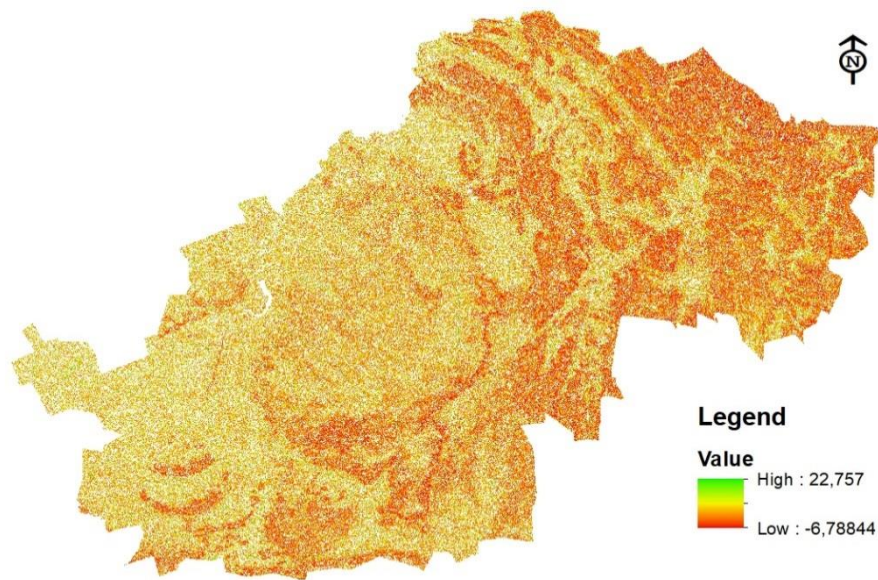


Figure 4.8 The spatial distribution map of topographic wetness index across the study area.

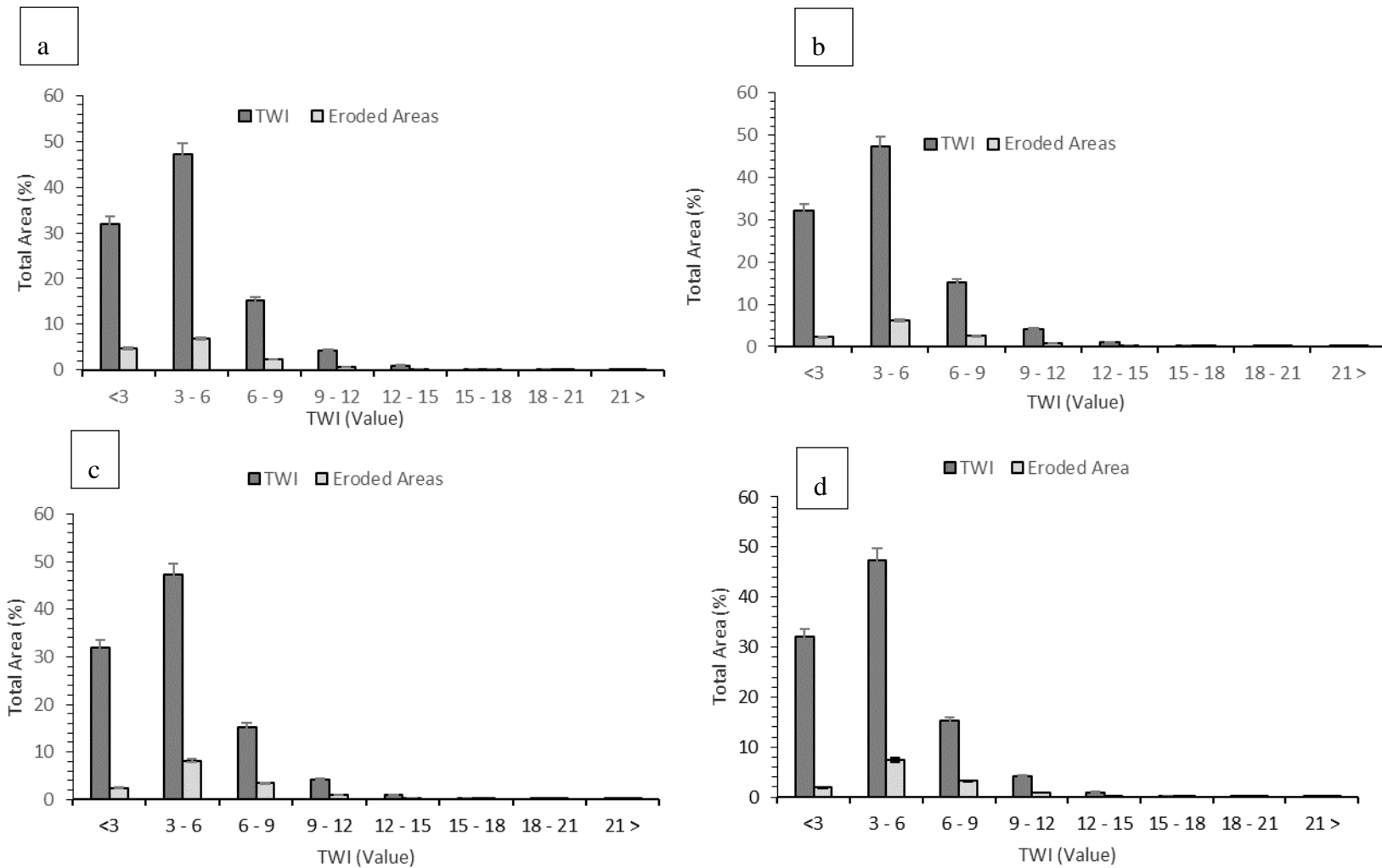


Figure 4.6: The relationship between TWI and area under erosion in 2002 (a. dry season b. wet season) and 2017 during (c. dry season d. wet season).

4.4. Discussion

The main essence of this study implemented a time-series analysis (2002 and 2017) of soil erosion in the former homelands of Sekhukhune, South Africa, using wet and dry season satellite data. Accurate mapping of eroded areas provides a critical input dataset required for policymaking and fulfilment of United Nation sustainable goals. Specifically, the study aimed assessing and mapping changes of eroded areas (wet and dry season), using multi-date Landsat products 8 Operational Land Imager (OLI) and 7 Enhanced Thematic Mapper (ETM+)), as well as to determine the changes among land cover types. Also, the study sought to find out if the variations in terms of eroded areas can be explained, using variations in the geology, slope, and TWI in the area.

Landsat series data was able to capture the extent of eroded areas in the area under study. The findings of this study show that eroded areas increased in Sekhukhune district between 2002 and 2017. For instance, during this period soil erosion increased by 3.1% in the dry season and 2.84 during the wet season. Shrubland and grasslands shrank from 53.26% to 49.29% during the dry season. Similarly, the same trend was observed for other land cover types considered in this study except for the built-up areas which increased by 3.51% during the dry season and 2.69% during the wet season. The observed findings can be attributed to increased population and pressure on land. Literature shows that population in Sekhukhune District increased 92922 between 2011 and 2016 (Toggle navigation Municipalities of South Africa, 2018). Since the area is more rural the land was exposed to overgrazing, for example, The Local Level Land Degradation Assessment (LADA) project conducted in the district indicated that Greater Sekhukhune District falls under Limpopo province and is among some of the areas which are badly degraded due to un-sustained human activities (Stronger et al. 2009).

Results of this study also show that the dominant geology type that suffered soil disturbances by erosion activities are the Lebowa granite (Red and Granite, Fine- to medium-grained) and Rustenburg layered its lithology strata is Pyroxenite, norite, anorthosite, chromitite, Gabbro, norite, anorthosite, Black magnetite gabbro). This could be attributed to the fact that these geology types are weakly structured; hence, they are highly affected by erosion activities. For

example, the literature shows that land surface areas characterized by the Norite, Dsjate, Dwars and granite rocks that form part of lebowa and Rustenburg parent material are more vulnerable to erosion the area under study (Efthimiou, 2018, Oparaku, and Iwar, 2018). The study conducted by Blom, (2012) indicated that for granite samples, erosion rates were higher for samples taken from high flow locations than for thalweg samples, although not to the extent found in the sandstone and basalt samples.

Moreover, the results of this study furthermore show that the influence of steepness of slope was observed mostly between 2-5% (1.1^0-3^0) particularly in the dry season of 2017. This steepness interval is nearly level where mostly anthropogenic/human activities take place including animal grazing lands and habitation. Therefore, we notice from this that extreme slope (45-70%), and Steeper slope (70-100%) have less influence on areas affected by erosion. In addition to the topographic effect, the highest TWI values that experienced much of erosion is between 3 and 6 TWI values in all the season of different years but the dry season of 2002 being slightly higher than the rest followed by 2017 dry season. From the TWI result, we can be concluded that dry season has too much influence on the capacity of erosion, particularly on minimum TWI values. However, the study by Seutloali et al. (2017) made the analysis of topographic variables extracted from DEM and indicated that highly eroded areas are characterized by steeper slope gradients and higher Stream power index (SPI) as compared to areas of low erosion levels. Previous studies have demonstrated that soil erosion increases with increasing slope gradient (Cerdà, 2007; Seutloali and Beckedahl, 2015). Nevertheless, in this study, areas that experienced much of erosion are within gentle slope in percentage and low TWI and this can be motivated by the fact that human activities are the main factor that contributes to affected areas. The study by Sheshukov et al. (2018) indicated that Topographic index models provide simplistic methods to predict the location and trajectory of the area affected by erosion. Even though this approach is certainly useful in assessing the extent of soil erosion related factors, only a few studies have used DEMs derived from satellite data for soil erosion studies (Vrieling, 2006; Sepuru and Dube, 2018;).

The results have demonstrated that areas of under erosion associated with Geology, slope, and TWI. Therefore, the improperly reclaimed farmland from grassland should be returned to grazing to minimize its vulnerability to erosion. Since grassland degradation is caused primarily by

overgrazing, rehabilitation of degraded grassland can be achieved by reducing grazing intensity to a sustainable level. The number of herds that can be supported by the grassland resource should be based strictly on grassland carrying capacity. Those severely overgrazed areas should be sealed off from grazing to give the grass a chance to regenerate. For instance, grazing should be banned temporarily toward wet season each year when the grass just turns green (Li et al., 2002).

4.5. Conclusions

The main aim of this study was to implement a time-series analysis (2002 and 2017) of soil erosion in the former homelands of Sekhukhune, South Africa was done, using wet and dry season satellite data. Additionally, the derived eroded areas were extracted and an overlay analysis was performed to assess whether and to what extent the observed erosional trends can be explained using geology, Topographic Wetness Index and the slope of the area under study. The results show that soil erosion increased significantly between 2002 and 2017. Further, it was observed from the results that soil moisture and geology i.e. Lebowa granite and Rustenburg layered had an influence on erosion occurrence when compared to slope characteristics. The results of this study can possibly assist in directing future studies in integrating remote sensing technologies with topographic characteristics for understanding soil erosion and devising sustainable erosion conservation strategies at a regional scale and particularly in resource-constrained Africa where costly and intensive field surveys are only reliable methods.

5. Chapter Five

ASSESSING THE USE OF MULTISPECTRAL REMOTE SENSING IN MAPPING THE SPATIO-TEMPORAL VARIATIONS OF SOIL EROSION: A SYNTHESIS

5.1. Introduction

Soil erosion is one of the major environmental problems in South Africa and the world-over (Wessels et al. 2004). The complex soil erosion problem and its associated various impacts have attracted research from different disciplines. However, most studies stated that human activities are central in deteriorating the state of the environment (e.g. Kellner 2002, Wessels et al. 2007). Among the anthropogenic activities that exacerbate soil erosion, land cover has been selected as the significant element. Although many researchers have studied various aspects of soil erosion, the spatial and temporal soil degradation paths and landscape developments have received little attention. Moreover, studies that looked at spatial and temporal soil degradation patterns focussed much in the developed world with limited application in resource constraint regions, due to the lack of high-resolution data. To overcome this challenge, therefore, there is need to consider the new crop of freely available new generation multispectral sensors, with improved sensing capabilities e.g. a large swath-width, high spatial resolution ($\pm 10\text{m}$) and improved noise-to-signal ratio. The focus of this research study was to therefore to assess the use of new generation multispectral remote sensing sensors in mapping and monitoring the spatio-temporal variations of soil erosion in the former homelands of Sekhukhune District, South Africa. Hence, the objectives of this study were to:

- i. determine the optimal new generation satellite data that can accurately map the spatial distribution of soil erosion in the former rural homelands of Sekhukhune, South Africa
- ii. map the seasonal and long term variations in soil erosion in the former homelands of Sekhukhune, Limpopo using multi-date satellite data

5.2. Comparing the effectiveness of Landsat 8 and Sentinel-2 data in mapping soil erosion

The review of literature indicated that that the new crop of sensors, such as Sentinel-2 and Landsat 8 OLI, with improved spatial, spectral radiometric and temporal resolutions have not been tested in soil erosion monitoring, despite the overwhelming capacity to provide the most

needed spatial tool for monitoring eroded areas at low costs (Sepuru and Dube, 2017). The aim of the study was to assess the use of multispectral remote sensing sensors in mapping and monitoring the spatio-temporal variations of soil erosion in the study area. Based on research findings from this study, the two new non-commercial multispectral remote sensing data: Landsat 8 OLI and Sentinel-2 MSI indicated their unique abilities in effectively assessing and mapping soil erosion (chapter 3). The magnitude of variation inaccuracies between the two sensors revealed that the integration of spectral bands and spectral vegetation indices showed that Sentinel-2 (OA = 83, 81%), slightly performed better than Landsat 8, with 82, 86%. However, the comparison of these sensors demonstrates Sentinel 2 MSI, as a better alternative for mapping and monitoring soil erosion at various scales given its high resolution and other related sensing characteristics. The slightly weaker performance of Landsat 8 when compared to Sentinel-2 can be associated with mixed pixel challenge (Dube, 2015). ANOVA results revealed that there are significant differences ($p < 0.05$) to discriminate eroded areas from other land cover types from Landsat 8 OLI and Sentinel-2 MSI. Sentinel-2 MSI bands located in the NIR (0.785-0.900 μm), red edge (0.698-0.785 μm) and SWIR (1.565-2.280 μm) regions were selected as the most optimal for discriminating degraded soils from other land cover types. However, for Landsat 8 OLI, only the SWIR (1.560-2.300 μm), NIR (0.845-0.885 μm) region were selected as the best regions. Of the eighteen spectral vegetation indices computed, Normalized Difference Vegetation Index (NDVI) and Soil Adjusted Vegetation Index (SAVI) and Global Environmental Monitoring Index (GEMI). The findings show that the lack of red edge bands in most multispectral sensors downplays their potential in mapping environmental properties (Korhonen et al. 2017).

5.3. Map the seasonal and long term variations in soil erosion in the former homelands of Sekhukhune, Limpopo using multi-date satellite data

Although sentinel 2 data demonstrated overwhelming performance in soil erosion, its applications on long-term soil erosion monitoring remains restricted due to the lack of backdating archival data. Based on research findings from this study, multi-date Landsat products 8 OLI and 7 ETM+ were used to determine and map the seasonal and long term variations in soil erosion in the former homelands of Sekhukhune, Limpopo. The results revealed changes of eroded areas (wet and dry season) amongst other land cover classes from 2002 to 2017

(chapter 4). For the dry season of 2002, 16.61 % (224733 ha) of the area was classified as eroded, whereas in 2017, 19.71% was noted. A similar trend was also observed in the wet season. The results also showed that the Lebowa granite and Rustenburg layered its lithology strata experienced more erosional disturbances than other geological types. This could be attributed to the fact that these geology types are weakly structured; hence, they are highly affected by erosion activities. For example, the literature shows that land surface areas characterized by the Norite, Dsjate, Dwars and granite rocks, which form part of lebowa and Rusternburg parent material, are more vulnerable to erosion the area under study (Efthimiou, 2018, Oparaku, and Iwar, 2018). The study conducted by Blom, (2012) indicated that for granite samples, erosion rates were higher for samples taken from high flow locations than for thalweg samples, although not to the extent found in the sandstone and basalt samples. Slopes between 2-5% (Nearly level) experienced more erosion and vice-versa. On the hand, the relationship between TWI and eroded areas showed that much erosion occurred between 3 and 6 TWI values in all the seasons for the two different years, however, the dry season of 2002 had a slightly higher relationship and vice-versa. The observed findings can be attributed to increased population and pressure on land (Schillaci, et al., 2017). Literature shows that population in more rural the land is exposed to overgrazing, leading to bad erosion due to un-sustained human activities (Stronger et al. 2009).

5.4. Conclusions

The overall aim of the study was to assess the use of multispectral remote sensing sensors in mapping and monitoring the spatio-temporal variations of soil erosion in the former homelands of Sekhukhune district, South Africa. The results of this study have demonstrated that the soil erosion can be mapped and monitored, using freely available new generation multispectral remote sensing dataset, particularly in countries similar to South Africa where purchasing data is a limitation in monitoring erosion as one of the major environmental problem.

Based on the results achieving the objectives of the study, the following was concluded:

- i. The new crop of sensors, such as Landsat 8 OLI and Sentinel-2 MSI series, with improved spatial, spectral radiometric and temporal resolutions provide the most needed spatial data for monitoring soil erosion at low costs.

- ii. The integration of Landsat 8 OLI and Sentinel-2 MSI derived raw spectral bands and vegetation indices significantly ($\alpha = 0.005$) improved the detection and mapping accuracies. Sentinel-2 MSI produced an overall classification accuracy of more than 80% whilst Landsat 8 OLI with more than 75% of all tested analytical stages. With this slight accuracy differences, the findings demonstrate that the new free multispectral sensors remain a potential primary data source for assessing soil erosion at the regional scale.
- iii. The results show that soil erosion increased significantly over the study period in the former homelands of Sekhukhune South Africa.
Further, soil moisture and geology i.e. Lebowa granite and Rustenburg layered had an influence on erosion occurrence when compared to topographic characteristics.

5.5. Recommendations

In view of the research findings and conclusions, the following recommendations for future research are suggested:

- i. Although the current study demonstrated accurate mapping and monitoring eroded areas from the use of new and freely available multispectral remote sensing sensors, it will be clearer for future research to further assess and compare the effectiveness of these sensors compared to those of high resolution such as hyperspectral data sets in mapping and monitoring eroded areas.
- ii. future experiments on the usefulness of these data sets need to be tested in mapping and monitoring different the levels of soil erosion (e.g. sheet, rills, and gullies),
- iii. There is need to develop a regional or national scale soil erosion mapping and monitoring if large-scale preventive and rehabilitation measures are to developed.

References

- Abbas, I.I., 2009. An overview of land cover changes in Nigeria, 1975-2005. *J. Geo. Reg. Plan.* 2 (4), 62.
- Adeyeri, O.E., Akinsanola, A.A., Ishola, K.A., 2017. Investigating surface urban heat island characteristics over Abuja: Nigeria: relationship between land surface temperature and multiple vegetation indices. *Remote Sens. Appl.: Soc. Environ.* 7, 57–68.
- Alatorre, L.C., Beguería, S., 2009. Identification of eroded areas using remote sensing in a badlands landscape on marls in the central Spanish Pyrenees. *Catena* 76 (3), 182–190.
- Alhawiti, R.H., Mitsova, D., 2016. Using Landsat-8 data to explore the correlation between urban heat island and urban land uses. *IJRET: Int. J. Res. Eng. Technol.* 5 (3), 457–466.
- Avdan, U., Jovanovska, G., 2016. Algorithm for automated mapping of land surface temperature using LANDSAT 8 satellite data. *J. Sens* 2016.
- Baade, J., Franz, S., Reichel, A., 2012. Reservoir siltation and sediment yield in the Kruger National Park, South Africa: a first assessment. *Land Degrad. Dev.* 23 (6), 586–600.
- Bai, Z., Dent, D., 2007. Land degradation and improvement in South Africa 1: identification by remote sensing. International Soil Reference and Information Centre (ISRIC), Wageningen (Report 2007/03).
- Balaguer-Puig, M., Marqués-Mateu, Á., Lerma, J.L., Ibáñez-Asensio, S., 2017. Estimation of small-scale soil erosion in laboratory experiments with Structure from Motion photogrammetry. *Geomorphology* 295, 285–296.
- Baret, F., Guyot, G., 1991. Potentials and limits of vegetation indices for LAI and APAR assessment. *Remote Sens. Environ.* 35 (2–3), 161–173.
- Baret, F., Jacquemoud, S., Hanocq, J.F., 1993. The soil line concept in remote sensing. *Remote Sens. Rev.* 7 (1), 65–82.
- Barnes, E.M., Baker, M.G., 2000. Multispectral data for mapping soil texture: possibilities and limitations. *Appl. Eng. Agric.* 16, 731–741.
- Beck, M.B., 1987. Water quality modeling: a review of uncertainty. *Water Resour. Res.* 23, 1393–1442.

- Beguería, S., 2006. Identifying erosion areas at basin scale using remote sensing data and GIS: a case study in a geologically complex mountain basin in the Spanish Pyrenees. *Int. J. Remote Sens.* 27 (20), 4585–4598.
- Bennett, J.P., 1974. Concepts of mathematical modeling of sediment yield. *Water Resour. Res.* 10, 485–492.
- Bennett, J.P., Palmer, A., Blackett, M., 2012. Range degradation and land tenure change: insights from a ‘released’ communal area of Eastern Cape Province, South Africa. *Land Degrad. Dev.* 23 (6), 557–568.
- Beven, K.J. and Kirkby, M.J., 1979. A physically based, variable contributing area model of basin hydrology/Un modèle à base physique de zone d'appel variable de l'hydrologie du bassin versant. *Hydrological Sciences Journal*, 24(1), pp.43-69.
- Blackburn, G.A., 1998. Spectral indices for estimating photosynthetic pigment concentrations: a test using senescent tree leaves. *Int. J. Remote Sens.* 19 (4), 657–675.
- Blom, T., 2012. Rock weathering effects on bedrock channel erosion determined via abrasion mill experiments (Doctoral dissertation, University of Colorado at Boulder).
- Blum, W.E.H., 2005. Functions of soil for Society and the environment. *Rev. Environ. Sci. Biotechnol.* 4, 75–79.
- Boardman, J., 2006. Soil erosion science: reflections on the limitations of current approaches. *Catena* 68, 73–86.
- Bocco, G., Valenzuela, C.R., 1988. Integration of GIS and image processing in soil erosion studies using ILWIS. *ITC J.* 4, 309–319.
- Botha, G.A., Wintle, A.G., Vogel, J.C., 1994. Episodic late quaternary palaeogully erosion in northern Kwazulu-Natal, South Africa. *Catena* 23, 327–340.
- Botha, J.H., Fouche, P.S., 2000. An assessment of land degradation in the northern province from satellite remote sensing and community perception. *South Afr. Geogr. Soc.* 82, 70–79.
- Brazier, R.E., Beven, K.J., Freer, J., Rowan, J.S., 2000. Equifinality and uncertainty in physically based soil erosion models: application of the GLUE methodology to WEPP—the Water Erosion Prediction Project—for sites in the UK and USA. *Earth Surf. Processes Landf.* 25 (8), 825–845.

- Clark, M.L., Kilham, N.E., 2016. Mapping of land cover in northern California with simulated hyperspectral satellite imagery. *ISPRS J. Photogramm. Remote Sens.* 119, 228–245.
- Coetzer, K.L., Erasmus, B.F., Witkowski, E.T. and Reyers, B., 2013. The race for space: tracking land-cover transformation in a socio-ecological landscape, South Africa. *Environmental management*, 52(3), pp.595-611.
- Croke, J., Mockler, S., 2001. Gully initiation and road-to-stream linkage in a forested catchment, southeastern Australia. *Earth Surface Processes and Landforms* 26 (2), 205–217.
- Dang, A., Zhang, S., He, X., Tang, L., Xu, H., 2003. Case study on soil erosion supported by GIS and RS.
- Davaasuren, N., 2001. Information System Design for Land Degradation Assessment, in Particular for Pasture Areas: Case Study of West Mongolia (Doctoral dissertation, International Institute for Aerospace Survey and Earth Sciences, Enschede, Netherlands).
- De Asis, A.M., Omasa, K., 2007. Estimation of vegetation parameter for modeling soil erosion using linear spectral mixture analysis of land sat ETMdata. *ISPRS J. Photo Gramme. Remote Sens.* 62, 309–324.
- De Jong, S.M., Paracchini, M.L., Bertolo, F., Folving, S., Megier, J., De Roo, A.P.J., 1999. Regional assessment of soil erosion using the distributed model SEMMED and remotely sensed data. *Catena* 37 (3), 291–308.
- Deeks, L.K., Duzant, J.H., Owens, P.N. and Wood, G.A., 2012. A decision support framework for effective design and placement of vegetated buffer strips within agricultural field systems. In *Advances in agronomy* (Vol. 114, pp. 225-248). Academic Press.
- Deering, D.W., Rouse, J.W., Haas, R.H., Schell, J.A., 1975. Measuring “forage production” of grazing units from Landsat MSS data. *Proceedings of the 10th International Symposium on Remote Sensing of Environment* 11, 1169–1178.
- Department Of Agriculture Forestry and Fisheries, 2015. *Economic Review of South African Agriculture for the Year Ended 31 December 2015*.
- Department of Agriculture, Forestry, and Fisheries, 2010. *Abstract of Agricultural Statistics*. South Africa, Pretoria.

- Department of Environmental Affairs and Tourism, (2005). Land degradation. Available at: <http://soer.deat.gov.za/themes> [accessed 10 February 2017].
- Department of Environmental Affairs, Tourism, 2006. South Africa Environment Outlook. A Report on the State of the Environment. Department of Environmental Affairs and Tourism, Pretoria. 371pp.
- Dhakal, A.S., Amada, T., Aniya, M., Sharma, R.R., 2002. Detection of areas associated with flood and erosion caused by a heavy rainfall using multitemporal landsat TM data. *Photogramm. Eng. Remote Sens.* 68 (3), 233–239.
- Dube, T., Mutanga, O., Sibanda, M., Seutloali, K., Shoko, C., 2017. Use of Landsat series data to analyse the spatial and temporal variations of land degradation in a dispersive soil environment: a case of King Sabata Dalindyebo local municipality in the Eastern Cape Province, South Africa. *Phys. Chem. Earth* 1–9.
- Dwivedi, R.S., Kumar, A.B., Tewari, K.N., 1997. The utility of multi-sensor data for mapping eroded lands. *Int. J. Remote Sens.* 18 (11), 2303–2318.
- Eswaran, H., Lal, R., Reich, P.F., 2001. Land degradation: an overview. In: Bridges, E.M.,
- Efthimiou, N., 2018. The importance of soil data availability on erosion modeling. *CATENA*, 165, pp.551-566.
- Fadul, H.M., Salih, A.A., Imad-eldin, A.A., Inanaga, S., 1999. Use of remote sensing to map gully erosion along the Atbara River, Sudan. *Int. J. Appl. Earth Obs. Geoinf.* 1 (3–4), 175–180.
- Finch, S., Samuel, A. and Lane, G.P., 2014. *Lockhart and Wiseman's Crop Husbandry Including Grassland*. Elsevier.
- Fistikoglu, O., Harmancioglu, N.B., 2002. Integration of GIS with USLE in assessment of soil erosion. *Water Resour. Manag.* 16 (6), 447–467.
- Flanagan, D.C., Laflen, J.M., 1997. USDA water erosion prediction project (WEPP). *Eurasia. Soil Sci.* 30, 524–530.
- Floras, S.A., Sgouras, I.D., 1999. Use of geoinformation techniques in identifying and mapping areas of erosion in a hilly landscape of central Greece. *Int. J. Appl. Earth Obs. Geoinf.* 1, 68–77.

- Fulajtar, E., 2001. Identification of severely eroded soils from remote sensing data tested in Risnovce, Slovakia. In: D.E., Stott, R.H., Mohtar and G.C., Steinhardt (Eds.), *Sustaining the Global Farm*. 1075–1081.
- Gandhi, M.G., Parthiban, S., Thummalu, N., Christy, A., 2015. Vegetation change detection using remote sensing and gis. A case study of Vellore District. *Procedia Comput. Sci.* 57, 1199–1210.
- Gao, B.C., 1996. NDWI—a normalized difference water index for remote sensing of vegetation liquid water from space. *Remote Sens. Environ.* 58 (3), 257–266.
- Garen, D., Woodward, D., Geter, F., 1999. A user agency's view of hydrologic, soil erosion and water quality modelling. *Catena* 37, 277–289.
- Garland, G.G., Hoffman, M.T., Todd, S., 2000. *Soil degradation*. M. T. Hoffman, Todd.
- Gavier-Pizarro, G.I., Kuemmerle, T., Hoyos, L.E., Stewart, S.I., Huebner, C.D., Keuler, N.S., Radeloff, V.C., 2012. Monitoring the invasion of an exotic tree (*Ligustrum lucidum*) from 1983 to 2006 with Landsat TM/ETM+ satellite data and Support Vector Machines in Córdoba, Argentina. *Remote Sens. Environ.* 122, 134–145.
- Geymen, A., Baz, I., 2008. The potential of remote sensing for monitoring land cover changes and effects on physical geography in the area of Kayisdagi mountain and its surroundings (Istanbul). *Environmental Monitoring and Assessment* 140 (1–3), 33–42
- Giannecchini, M., Twine, W. and Vogel, C., 2007. Land-cover change and human-environment interactions in a rural cultural landscape in South Africa. *The Geographical Journal*, 173(1), pp.26-42.
- Gibbs, H.K. and Salmon, J.M., 2015. Mapping the world's degraded lands. *Applied Geography*, 57, pp.12-21.
- Gitelson, A.A., Kaufman, Y.J., Stark, R., Rundquist, D., 2002. Novel algorithms for remote estimation of vegetation fraction. *Remote Sens. Environ.* 80 (1), 76–87.
- Gitelson, A.A., Merzlyak, M.N., Lichtenthaler, H.K., 1996. Detection of red edge position and chlorophyll content by reflectance measurements near 700 nm. *J. Plant Physiol.* 148 (3–4), 501–508.

- Gitelson, A.A., Vina, A., Ciganda, V., Rundquist, D.C., Arkebauer, T.J., 2005. Remote estimation of canopy chlorophyll content in crops. *Geophys. Res. Lett.* 32 (8).
- Gualtieri, J.A., Chettri, S.R., Crompton, R.F., Johnson, L.F., 1999. Support vector machine classifiers as applied to AVIRIS data.
- Guidici, D., Clark, M.L., 2017. One-Dimensional Convolutional Neural Network Land- Cover Classification of Multi-Seasonal Hyperspectral Imagery in the San Francisco Bay Area California. *Remote Sens.* 9 (6) p.629.
- Hannam, I.D., Oldeman, L.R., Penning de Vries, F.W.T., Scherr, S.J., Sombatpanit, S. (Eds.), Response to land degradation. Science Publishers Inc, Enfield, NH, USA, pp. 20–35.
- Haubrock, S.N., Chabrillat, S., Lemmertz, C., Kaufmann, H., 2008. Surface soil moisture quantification models from reflectance data under field conditions. *Int. J. Remote sens.* 29 (1), 3–29.
- Hermes, L., Frieauff, D., Puzicha, J., Buhmann, J.M., 1999. Support vector machines for land usage classification in Landsat TM imagery. Hamburg, Germany pp. 348–350.
- Hochschild, V., Märker, M., Rodolfi, G., Staudenrausch, H., 2003. Delineation of erosion classes in semiarid southern African grasslands using vegetation indices from optical remote sensing data. *Hydrol. Process.* 17, 917–928.
- Hoffman, M.T., 2014. Changing patterns of rural land use and land cover in South Africa and their implications for land reform. *Journal of Southern African Studies*, 40(4), pp.707-725.
- Huang, C., Davis, L.S., Townshend, J.R.G., 2002. An assessment of support vector machines for land cover classification. *Int. J. Remote Sens.* 23 (4), 725–749.
- Huang, C.H., Laflen, J.M., Bradford, J.M., 1996. Evaluation of the detachment-transport coupling concept in the WEPP rill erosion equation. *Soil Sci. Soc. Am. J.* 60 (3), 734–739.
- Hudson, N.W., 1995. Soil Conservation. BT Batsford Limited, London.
- Huete, A., Justice, C., Van Leeuwen, W., 1999. MODIS vegetation index (MOD13). Algorithm Theor. Basis Doc. 3 p.213.
- Huete, A.R., 1988. A Soil Adjusted Vegetation Index (SAVI). *Remote Sens. Environ.* 25 (3), 295–309.

- Huete, A.R., Liu, H.Q., 1994. An error and sensitivity analysis of the atmosphere- and soil correcting variants of the NDVI for the MODIS-EOS. *IEEE Trans. Geosci. Remote Sens.* 32 (4), 897–905.
- Ighodaro, I.D., Lategan, F.S., Yusuf, S.F., 2013. The impact of soil erosion on agricultural potential and performance of Sheshegu community farmers in the Eastern Cape of South Africa. *J. Agric. Sci.* 5 (5), p.140.
- IPCC (Intergovernmental Panel on Climate Change), 2001. *Climate change 2001: Impacts, adaptation and vulnerability* [online]. Available from http://www.grida.no/climate/ipcc_tar/wg2/index.htm [Accessed 26 May 2017].
- Irons, J.R., Weismiller, R.A., Petersen, G.W., 1989. Soil reflectance. In: Asrar, G.E. (Ed.),
- Jackson, R.D., and A.R. Huete, 1991. Interpreting vegetation indices. *Remote Sensing of the Environment*, 11:185-200.
- Jahun, B.G., Ibrahim, R., Dlamini, N.S., Musa, S.M., 2015. Review of soil erosion assessment using RUSLE model and GIS. *J. Biol. Agric. Healthcare* 5 (9), 36–47.
- Jensen, J.R., 2005. *Introductory digital image processing*, 3rd ed. Pearson Prentice Hall, United States of America.
- Jetten, V., Govers, G., Hessel, R., 2003. Erosion Models: quality of Spatial Predictions. *Hydrol. Process.* 17 (5), 887–900.
- Jordán, A. and Martínez-Zavala, L., 2008. Soil loss and runoff rates on unpaved forest roads in southern Spain after simulated rainfall. *Forest Ecology and Management*, 255(3-4), pp.913-919.
- Kakembo, V. and Rowntree, K.M., 2003. The relationship between land use and soil erosion in the communal lands near Peddie Town, Eastern Cape, South Africa. *Land Degradation & Development*, 14(1), pp.39-49.
- Karami, A., Khorani, A., Noohegar, A., Shamsi, S.R.F., Moosavi, V., 2015. Gully erosion mapping using object-based and pixel-based image Classification methods. *Environ. Eng. Geosci.* 27 (2), 101–110.
- Keesstra, S.D., Bouma, J., Wallinga, J., Tiftonell, P., Smith, P., Cerdà, A., Montanarella, L., Quinton, J.N., Pachepsky, Y., van der Putten, W.H. and Bardgett, R.D., 2016. The significance of soils

- and soil science towards realization of the United Nations Sustainable Development Goals. *Soil*, 2(2), p.111.
- Khan, N.I., Islam, A., 2003. Quantification of erosion patterns in the brahmaputrajamuna river using geographical information system and remote sensing techniques. *Hydrol. Process.* 17 (5), 959–966.
- Kimura, R., 2007. Estimation of moisture availability over the Liudaogou river basin of the Loess Plateau using new indices with surface temperature. *J. Arid. Environ.* 70, 237–252.
- King, C., Baghdadi, N., Lecomte, V., Cerdan, O., 2005. The application of remote-sensing data to monitoring and modelling of soil erosion. *Catena* 62 (2), 79–93.
- Kirui, O., Mirzabaev, A., 2015. Costs of land degradation in Eastern Africa. In: 2015 Conference. August 9–14, 2015, Milan, Italy (No. 212007), International Association of Agricultural Economists.
- Kiusi, R.B., Meadows, M.E., 2006. Assessing land degradation in the monduli district, northern Tanzania. *Land Degrad. Dev.* 17, 509–525.
- Knight, J., Spencer, J., Brooks, A., Phinn, S., 2007. Large area, high-resolution remote sensing based mapping of alluvial gully erosion in Australia’s tropical rivers. In *Proceedings of the 5th Australian Stream Management Conference: Australian Rivers: Making a difference*, New South Wales, Australia, pp. 199–204.
- Korhonen, L., Packalen, P., Rautiainen, M., 2017. Comparison of Sentinel-2 and Landsat 8 in the estimation of boreal forest canopy cover and leaf area index. *Remote Sens. Environ.* 195, 259–274.
- Korhonen, L., Packalen, P., Rautiainen, M., 2017. Comparison of Sentinel-2 and Landsat 8 in the estimation of boreal forest canopy cover and leaf area index. *Remote Sens. Environ.* 195, 259–274.
- Kwanele, P., Njoya, S.N., 2017. Mapping soil erosion in a Quaternary catchment in Eastern Cape using Geographic information system and remote sensing. *South Afr. J. Geomat.* 6 (1), 11–29.
- LADA (Land Degradation Assessment in Drylands), 2002. *Land Degradation in Drylands. Proceedings of the FAO workshop held 5-7 December 2002.* Rome: Food and Agriculture Organisation.

- Lafarge, F., Descombes, X., Zerubia, J., 2005. Textural kernel for SVM classification in remote sensing: Application to forest fire detection and urban area extraction.
- Lafren, J.M., Flanagan, D.C., Engel, B.A., 2004. Soil erosion and sediment yield prediction accuracy using WEPP. *JAWRA J.Am. Water Res.Assoc.* 40 (2), 289–297.
- Lal, R., 1994. Soil erosion research methods. Soil and Water Conservation Society, Ankeny.
- Lal, R., 2001. World cropland soils as a source or sink for atmospheric carbon. *Adv. Agron.* 71, 145–191.
- Lawrence, R.L., Ripple, W.J., 1998. ‘Comparison among vegetation indices and bandwise regression in a highly disturbed heterogeneous landscape: mount St. Helens, Washington’. *Remote Sens. Environ.* 64 (1), 91–102.
- Le Roux, J., Newb T.S., and Sumner P.D, 2007. "Monitoring soil erosion in South Africa at a regional scale: review and recommendations." *South African Journal of Science* 103(7-8): 329-335
- Le Roux, J.J. and Germishuys, T., 2007. Modelling sediment yield for an agricultural research catchment in KwaZulu-Natal.
- Le Roux, J.J., Morgenthal, T.L., Malherbe, J., Pretorius, D.J., Sumner, P.D., 2008. Water erosion prediction at a national scale for South Africa. *Water SA* 34 (3), 305–314.
- Le Roux, J.J., Newby, T.S., and Sumner, P.D., 2007. Monitoring soil erosion in South Africa at a regional scale: review and recommendations. *South African Journal of Science*, 103(7-8), pp.329-335.
- Liggitt, B., 1988. An investigation into soil erosion in the Mfolozi catchment.
- Lillesand, T.M., Kiefer, R.W., 1994. *Remote Sensing and Image Interpretation*. John Wiley and Sons, Inc, New York.
- Lo Curzio, S., Magliulo, P., 2010. Soil erosion assessment using geomorphological remote sensing techniques: an example from southern Italy. *Earth Surf. Processes Landf.* 35 (3), 262–271.
- Lu, D., Weng, Q., 2007. A survey of image classification methods and techniques for improving classification performance. *Int. J. Remote Sens.* 28 (5), 823–870.

- Luleva, M.I., van de Werff, H., van der Meer, F., Jetten, V., 2012. Gaps and opportunities in the use of remote sensing for soil erosion assessment. *Chem.: Bulg. J. Sci. Educ.* 21 (5), 748–764.
- Madikizela, P.N.T., 2000. Spatial and temporal aspects of soil erosion in Mt Ayliff and MtFrere, Eastern Cape province, South Africa.
- Maskey, R.B., Binod, P., Sharma, S. and Joshi, M., 2003, October. Human dimensions in sustainable land use management in degraded land areas of Nepal. In *The open meeting of the global environmental change research community*.
- Mathieu, R., King, C., Le Bissonnais, Y., 1997. Contribution of multi-temporal SPOT data to the mapping of a soil erosion index. The case of the loamy plateau of northern France. *Soil Technol.* 10 (2), 99–110.
- Matongera, T.N., Mutanga, O., Dube, T., Sibanda, M., 2017. Detection and mapping the spatial distribution of bracken fern weeds using the Landsat 8 OLI new generation sensor. *Int. J. Appl. Earth Obs. Geoinf.* 57, 93–103.
- McFeeters, S.K., 1996. The use of the Normalized Difference Water Index (NDWI) in the delineation of open water features. *Int. J. Remote Sens.* 17 (7), 1425–1432.
- Merritt, W.S., Letcher, R.A., Jakeman, A.J., 2003. A review of erosion and sediment transport models. *Environ. Model. Softw.* 18, 761–799.
- Metternicht, G.I., Zinck, J.A., 1998. Evaluating the information content of JERS-1 SAR and Landsat TM data for discrimination of soil erosion features. *ISPRS J. Photogramm. Remote Sens.* 53 (3), 143–153.
- Mhangara, P., 2011. Land use/cover change modelling and land degradation assessment in the Keiskamma catchment using remote sensing and GIS (Doctoral dissertation).
- Millington, A.C., Townshend, J.R.G., 1984. Remote sensing applications in African erosion and sedimentation studies. *Challenges in African hydrology and water resources* 144. IAHS Press IAHS Publ., Wallingford, UK, pp. 373–384.
- Mondal, A., Khare, D., Kundu, S., 2017. Uncertainty analysis of soil erosion modelling using different resolution of open-source DEMs. *Geocarto Int.* 32 (3), 334–349.

- Morgan, R.P.C., 2005. Soil erosion and conservation, 3rd ed. Blackwell Publishing, Malden, Oxford, Victoria.
- Mousazadeh, F. and Salleh, K.O., 2014. The influence of lithology and soil on the occurrence and expansion of gully erosion, Toroud Basin–Iran. *Procedia-Social and Behavioral Sciences*, 120, pp.749-756.
- Mpandeli, S., Nesamvuni, E., Maponya, P., 2015. Adapting to the impacts of drought by smallholder farmers in sekhukhune district in limpopo province, South Africa. *J. Agric. Sci.* 7 (2), p.115.
- Muttitanon, W. and Tripathi, N.K., 2005. Land use/land cover changes in the coastal zone of Ban Don Bay, Thailand using Landsat 5 TM data. *International Journal of Remote Sensing*, 26(11), pp.2311-2323.
- Nearing, M.A., Pruski, F.F., O’Neal, M.R., 2004. Expected climate change impacts on soil erosion rates, a review. *J. Soil Water Conserv.* 59 (1), 43–50.
- Nichol, J.E., Shaker, A., Wong, M.S., 2006. Application of high-resolution stereo satellite images to detailed landslide hazard assessment. *Geomorphology* 76 (1), 68–75.
- Nigel, R., Rughooputh, S., 2010. Mapping of monthly soil erosion risk of mainland Mauritius and its aggregation with delineated basins. *Geomorphology* 114, 101–114.
- Nkonya, E., von Braun, J., Mirzabaev, A., Le, Q.B., Kwon, H.Y., Kirui, O., 2013. *Economics of Land Degradation Initiative: Methods and Approach for Global and National Assessments*.
- Oldeman, L.R., Hakkeling, R.U., Sombroek, W.G., 1990. World map of the status of human-induced soil degradation: an explanatory note. *Int. Soil. Ref. Inf. Cent.*
- Omuto, C.T., Shrestha, D.P., 2007. Remote sensing techniques for rapid detection of soil physical degradation. *Intern. J. Remote Sens.* 28, 4785–4805.
- Onyando, J.O., Kisoyan, P., Chemelil, M.C., 2005. Estimation of potential soil erosion for river perkerra catchment in Kenya. *Water Resour. Manag.* 19, 133–143.
- Oparaku, L.A. and Iwar, R.T., 2018. Relationships between average gully depths and widths on geological sediments underlying the Idah-Ankpa Plateau of the North Central Nigeria. *International Soil and Water Conservation Research*.

- Petter, P., 1992. GIS and Remote Sensing for Soil Erosion Studies in Semiarid Environments. Ph.D. Thesis. University of Lund, Lund.
- Pickup, G., Nelson, D.J., 1984. Use of Landsat radiance parameters to distinguish soil erosion, stability and deposition in arid central Australia. *Remote Sens. Environ.* 16 (3), 195–209.
- Pinty, B., Verstraete, M.M., 1992. GEMI: a non-linear index to monitor global vegetation from satellites. *Plant Ecol.* 101 (1), 15–20.
- Pontius Jr, R.G., Millones, M., 2011. Death to Kappa: birth of quantity disagreement and allocation disagreement for accuracy assessment. *Int. J. Remote Sens.* 32 (15), 4407–4429.
- Pretorius, D.J., 1998. The Development of Land Degradation Monitoring and Auditing Techniques with the Aid of Remote Sensing and GIS Technology. ISCW Report No. GW/A/98/27. ARC – Institute for Soil, Climate, and Water, Pretoria, South Africa.
- Price, K.P., 1993. Detection of soil erosion within pinyon-juniper woodlands using Thematic Mapper (TM) data. *Remote Sens. Environ.* 45 (3), 233–248.
- Qi, J., Chehbouni, A., Huete, A.R., Kerr, Y.H., Sorooshian, S., 1994. A modified soil adjusted vegetation index. *Remote Sens. Environ.* 48 (2), 119–126.
- Randall, L.A., 1993. Towards the Delineation of Sediment Production Areas Using Satellite Data and GIS. In: Lorentz, S.A., Kienzle, S.W., Dent, M.C. (Eds.), *Proceedings of the Sixth South African National Hydrological Symposium 11*. University of Natal, Pietermaritzburg, South Africa, pp. 531–538.
- Renschler, C., 1996. Soil erosion hazard mapping by means of Geographical Information systems (GIS) and Hydrological modelling (MSc). Technical University of Braunschweig, Braunschweig.
- Richards, J.A., Jia, X., 2006. *Remote sensing digital image analysis: An introduction*, 4th ed. Springer Verlag Berlin Heidelberg, Germany.
- Richardson, A.J., Wiegand, C.L., 1977. Distinguishing vegetation from soil background information. *Photogramm. Eng. Remote Sens.* 43 (12), 1541–1552.
- Roli, F., Fumera, G., 2001. Support Vector Mach. *Remote Sens. Image Classif.* 4170, 160–166.

- Rosewell, C.J., 2001. Evaluation of WEPP for runoff and soil loss prediction in Gunnedah. NSW, Australia. *Austr. J. Soil Res.* 9, 230–243.
- Roujean, J.L., Breon, F.M., 1995. Estimating PAR absorbed by vegetation from bidirectional reflectance measurements. *Remote Sens. Environ.* 51 (3), 375–384.
- Rouse, J.W., Haas, R.H., Schell, J.A., Deering, D.W., 1973. ‘Monitoring vegetation systems in the Great Plains with ERTS’. In: *Proceedings of the 3rd ERTS Symposium, NASA, Washington DC. S., Ntshona, Z., Turner, S (Ed.), A National Review of Land Degradation in South Africa. Pretoria, South Africa: South African National Biodiversity Institute. pp. 69–107.*
- Sanchez, P.A. and Swaminathan, M.S., 2005. Hunger in Africa: the link between unhealthy people and unhealthy soils. *The Lancet*, 365(9457), pp.442-444.
- Sanchez, P.A., 2002. Soil fertility and hunger in Africa. *Science*, 295(5562), pp.2019-2020.
- Schillaci, C., Acutis, M., Lombardo, L., Lipani, A., Fantappie, M., Märker, M. and Saia, S., 2017. Spatio-temporal topsoil organic carbon mapping of a semi-arid Mediterranean region: The role of land use, soil texture, topographic indices and the influence of remote sensing data to modelling. *Science of The Total Environment*, 601, pp.821-832.
- Scottish Environment Protection Agency, 2001. *State of the Environment Soil Quality Report.*
- Sepuru, T.K. and Dube, T., 2017. An appraisal on the progress of remote sensing applications in soil erosion mapping and monitoring. *Remote Sensing Applications: Society and Environment* 9 (2018) 1–9
- Sepuru, T.K. and Dube, T., 2018. Understanding the spatial distribution of eroded areas in the former rural homelands of South Africa: Comparative evidence from two new non-commercial multispectral sensors. *International Journal of Applied Earth Observation and Geoinformation*, 69, pp.119-132.
- Servenay, A., Prat, C., 2003. Erosion extension of indurated volcanic soils of Mexico by aerial photographs and remote sensing analysis. *Geoderma* 117 (3–4), 367–375.
- Seutloali, K.E. and Beckedahl, H.R., 2015. Understanding the factors influencing rill erosion on roadcuts in the south eastern region of South Africa. *Solid Earth*, 6(2), p.633.

- Seutloali, K.E., Dube, T. and Mutanga, O., 2017. Assessing and mapping the severity of soil erosion using the 30-m Landsat multispectral satellite data in the former South African homelands of Transkei. *Physics and Chemistry of the Earth, Parts A/B/C*, 100, pp.296-304.
- Seutloali, K.E., Dube, T., Mutanga, O., 2016. Assessing and mapping the severity of soil erosion using the 30-m Landsat multispectral satellite data in the former South African homelands of Transkei (viewed 06 June 2017). *Phys. Chem. Earth*. [http://dx. doi.org/10.1016/j.pce.2016.10.001](http://dx.doi.org/10.1016/j.pce.2016.10.001).
- Shoko, C., Mutanga, O., 2017. Examining the strength of the newly-launched Sentinel 2 MSI sensor in detecting and discriminating subtle differences between C3 and C4 grass species. *ISPRS J. Photogramm. and Remote Sens.* 129, 32–40.
- Shoko, C., Mutanga, O., Dube, T., 2016. Progress in the remote sensing of C3 and C4 grass species aboveground biomass over time and space. *ISPRS J. Photogramm. Remote Sens.* 120, 13–24.
- Siambi, M., Simalenga, T., Mpandeli, N.S., Liphadzi, K., Mailula, N., Mkhari, J., Ramugondo, R., 2007. Increased food security and income in the Limpopo Basin through integrated crop, water and soil fertility options and public-private partnerships. In: *Proceedings of the CGIAR Challenge Program on Water and Food*. Addis Ababa, Ethiopia.
- Siambi, M., Simalenga, T., Mpandeli, N.S., Liphadzi, K., Mailula, N., Mkhari, J., Ramugondo, R., 2007. Increased food security and income in the Limpopo Basin through integrated crop, water and soil fertility options and public-private partnerships. In: *Proceedings of the CGIAR Challenge Program on Water and Food*. Addis Ababa, Ethiopia.
- Sibanda, M., Mutanga, O., Rouget, M., 2016. Discriminating rangeland management practices using simulated HypSIRI, landsat 8 OLI, sentinel 2 MSI, and VEN(S spectral data. *IEEE J. Sel. Top. Appl. Earth Obs. Remote Sens.* 9 (9), 3957–3969.
- Sibanda, M., Mutanga, O., Rouget, M., 2016. Discriminating Rangeland Management Practices Using Simulated HypSIRI, Landsat 8 OLI, Sentinel 2 MSI, and VEN μ S Spectral Data. *IEEE. J. Sel. Top. Appl. Earth Obs. Remote Sens.* 9 (9), 3957–3969.
- Sibanda, M., Mutanga, O., Rouget, M., Odindi, J., 2015. Exploring the potential of in situ hyperspectral data and multivariate techniques in discriminating different fertilizer treatments in grasslands. *J. Appl. Remote Sens.* 9 (1), 096033.

- Singh, D., Herlin, I., Berroir, J.P., Silva, E.F., Meirelles, M.S., 2004. An approach to correlate NDVI with soil colour for erosion process using NOAA/AVHRR data. *Adv. Space Res.* 33 (3), 328–332.
- Sobrino, J.A., Raissouni, N., 2000. Toward remote sensing methods for land cover dynamic monitoring: application to Morocco. *Intern. J. Remote Sensing* 21, 353–366.
- Sonawane, K.R., Bhagat, V.S., 2017. Improved change detection of forests using Landsat TM and ETM+ data. *Remote Sens. Land* 1, 18–40.
- South Africa. University of Waterloo Master's thesis.
- Stronkhorst, L., Trytsman, G., Breytenbach, F., Matlou, M., Kidson, M., Lotter, L., Pollard, C., 2009. Report: Local Level Land Degradation Assessment in the Mphanama Village, Agricultural Research Council – Institute for Soil, Climate and Water Report No: GW/ A/2009/69 Project No: GW/56/017.
- Sujatha, G., Dwivedi, R.S., Sreenivas, K., Venkataratnam, L., 2000. Mapping and monitoring of degraded lands in part of jaunpur district of uttar pradesh using temporal spaceborne multispectral data. *Int. J. Remote Sens.* 21 (3), 519–531.
- Symeonakis, E., Drake, N., 2004. Monitoring desertification and land degradation over sub-Saharan Africa. *Int. J. Remote Sens.* 25 (3), 573–592.
- Tanser, F.C., Palmer, A.R., 1999. The application of a remotely-sensed diversity index to monitor degradation patterns in a semi-arid, heterogeneous, South African landscape. *J. Arid Environ.* 43 (4), 477–484.
- Taruvinga, K., 2008. Gully Mapping using Remote Sensing: case Study in KwaZulu-Natal, South Africa (Unpublished M.Sc. Thesis). University of Waterloo, Ontario, Canada.
- Tesfamichael, S.G., 2004. Mapping potential soil erosion using RUSLE, Remote Sensing, and GIS: the case study of Weenen game reserve (Kwazulu-Natal. M.Sc. Dissertation). University of KwaZulu-Natal, South Africa.
- Thiam, A.K., 2003. The causes and spatial pattern of land degradation risk in southern Mauritania using multitemporal AVHRR-NDVI imagery and field data. *Land Degrad. Dev.* 14 (1), 133–142.

- Thompson, A., 2017. Soil Erosion in Africa: Causes and Efforts to Control. Available at: <https://www.thoughtco.com/soil-erosion-in-africa-43352> (accessed 06 July 2017).
- Thompson, M., Vlok, J., Rouget, M., Hoffman, M., Balmford, A., Cowling, R., 2009. Mapping grazing-induced degradation in a semi-arid environment: a rapid and cost effective approach for assessment and monitoring. *Environ. Manag.* 43 (4), 585–596.
- Toggle navigation Municipalities of South Africa, 2018. Accessed on 07 may 2018 at: [<https://municipalities.co.za/demographic/127/sekhukhune-district-municipality>]
- Tully, K., Sullivan, C., Weil, R. and Sanchez, P., 2015. The state of soil degradation in Sub-Saharan Africa: Baselines, trajectories, and solutions. *Sustainability*, 7(6), pp.6523-6552.
- Vågen, T.G., Winowiecki, L.A., Abegaz, A., Hadgu, K.M., 2013. Landsat-based approaches for mapping of land degradation prevalence and soil functional properties in Ethiopia. *Remote Sens. Environ.* 134, 266–275.
- Vaidyanathan, N.S., Sharama, G., Sinha, R., Dikshit, O., 2002. Mapping of erosion intensity in the Garhwali Himalaya. *Int. J. Remote Sens.* 23 (20), 4125–4129.
- Voortman, R.L., Sonneveld, B.G., Keyzer, M.A., 2003. African land ecology: opportunities and constraints for agricultural development. *Ambio: J. Hum. Environ.* 32 (5), 367–373.
- Vrieling, A., 2006. Satellite remote sensing for water erosion assessment: a review. *Catena* 65 (1), 2–18.
- Vrieling, A., 2007. Mapping erosion from space (Doctoral Thesis). Wageningen University.
- Vrieling, A., De Jong, S.M., Sterk, G. and Rodrigues, S.C., 2008. Timing of erosion and satellite data: A multi-resolution approach to soil erosion risk mapping. *International Journal of Applied Earth Observation and Geoinformation*, 10(3), pp.267-281.
- W.H. Wischmeier, D.D. Smith 1978. Predicting rainfall erosion losses-a guide to conservation planning. *Predicting rainfall erosion losses-a guide to conservation planning.*
- Wang, J., Xiao, X., Qin, Y., Dong, J., Geissler, G., Zhang, G., Cejda, N., Alikhani, B., Doughty, R.B., 2017. Mapping the dynamics of eastern redcedar encroachment into grasslands during 1984–2010 through PALSAR and time series Landsat images. *Remote Sens. Environ.* 190, 233–246.

- Watson, H.K., Ramokgopa, R., 1997. Factors influencing the distribution of gully erosion in KwaZulu Natal's Mfolozi catchment—land reform implications. *S. Afr. Geogr. J.* 79 (1), 27–34.
- Wentzel, K., 2002. Determination of the overall soil erosion potential in the Nsikazi district (Mpumalanga Province, South Africa) Using Remote and GIS. *Can. J. Remote Sens.* 28 (2), 322–327.
- Wessels K.J., (2005). Monitoring land degradation in Southern Africa by assessing changes in primary productivity.
- Wessels, K.J., Prince, S.D., Frost, P.E., van Zyl, D., 2004. Assessing the effects of human induced land degradation in the former homelands of northern South Africa with a 1km AVHRR NDVI time-series. *Remote Sens. Environ.* 91, 47–67.
- Wessels, K.J., Prince, S.D., Malherebe, J., Small, J., Frost, P.E., 2007. Can human-induced land degradation be distinguished from the effects of rainfall variability? A case study in South Africa. *J. Arid Environ.* 68, 271–297.
- Wessels, K.J., Prince S.D., Frost P.E., and Zyl D., (2004). "Assessing the effects of human-induced land degradation in the former homelands of northern South Africa with a 1 km AVHRR NDVI time-series." *Remote Sensing of Environment* 91(1): 47-67.
- Whitlow, R., 1986. Mapping erosion in Zimbabwe: a methodology for rapid survey using aerial photographs. *Appl. Geogr.* 6 (2), 149–162.
- Wulder, M.A., Wulder, J.C., White, S.N., Goward, J.G., Masek, J.R., Irons, M., Herold, W.B., Cohen, T.R., Loveland, C.E., 2008. Woodcock Landsat continuity: issues and opportunities for land cover monitoring. *Remote Sens. Environ.* 112, 955–969.
- Wulder, M.A., Wulder, J.G., Masek, W.B., Cohen, T.R., Loveland, C.E., 2012. Woodcock Opening the archive: how free data has enabled the science and monitoring promise of Landsat. *Remote Sens. Environ.* 122, 2–10.
- Xue, J., Su, B., 2017. Significant remote sensing vegetation indices: a review of developments and applications. *J. Sens.*
- Xulu, S., 2014. Land degradation and settlement intensification in Umhlathuze Municipality (Doctoral dissertation, Stellenbosch: Stellenbosch University).

- Yavaşlı, D.D., 2016. Estimation of above ground forest biomass at Muğla using ICESat/GLAS and Landsat data. *Remote Sens. Appl.: Soc. Environ.* 4, 211–218.
- Zhang, C., Denka, S., Cooper, H., Mishra, D.R., 2017. Quantification of sawgrass marsh aboveground biomass in the coastal Everglades using object-based ensemble analysis and Landsat data. *Remote Sens. Environ.*
- Zhou, P., Luukkanen, O., Tokola, T., Nieminen, J., 2008. Effect of vegetation cover on soil erosion in a mountainous watershed. *Catena* 75 (3), 319–325.
- Zimdahl, R.L., 2012. *Agriculture's ethical horizon*. Elsevier.